THEORETICAL INVESTIGATION OF TRANSPORT AND REFLECTION OF THERMAL WAVES

By

YE TIAN

Bachelor of Science
Xi'an Jiaotong University
Xi'an, China
1983

Master of Science
Xi'an Jiaotong University
Xi'an, China
1986

Submitted to the Faculty of the
Graduate College of the
Oklahoma State University
in partial fulfillment of
the requirements for
the Degree of
DOCTOR OF PHILOSOPHY
July, 1995

THEORETICAL INVESTIGATION OF TRANSPORT AND REFLECTION OF THERMAL WAVES

Thesis Approved:

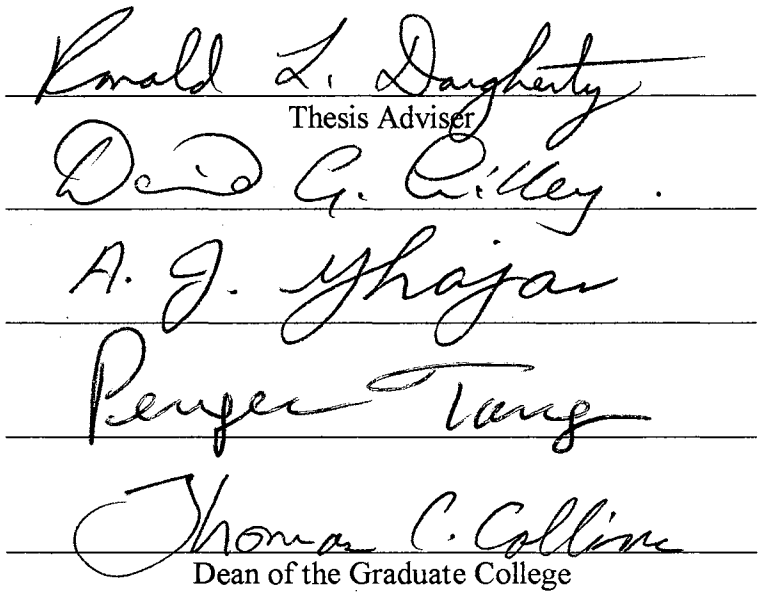

Thesis Adviser

Dean of the Graduate College

ACKNOWLEDGEMENTS

I wish to express my sincere appreciation to my adviser, Dr. Ronald L. Dougherty for his intelligent supervision, constructive guidance, strong encouragement, inspiration and friendship. My sincere appreciation extends to my other committee members Dr. Bruce J. Ackerson, Dr. Afshin J. Ghajar, Dr. David G. Lilley, and Dr. P. Tong whose guidance, assistance, encouragement, and friendship are also invaluable.

Moreover, I wish to express my sincere gratitude to those who provided suggestions and assistance for this study: Dr. Jiaqi Cai, Mr. Lap Mou Tam, Dr. Mingchun Dong, Mr. Tzer-Kun Lin, Mr. Wen-Chieh Tang, and many other friends.

I would also like to give my special appreciation to my wife, Liu Bin, for her precious suggestions on my research, her strong encouragement in times of difficulty, love and understanding throughout this whole process. Thanks also go to my parents, Tian, Jiu-Ting and Zhou, Yi-Xing, my aunt Sarah Chu, my uncle Rommie Chu. my brother Yuan Tian, for their support and encouragement.

Finally, I would like to thank the School of Mechanical and Aerospace Engineering for support during my doctoral study.

TABLE OF CONTENTS

LIST OF FIGURES AND TABLES

Table

NOMENCLATURE

a(t)	function in Eq. (2-1).
A	coefficients in the finite difference Eqs. (5-50) - (5-55).
[A]	matrix defined by Eq. (5-18).
B_i	Biot number defined by Eq. (3-27).
B_p	source term in the finite difference Eqs. (5-50) and (5-56).
[B]	matrix defined by Eq. (5-19).
$[\tilde{B}]$	matrix defined by Eq. (5-18).
b(t)	a function used in Eq. (2-1).
C	propagation speed of a thermal wave (m/s).
c_p	constant pressure specific heat (J/kgK).
$\bar{c}_v$	constant volume specific heat (J/m^3K).
c_v	constant volume specific heat (J/kgK).
E	internal energy (J/m^3).
$\bar{E}$	dimensionless internal energy defined by Eq. (7-60).
$\vec{F}$	vector of temperature and heat flux (see Eq. (5-16)).
f(t)	function of time.
$\vec{G}$	vector of temperature and heat flux (see Eqs. (5-26) and (5-29)).
HHC	hyperbolic heat conduction.
h	convective heat transfer coefficient (W/m^2K).
$\hbar$	Planck's constant (Js).
i	$\sqrt{-1}$
I	phonon transport intensity (J/m^3 ster).

$\bar{I}$ approximate phonon transport intensity (J/m^3 ster).

J heat flux (W/m^2) (see Chapter VII).

K thermal conductivity (W/mK).

k Boltzmann constant (J/K).

k extinction coefficient (Chapters II-VI).

$\hat{k}$ imaginary part ratio of the complex refractive indexes of two materials.

$\tilde{k}$ extinction coefficient for two-dimensional reflection (see Eq. (4-28)).

L reference length, or the thickness of a one-dimensional material (m).

N number of atoms per unit volume of crystal ($1/m^3$).

n refractive index.

$n_{p,q}$ phonon distribution number in Chapter VII.

$\bar{n}$ complex refractive index.

$\hat{n}$ real part ratio of the complex refractive indexes of two materials.

$\tilde{n}$ refractive index for two-dimensional reflection (see Eq. (4-28)).

P variable representing flux at the interface of two control volumes (see Eqs. (5-30)-(5-33)).

p pressure (N/m^2).

PHC parabolic heat conduction.

PTE phonon transport equation.

$\bar{q}$ heat flux (W/m^2).

q heat flux in Chapters I - VI (W/m^2), and modulus of wave vector in Chapter VII (1/m).

$\mathbf{q}$ wave vector (1/m).

$\hat{q}$ heat flux defined by Eq. (5-2) (K).

Q heat transfer normal to the interface or boundary (W).

$\dot{Q}$ heat generation (Eq. (2-1)) (W/m^3).

R Debye's radius (m^{-1}) (see Eq. (7-9)).

R equal to $c_p - c_v$ in Eq. (2-2) (J/kgK).

[R] eigenvector matrix.

Re( ) real part of a complex number.

$\vec{r}^{\,o}$ unit directional vector.

$\vec{r}$ phonon propagation directional vector.

S source term in finite difference equation (Eqs. (5-41) and (5-42)).

$\vec{S}$ source term vector in Eqs. (5-20) - 5-30).

s_p phase speed of a elastic wave (m/s).

T temperature (K).

T_B boundary temperature (K).

TD dimensionless parameter defined in Chapter III.

TD_B dimensionless parameter defined in Chapter III.

t time (s).

$\bar{t}$ dimensionless time (see Eqs. (5-2) and (7-37)).

U_m m^{th} order of moment of phonon intensity (J $ster^{m-1}$).

V control volume, or the crystal volume (m^3).

$\bar{v}$ acoustic velocity (m/s).

$\vec{v}$ phonon velocity (m/s).

x coordinate (m).

$\bar{x}$ dimensionless x coordinate (see Eqs. (5-2) and (7-37)).

y coordinate (m).

$\bar{y}$ dimensionless y coordinate.

Greek

α thermal diffusivity (m^2 /s).

β ratio of thermal capacities of two materials (see Eq. (5-3b)).

γ ratio of relaxation times of two materials (see Eq. (5-2)).

Γ dimensionless parameter defined by Eqs. (3-27) and (5-2).

δ transmission angle.

δ_o real transmission angle.

Δ parameter defined by Eq. (5-35).

ε angle defined by Eq. (4-14).

ς parameter defined by Eq. (5-45).

ξ parameter defined by Eq. (5-45).

η parameter defined by Eq. (4-19).

Θ Debye's temperature (K).

θ incident angle.

κ Boltzmann constant (Chapter VII).

λ wavelength (m).

$\tilde{\lambda}$ eigen values of the wave equations in Chapters V and VII.

Λ phonon mean free path (m).

μ cosine of the polar angle.

ν frequency of phonon wave (1/s).

Ξ phonon scattering function in the phonon transport equation (Eq. (7-18)).

ρ density of the material (kg/m^3).

$\rho_{\lambda r}$ reflectivity of a single wavelength complex thermal wave.

$\tilde{\rho}_{\lambda}$ reflectivity of a single wavelength real wave.

$\tilde{\rho}$ reflectivity of a real thermal wave.

$\tilde{\rho}_m$ time-averaged reflectivity of a real thermal wave.

σ angle defined by Eq. (3-10).

$\hat{\sigma}$ sign defined by Eq. (5-33).

τ relaxation time (s).

$\tilde{\tau}_m$ time-averaged transmissivity.

ϕ angle defined by Eq. (4-17).

Φ auxiliary function defined by Eq. (7-54).

φ reflection angle.

χ parameter defined by Eq. (5-34).

ψ angle defined by Eqs. (3-39) and (4-31).

Ψ auxiliary function defined by Eq. (7-53).

Ω solid angle in space (ster).

ω wave frequency (s^{-1}).

Subscript

A node before the central node.

B node after the central node.

E node east of the central node.

e east boundary of control volume.

i incident.

I imaginary part.

l longitudinal wave.

M magnitude.

m order of moment.

N node north of central node.

n north boundary of the control volume.

o initial time.

P central node.

p polarization mode.

q wave vector.

r reflected.

R real part.

S node south of the central node.

s south boundary of control volume.

t transmitted.

$\bar{t}$ derivative with respect to time.

x component on x-axis.

$\bar{x}$ derivative with respect to $\bar{x}$ coordinate.

y component on y-axis.

W node west of the central node.

w west boundary of control volume.

Ω in solid angle $d\Omega$.

λ for given wavelength.

1 material 1.

2 material 2.

Superscript

o represents previous time step in Chapter V, and steady state in Chapter VII.

n at current time step.

n+1 at next time step.

CHAPTER I

INTRODUCTION

The classical heat conduction theory (parabolic heat conduction model) has been used successfully in most thermal engineering applications. However, in the cases such as at extremely low temperature (nearly absolute zero K), or for an extremely short time period, or a very thin material, the heat transfer is no longer a diffusion phenomenon as described by the classical theory. It is observed that thermal energy then propagates like a wave (thermal wave) with a constant speed. Therefore, different heat conduction models are used to describe the wave-propagation process of heat conduction. In these models, the hyperbolic heat conduction model and phonon transport theory are the two most important models with strong physical background and have been studied by many investigators.

In this chapter, we are going to introduce the background and the applications of thermal waves which will be studied in this research.

1.1 Background

Heat conduction processes based on the classical theory and the wave models are very different. In the classical theory, thermal energy is transferred with an infinite propagation speed. However, according to the wave models, the propagation speed is finite and the thermal energy can be reflected at an interface between two different media. In order to understand the differences between these heat conduction models, we will discuss the one-dimensional heat conduction problem as shown in Fig. 1-1.

According to the classical parabolic heat conduction theory (PHC), the temperature and heat flux satisfy the energy conservation equation and Fourier's law

$$-\frac{\partial q}{\partial x} = \rho c_p \frac{\partial T}{\partial t} \tag{1-1}$$

$$q = -K\frac{\partial T}{\partial x} \tag{1-2}$$

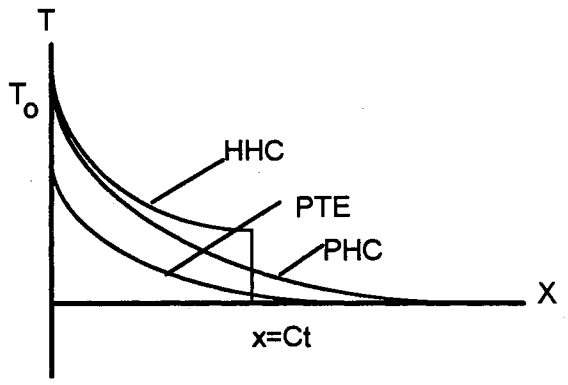

Fig. 1-1 The One-Dimensional Heat Conduction by Diffusive, Hyperbolic, and Phonon Transport Heat Conduction

The solution of the temperature field of the problem shown in the Fig. 1-1 is

$$\frac{[T(x,t)-T_b]}{[T_o-T_b]} = 1 - erfc\left\{\frac{x}{2\sqrt{\alpha \cdot t}}\right\} \tag{1-3}$$

where T_b is the initial temperature of the medium.

From this solution, we find that a thermal disturbance at the boundary x = 0 is instantaneously felt at any point in the medium. This result implies that the thermal energy is transferred in an infinite speed. Obviously, this is not realistic. Despite its unrealistic physical interpretation, this result is a very good approximation for most situations of common experience. However, when we study transient heat transfer in extremely short time periods (10^{-10} s), or at extremely low temperatures approaching absolute zero, this classical solution breaks down because of the wave behavior of heat propagation. In this case, the hyperbolic model of heat conduction is used to describe the heat transfer process. The hyperbolic model proposed by Vernotte (1958) is

$$q + \tau\frac{\partial q}{\partial t} = -K\frac{\partial T}{\partial x} \tag{1-4}$$

where τ is the relaxation time. According to this equation, the heat flow does not start instantaneously after the temperature gradient has been imposed on the medium, but grows gradually with a relaxation time τ after the application of the temperature gradient. The temperature profile according to this model is illustrated in Fig. 1-1 by the curve labeled HHC. We can see that there is an obvious wave front along the propagation direction. The temperature in the region ahead of the front is not affected by the boundary condition. The wave front moves forward along the x-axis with a constant propagation speed C. This speed is related to the relaxation time and the thermal diffusivity as (Baumeister and Hamill, 1969)

$$C^2 = \frac{\alpha}{\tau} \tag{1-5}$$

When the relaxation time is very small, the hyperbolic model reduces to the classical parabolic model. For most materials, the relaxation time is very small; therefore, the parabolic model is accurate enough for engineering applications when a long time period of heat conduction is of interest. However, for very short time period processes, the hyperbolic model should be used.

The hyperbolic model, Eq. (1-4), is for isotropic and homogeneous media. For anisotropic and non-homogeneous media, the hyperbolic model is not correct because the thermal properties and relaxation time may not be constant, and the anisotropic scattering of thermal waves by particles, such as the impurities in the materials, should be considered.

The temperature distribution based on the phonon transport theory is different from those of PHC and HHC as illustrated in Fig. 1-1. The phonon theory was first developed by Debye (Roberts and Miller, 1960) and have been studied by many physicists. According to this theory, heat transfer actually is the propagation of elastic waves in materials. Therefore, the propagation speed of the thermal wave is the same as the

acoustic speed of the material. The energy of an elastic waves is quantized and the quantum is called a phonon. Phonon theory has been successfully used to predict the thermodynamic properties of a variety materials (Roberts and Miller, 1960). These properties include thermal conductivity and specific heat. When the temperature of the material is very low, phonon transport process is similar to the photon transport process in radiative heat transfer (Bak, 1964).

1.2 Applications of Thermal Waves in Engineering

Thermal waves have found many applications in engineering. One important application is the heat conduction process encountered in cryogenic engineering (Bertman and Sandiford, 1970). The heat transfer in a super-conductor is a kind of thermal wave propagation. The manufacturing of very pure materials such as crystals has the same heat conduction problems which can be treated with thermal wave theory. The study of the propagation of thermal wave in anisotropic materials is useful for the measurement of impurities in materials, and the study of physical properties of the impurities. With the advent of laser technology, the use of laser pulses of extremely short duration has found numerous applications for purposes such as the annealing of semiconductors and surface heating and melting of materials (Hess et al., 1981; Stritzker et al., 1981; Maher and Hall, 1980). In these situations, the thermal wave plays an important role in establishing the temperature field. There are still other applications of thermal waves: in low-pressure gases (Chan et al., 1971), nuclear engineering (Hus, 1962), and seismology (Luikov et al., 1976). It is also suggested that hyperbolic model be used in chemical and process engineering (Luikov, 1966). Hyperbolic heat conduction is also found to be useful in nuclear engineering. Kazimi and Erdman (1975) studied the temperature change of two suddenly contacting materials which is encountered in nuclear reactors.

Thermal waves may also have important applications in non-destructive testing of flaw and corrosion in composite materials and corrosion in metals by thermal imaging.

One specific use of this technology may be the non-destructive detection of corrosion in aircraft (Dougherty and Price, 1994).

In recent years, as the development of electronic and computer industry, super-conductive thin films which are a few microns in thickness are applied in many computer components. The study of heat transfer in such thin films is of interest and has become an important branch of heat transfer called microscale heat transfer. The phonon transport theory has been rapidly developing, and has been applied as the basic theory of heat conduction in this field (Ziman, 1960, Bak, 1964, Goodson and Flik, 1993, Klitsner et al., 1990, Majumdar, 1993).

1.3 Purpose of this Research

The purpose of this research is to study the propagation of the thermal wave in isotropic and non-homogeneous media. To achieve our purpose, we need to develop the thermal wave transport equation in such media. The reflection and transmission of the thermal wave at an interface of two different media will also be studied. Numerical methods will be developed to solve for the thermal waves in one- and two-dimensional materials. Based on the numerical solutions of thermal waves in different situations, we will study the mechanism of the propagation of thermal waves, and develop thermal wave transport theory. We will study the relationship between the different heat conduction models (PHC, HHC, and PTE). By comparing these models, we will find their similarities and differences.

This thesis includes eight chapters. The study of hyperbolic thermal waves (HHC) is presented in Chapters III to VI. Chapter VII is the research on phonon transport theory, and the comparison of the three heat conduction models. Parabolic heat conduction is not discussed unless it is needed. This is because the parabolic heat conduction theory has been developed completely elsewhere (Ozisik, 1980).

CHAPTER II

REVIEW OF LITERATURE

The investigation of thermal waves started in the 1940's. However, the problem had been proposed much earlier. Many investigators realized that the infinite propagation speed implied by the classical theory is unrealistic. But this problem was not considered important because most engineering heat conduction processes in our common experience can be treated accurately using the classical theory. Also we did not find experimental evidence of thermal waves until Peshkov (1944) first observed them in super fluid helium. Since then, limited studies have been done. Table 1 lists the most important studies in this field. These investigations can be classified into three categories: experimental studies, basic theory, and applications.

2.1 Experimental Studies

A very basic experimental study was the observation of the thermal wave in super fluid helium performed by Peshkov in 1944. The experiment showed an oscilloscope trace of a pulsed energy source propagating at a constant speed in helium at about 1K. Peshkov found from his experiment that the propagation speed was 19 m/s at 1.4K, an order of magnitude smaller than the ordinary magnitude of sound speed in helium. The thermal wave in super fluid helium was explained in Bak's book (1964) using phonon and roton interaction theory, and it was found that these waves are not pure phonon transport processes. The same experiment was also described by Bertman and Sandiford (1970). These are the direct proofs of the existence of thermal wave phenomena.

According to Bertman and Sandiford, the thermal wave cannot be observed in most of materials which are not pure enough; because the impurities in the materials scatter the thermal wave frequently, and the scattering processes will cause several changes in the propagation direction of the thermal wave. At extremely low temperatures, helium is very

pure. Therefore, the scattering of the thermal wave by impurities is negligible, and the thermal wave becomes important. Most solids have many point defects such as chemical and impurities, and they also have many crystal imperfections such as dislocations in the crystal lattice. All of these defects scatter the thermal wave strongly. The scattering interactions take place much more frequently than the normal (wave propagation) processes. However, with the development of the technology for purifying materials, we can expect to observe thermal waves in other substances. On the other hand, as the increasing applications of very thin films in electronic and computer industry, wave behavoir of heat transfer in such thin films is significant.

An indirect proof of thermal waves was obtained in exothermic catalytic reactions in which the maximum temperatures in crystals can occur in extremely short time periods, about 10^{-13} s. Cusumano and Low (1970) have shown experimentally the anomalous temperature rise which is caused by the heat of reaction of O_2 on SiO_2 supported by Ni. Harrington's (1966) experiments show that the temperature rise is in the range from 2000 to 3000 K. However, the theoretical results based on the classical theory are much smaller than the experimental results. Prater's (1958) prediction by using the classic heat conduction model (PHC) was 2 K, and Luss and Amundson's (1969) solution by PHC was 250K. Using the hyperbolic model (HHC), Chan et al. (1971) predicted a temperature rise ranging from 1100 to 2500K. These studies demonstrate that the heat conduction in extremely short time periods is a wave phenomenon.

TABLE 1. Previous Studies

Investigator	Results of Study
Bak (Editor) (1964)	Phonon Theory.
Berkovsky & Bash (1977)	Derivation of hyperbolic model using kinetic theory.
Baumeister & Hamill (1969)	Solution of HHC in semi-infinite 1-D medium.

TABLE 1. Previous Studies (Continued)

Bertman & Sandiford (1970)	Explained thermal waves in helium as second sound.
Chan et al. (1971)	Solution of HHC in 1-D medium in catalytic supported crystallites.
Chester (1963)	Discussion of thermal wave.
Cheng (1989)	Solution of 1-D problem using a discrete microscopic model.
Curtin & Pipkin (1969)	General equations of thermal waves based on thermodynamics.
Frankel et al. (1987)	Solution of hyperbolic heat conduction in composite media.
Goodson & Flik (1993)	Study of phonon heat conduction in superconducting film.
Harrington (1966)	Surface heating process.
Hus (1962)	Studied the size effect on heat transfer in nuclear system.
Kaminiski (1990)	Measurement of relaxation time for non-homogeneous media.
Kittel (1986)	Application of phonon theory in solid physics.
Klitsner et al. (1990)	Phonon radiative heat transfer and boundary scattering.
Luikov (1966)	Application of HHC in chemical and process engineering.
Luikov et al. (1976)	Solved HHC using numerical method.
Majumdar (1993)	Developed phonon transport equation
Ozisik (1984)	Solution of HHC for 1-D problem in finite medium.
Peshkov (1944)	Observation of thermal wave in helium.
Roberts & Miller (1960)	Using phonon theory to predict thermodynamic properties.
Tzou (1989)	Thermal shock wave.
Tzou (1993)	Harmonic analysis of reflection of thermal waves.
Vick & Ozisik (1993)	Solution of HHC for 1-D problem.
Yang (1990, 1992)	One and two-dimensional numerical solution of HHC.
Weymann (1967)	Discussed wave speed of HHC using random walk model.
Wiggert (1977)	Early time transient heat conduction by HHC.
Ziman (1960)	Phonon and electron theory.

Heat conduction in a non-homogeneous medium with inner-structure such as a porous material, e.g. sand, can also be treated by the hyperbolic model. Kaminski (1990)

explained the physical meaning of the relaxation time τ of such a medium as the time period needed for accumulating the thermal energy required for propagative transfer to the next nearest element of the inner structure. He measured the relaxation time for several materials. The results are listed in Table 2. From these results we find that the relaxation times based on Kaminski's definition are very significant. Compared with the relaxation times of homogeneous materials (in the range from 10^{-8} to 10^{-12} s), the wave effect in non-homogeneous media is very important. The propagation speed listed in Table 2 is very small. The temperature profile and heat flux predicted using the hyperbolic model agree very well with experiment and much better than the results based on the parabolic model (Kaminski, 1990). The relaxation times of non-homogeneous materials can range from 10^{-3} to 10^{3} s (Luikov, 1966).

TABLE 2(a). The Properties of Experimental Materials

Materials	Mean Particle Diameter (mm)	Moisture content kg(mos)/kg(dry)	Bulk density kg/m^3
H Acid	19.3	0.129	439
$NaHC_3$	96.4	0.185	1236
Sand	187.0	0.0098	1551
Ion exchanger	206.0	0.069	1607
Glass Ballotini	602.0	0.181	862

TABLE 2(b). Parameters of the Thermal Wave

Materials	Thermal diffusivity (mm^2/s)	Propagation Speed (mm/s)	Relaxation Time (s)
H Acid	0.260	0.103	24.5
$NaHC_3$	0.310	0.104	28.7
Sand	0.408	0.143	20.0
Ion exchanger	0.220	0.064	53.7
Glass Ballotini	0.251	0.152	10.9

2.2 Basic Theory

Since Peshkov's (1944) observation of thermal waves in superfluid helium, the wave phenomena was realized to be important in both heat conduction theory and engineering applications. It raised two questions that need to be explained theoretically. What actually are thermal waves; and how do they propagate in materials?

Vernotte (1958) suggested the hyperbolic model, (Eq. (1-4)) to explain the second question. This model (HHC) is a macroscopic description of thermal waves, and cannot explain the microscopic mechanism of thermal wave phenomena. Therefore, this model itself may not be correct. Many investigators have attempted to explain this model in different ways. Chester (1963) justified the existence of the thermal wave based on the results of Maxwell (1867). It was shown that the hyperbolic model is actually a truncated form of a more general relation originally derived by Maxwell. Weymann (1967) used a random walk model to derive the hyperbolic model. He interpreted the relaxation time as the time period needed for a moving point to walk one step in distance $\pm\ell$. Taitel (1972) derived Eq. (1-4) using a discrete model. He concluded that Eq. (1-4) is still an approximation which is valid for extremely short time periods because Eq. (1-4) is a second order approximation. Curtin and Pipkin (1969) obtained a general integro-differential equation for heat conduction of non-linear materials with memory. Their equation is hyperbolic and includes the effect of the memory of materials:

$$\frac{\partial^2 T(x,t)}{\partial t^2} + b(t=0)\frac{\partial T(x,t)}{\partial t} + \int_0^\infty b(t')\frac{\partial T(x,t-t')}{\partial t}dt'$$
$$= a(t=0)\Delta T(x,t) + \int_0^\infty a(t')\Delta T(x,t-t')dt' + \dot{Q} \qquad (2\text{-}1)$$

The effect of the memory of materials is considered by the function b(t) and a(t) and the integrals in the above equation.

Cheng (1989) solved the Boltzmann transport equation for the propagation of a temperature disturbance in a fluid using a discrete velocity microscopic model. He showed

that heat conduction indeed possesses wave like properties and a characteristic propagation speed. Luikov et al. (1976) used the concept of isotherms to derive Eq. (1-4).

The above research has proven that wave behavior is a basic property of heat conduction. Although the hyperbolic model was derived by many investigators using different methods, the relaxation time is still a problem that has not been solved. Some formulas are available to calculate the relaxation times theoretically for some special materials, but there is no experimental method to determine this important property for homogeneous media because it is so small that so far we still have no method to measure it accurately. Cheng (1989) has given an equation to calculate the propagation speed C for gases.

$$C^2 = \frac{5}{2}\left[\frac{c_p}{c_v} - 1\right]RT \qquad (2\text{-}2)$$

This equation shows that the speed decreases with a decrease in temperature, so the wave behavior will be more important at low temperature than at high temperature.

Besides the HHC model, other forms of thermal wave models have been developed. One such model was developed by Berkovsky and Bashtovoi (1977). They obtained a power form heat conduction law using a modified collision term in the Boltzmann equation and then calculated the heat flux from the molecular distribution function. However, these models are not commonly used.

Since the hyperbolic heat conduction model (HHC) cannot explain the basic mechanism of heat conduction in solid materials, it is believed that this model is still not the exact solution of the problem. Heat conduction in solids has been explained by using the phonon theory by many physicists (Ziman, 1960, Bak, 1964, Kittel, 1986, Roberts and Miller, 1960). From this theory, heat conduction is explained as the propagation of elastic waves in a solid. The energy of the elastic waves is quantized and can be treated as a phonon gas. By studying phonon transport in solid, heat conduction can be quantitatively described. It is believed that the Boltzman transport equation for phonons is the general

equation to describe heat conduction in solids. Parabolic heat conduction and hyperbolic heat conduction can be derived from the Boltzman transport equation under certain assumptions (Ziman, 1960, Majumdar, 1993). The phonon theory can explain both the mechanism and the mode of propagation of thermal waves in solid materials. Therefore, thermal waves should be correctly predicted by using the Boltzman equation.

2.3 Applications

Many studies of hyperbolic heat conduction have been published. It appears that all of these studies are limited to one-dimensional problems. Baumeister and Hamill (1969) solved the heat conduction problem in a semi-infinite body. His solution shows the discontinuous temperature distribution at the front of a thermal wave. There is a significant difference between the classical theory and hyperbolic heat conduction. According to the classical theory (Fourier's law), the heat flux due to a step change in temperature is infinite because of the infinite temperature gradient. However, Baumeister and Hamill's result proved that the heat flux calculated using the hyperbolic model is finite. Wiggert (1977) studied hyperbolic heat conduction in a one-dimensional finite medium by using the method of characteristics. He proved that the characteristics method is very accurate for solving the hyperbolic heat conduction equations.

Ozisik (1984) discussed in detail the propagation and reflection of a hyperbolic thermal wave produced by a pulsed energy source in a one-dimensional medium. He also showed that the temperatures at the boundaries are the superposition of the incident temperature wave and the reflected temperature wave.

Chan et al. (1971) studied hyperbolic heat conduction in catalytic supported crystallites. Tzou (1989) studied the thermal shock produced by a moving source. He found that the thermal shock is very similar to the sound shock in supersonic flow. Hus (1962) developed a semi-infinite conduction model for the inception of nucleate boiling, in which times on the order of 10^{-6} sec need to be considered.

There are very limited studies related to two-dimensional thermal waves. Tzou (1989) has studied the two-dimensional thermal shock caused by a moving source. Yang (1992) has solved several two-dimensional thermal wave problems by using numerical methods.

Ziman (1960) has studied boundary scattering phenomenon using the steady state phonon transport equation (Boltzman transport equation). Klitsner et al. (1990) also investigated phonon radiation and surface scattering under steady state and at very low temperature. Majumdar (1993) solved a steady state transport equation to investigate the heat conduction in diamond films. These studies did not discuss the wave properties because they were all under steady state.

From the review of the previous literature, we know that both HHC and PHC models are based on particle transport theory (either atoms for gases or phonons for solids). But we still have questions that are not answered by the literature. They are (1) are these models correct? (2) if they are correct, what are the conditions for using these models? For steady state heat conduction, Majumdar (1993) has shown that HHC is an approximation of the phonon transport equation for very thick materials (large acoustic thickness). However, for transient heat conduction processes, especially for the process during an extremely short time period, the HHC and PHC models still need to be examined for their accuracy.

So far, we have found very limited studies of thermal waves in one-dimensional composite materials and non-homogeneous materials (Tzou, 1993, Frankel et al., 1987). No study has been found for two-dimensional media. Although Tzou has developed a closed form solution for the reflectivity, the solution was not compared with the numerical solution of the hyperbolic heat conduction, and therefore, the physical process of reflection was not explained very carefully. Since studies of the reflection process for thermal waves are very limited, there is not much knowledge about the wave propagation in non-homogeneous materials in which the thermal waves are scattered by the impurities.

Applications of thermal waves in corrosion detection is another important field. Thermal imaging technology for non-destructive testing of flaws in solid materials has been reviewed by Dougherty and Price (1994). Much research on thermal imaging using the PHC model has been published (Maldague et al., 1991, Del Grande et al., 1993).

CHAPTER III

ONE-DIMENSIONAL THERMAL WAVE

A one-dimensional thermal wave is a basic type of thermal wave. Since it has the basic wave properties which all kinds of thermal waves have, the study of this special wave is very important for the next level of study on multi-dimensional thermal waves. On the other hand, the one-dimensional thermal wave has been found to be very useful in engineering applications. Therefore, in this chapter, we will study this specific thermal wave and its basic properties.

3.1 One-Dimensional Thermal Wave Equations

We consider one-dimensional hyperbolic heat conduction in an isotropic and homogeneous medium. From Eq. (1-1) and Eq. (1-4), we can easily derive the following wave equations for temperature T and heat flux q:

$$\frac{1}{C^2}\frac{\partial^2 T}{\partial t^2} = \frac{\partial^2 T}{\partial x^2} - \frac{(\partial T/\partial t)}{\alpha} \tag{3-1}$$

$$\frac{1}{C^2}\frac{\partial^2 q}{\partial t^2} = \frac{\partial^2 q}{\partial x^2} - \frac{(\partial q/\partial t)}{\alpha} \tag{3-2}$$

where $C^2 = \frac{\alpha}{\tau}$.

From Eqs. (3-1) and (3-2), we find that the temperature and heat flux are the same kind of waves, therefore their properties are similar to each other. The terminology "thermal wave" indicates both the temperature wave and the heat flux wave.

In Eqs. (3-1) and (3-2), the second terms on the right side represent the extinction of thermal waves in space during propagation. When the thermal diffusivity is very large (due to very large thermal conductivity or very small heat capacity), the extinction term will be negligible, so these equations become the standard wave equations (Kreyszig, 1983)

$$\frac{1}{C^2}\frac{\partial^2 T}{\partial t^2}=\frac{\partial^2 T}{\partial x^2} \tag{3-1a}$$

$$\frac{1}{C^2}\frac{\partial^2 q}{\partial t^2}=\frac{\partial^2 q}{\partial x^2} \tag{3-2a}$$

The thermal waves described by the above equations do not include extinction during the propagation. We call this kind of thermal wave the ideal thermal wave.

In Eqs. (3-1) and (3-2), it seems that temperature and heat flux are independent. However, this is not true. The temperature wave and heat flux wave exist together, and they are related to each other according to Eq. (1-1). Therefore, if there is a temperature wave, there must be a corresponding heat flux wave. We cannot separate them simply according to Eqs. (3-1) and (3-2). This is very important. The relationship between heat flux and temperature illustrates the conversion of energy between heat flow and the internal energy (temperature) of the material. Therefore, the propagation of a thermal wave or heat transfer is realized by a series of energy conversion processes. This heat conduction mechanism will be discussed in more detail in the following chapter.

For one-dimensional thermal waves, the harmonic thermal wave is extremely important since all of the other waves can be composed of harmonic thermal waves using Fourier transform theory. The harmonic thermal wave of frequency ω can be expressed by the following equations

$$q = q_M \exp\left[i\omega\left(t-\frac{\bar{n}x}{C}\right)\right] \tag{3-3}$$

$$T = T_M \exp\left[i\omega\left(t-\frac{\bar{n}x}{C}\right)\right] \tag{3-4}$$

where ω is the frequency and λ is the wavelength which is related to the frequency by

$$\omega=\frac{2\pi C}{\lambda} \tag{3-5}$$

In Eqs. (3-3) and (3-4), $\bar{n}$ is the complex refractive index of the thermal wave, and it is defined as

$$\bar{n} = n - ik \tag{3-6}$$

where n is called the real refractive index (or refractive index) and k is called the extinction coefficient. From the thermal wave Eqs. (3-1) and (3-2) and Eqs. (3-3) and (3-4), we can obtain

$$n^2 = \frac{1}{2}\left\{1+\left[1+\left(\frac{1}{\omega\tau}\right)^2\right]^{1/2}\right\} \tag{3-7}$$

$$k^2 = \frac{1}{2}\left\{-1+\left[1+\left(\frac{1}{\omega\tau}\right)^2\right]^{1/2}\right\} \tag{3-8}$$

These same equations were also derived by Weymann (1967). Physically, n represents the phase change of the harmonic thermal wave, and k represents the extinction of the thermal wave during the propagation. When the extinction coefficient is zero, the wave is termed an ideal thermal wave. This kind of wave actually does not exist because, for all materials, the thermal capacity is not zero and conductivity is finite. When the relaxation time is very small, or the wave has a very small frequency, the thermal wave will die out very quickly, and in this case, heat conduction is a diffusion process which can be predicted by using the classical parabolic heat conduction theory (Weymann, 1967).

The refractive index and the extinction coefficient are shown in Fig. 3-1 as a function of $\omega\tau$. From the figure, we can see that the refractive index and the extinction coefficient are significantly different in the region of $1/\omega\tau$ less than 1.0. In this region, heat conduction is a wave propagation process. When $1/\omega\tau$ is very large, the refractive index and the extinction coefficient are equal; thus heat conduction is a diffusion process. Since for most materials, the relaxation time is very small (10^{-13} to 10^{-8} s) (Ozisik, 1984), the thermal wave is important only when heat conduction takes place in an extremely short time period, for example, during the initial time to build a temperature gradient. When the temperature is extremely low, approaching 0K, the relaxation time can be significant and thermal waves also become important.

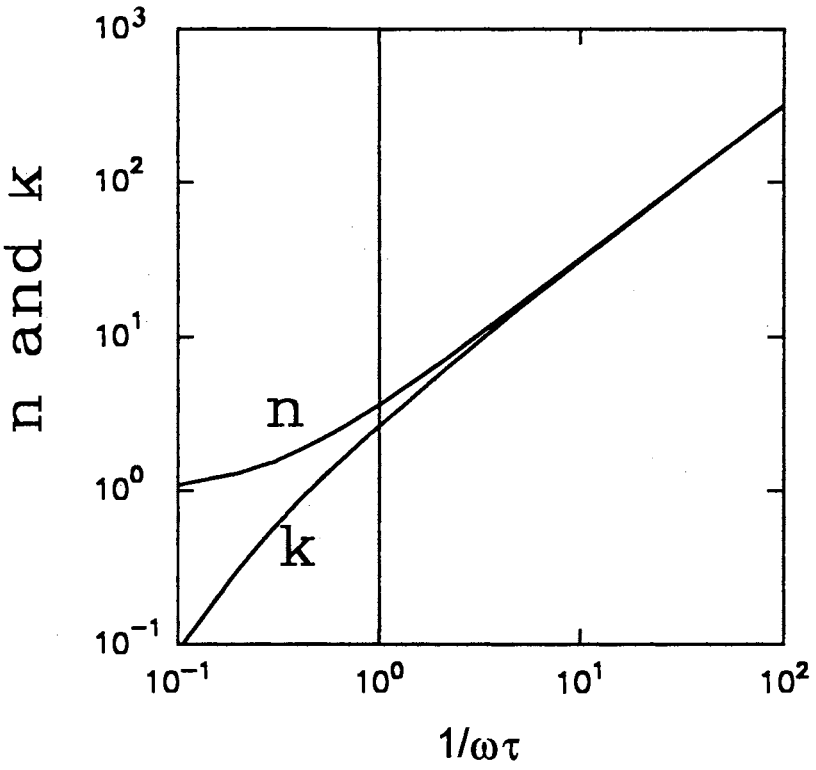

Fig. 3-1 Refractive Index and Extinction Coefficient

The heat flux and temperature waves are not independent of each other. From Eqs. (1-1), (3-3) and (3-4), we can obtain

$$T_M = \frac{\bar{n}}{C\rho c_p} q_M \tag{3-9}$$

Therefore, the heat flux and temperature waves exist simultaneously. This relationship shows that the magnitude of temperature is directly proportional to the magnitude of heat flux. If we define angle σ by

$$\frac{\bar{n}}{|\bar{n}|} = \exp(-i\sigma) \tag{3-10}$$

then from Eqs. (3-4), (3-9) and (3-10), we can obtain

$$T_\lambda = \frac{|\bar{n}|}{C\rho c_p} q_M \exp\left[i\omega\left(t - \frac{\bar{n}x}{C}\right) - i\sigma \right] \tag{3-11}$$

Comparing the above equation with Eq. (3-3), we find that there is a phase difference between the temperature wave and the heat flux wave. When the extinction coefficient k is zero, or the frequency is very large, the phase difference σ is $\pi/2$. When heat conduction is a diffusion process, the phase difference is $\pi/4$. These solutions can be tested by using numerical experiments to solve for the thermal waves for small frequency.

3. 2 Reflection of a Thermal Wave at an Interface

Since the one-dimensional thermal wave Eqs. (3-1) and (3-2) have the same form as the one-dimensional electromagnetic wave equations (Siegel and Howell, 1981), we can use the method for deriving the reflection of the electromagnetic wave to derive the reflection of a one-dimensional thermal wave at an interface between two materials.

To study the reflection of a thermal wave at the interface of two different materials, we consider an incident plane wave along the x' direction as shown in Fig. 3-2. The reflected and transmitted waves are also shown in the figure. Because both the incident wave and the reflected wave, as well as the transmitted wave, satisfy the wave equations discussed in the previous section, we can express them as harmonic waves, i.e.

$$T_{\lambda i} = T_{Mi} \exp\left[i\omega(t - \frac{\overline{n}_1 x'}{C_1}) \right] \tag{3-12a}$$

$$T_{\lambda r} = T_{Mr} \exp\left[i\omega(t - \frac{\overline{n}_1 x''}{C_1}) \right] \tag{3-12b}$$

$$T_{\lambda t} = T_{Mt} \exp\left[i\omega(t - \frac{\overline{n}_2 x'''}{C_2}) \right] \tag{3-12c}$$

$$q_{\lambda i} = q_{Mi} \exp\left[i\omega(t - \frac{\overline{n}_1 x'}{C_1}) \right] \tag{3-12d}$$

$$q_{\lambda r} = q_{Mr} \exp\left[i\omega(t - \frac{\overline{n}_1 x''}{C_1}) \right] \tag{3-12e}$$

$$q_{\lambda t} = q_{Mt} \exp\left[i\omega(t - \frac{\overline{n}_2 x'''}{C_2}) \right] \tag{3-12f}$$

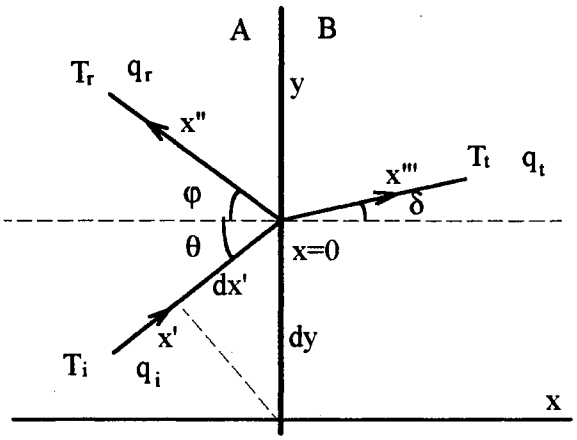

Fig. 3-2 Reflection and Transmission of a Thermal Wave at an Interface

From Fig. 3-2, we can see that the coordinates involved in the above equations have the following relationships

$$y = x' / \sin\theta = x'' / \sin\varphi = x''' / \sin\delta \tag{3-13}$$

At the interface x=0, we have the following boundary conditions:

1. Energy conservation condition in the direction normal to the interface.

At the interface, the incident energy, the reflected energy and the transmitted energy in the direction normal to the interface must satisfy the energy conservation equation as

$$[Q_i - Q_r = Q_t]_{x=0} \tag{3-14a}$$

or

$$[q_{\lambda i}\cos\theta - q_{\lambda r}\cos\varphi = q_{\lambda t}\cos\delta]_{x=0} \tag{3-14b}$$

2. Continuity of temperature at the interface.

The temperature at the interface must be continuous. On the left side of the interface, the temperature wave is the superposition of the incident wave and

the reflected wave. On the right side of the interface, the temperature wave is the transmitted wave. The continuity condition therefore is written as

$$\left[T_{\lambda i} + T_{\lambda r} = T_{\lambda t}\right]_{x=0} \tag{3-15}$$

From Eq. (3-11) we can obtain the relationship between heat flux and temperature

$$T_\lambda = \frac{\bar{n}}{C\rho c_p} q_M \exp\left[i\omega(t - \frac{\bar{n}x}{C})\right] \tag{3-16}$$

From Eqs. (3-12d-f), (3-13) and (3-14), we derive

$$\begin{aligned} &q_{iM}\cos\theta\exp\left[i\omega(t - \frac{\bar{n}_1 y}{C_1}\sin\theta)\right] - q_{rM}\cos\varphi\exp\left[i\omega(t - \frac{\bar{n}_1 y}{C_1}\sin\varphi)\right] \\ &= q_{tM}\cos\delta\exp\left[i\omega(t - \frac{\bar{n}_2 y}{C_2}\sin\delta)\right] \end{aligned} \tag{3-17}$$

Since this equation is true for any y, the following equation must be satisfied

$$\sin\theta = \sin\varphi = \frac{\bar{n}_2}{\bar{n}_1}\frac{C_1}{C_2}\sin\delta \tag{3-18}$$

Therefore, the incident angle θ is equal to the reflected angle φ. This equation is very similar to Snell's law in electromagnetic theory (Siegel and Howell 1981). Actually, the thermal wave Eqs. (3-1) and (3-2) have the same form as the electromagnetic wave equation (Siegel and Howell 1981). The angle δ is a complex number and it cannot be intepreted as the transmission angle for all cases. Substituting Eq. (3-18) into (3-17) we obtain

$$q_{iM}\cos\theta - q_{rM}\cos\varphi = q_{tM}\cos\delta \tag{3-19}$$

Substituting Eqs. (3-9), (3-12a-c), (3-13), (3-16), and (3-18) into Eq. (3-15) yields

$$q_{iM}\left(\frac{\bar{n}}{C\rho c_p}\right)_1 + q_{rM}\left(\frac{\bar{n}}{C\rho c_p}\right)_1 = q_{tM}\left(\frac{\bar{n}}{C\rho c_p}\right)_2 \tag{3-20}$$

Eliminating q_{tM} by substituting Eq. (3-19) into Eq. (3-20), we find that

$$q_{iM}\left[\left(\frac{\overline{n}}{C\rho c_p}\right)_2\cos\theta-\left(\frac{\overline{n}}{C\rho c_p}\right)_1\cos\delta\right]=q_{rM}\left[\left(\frac{\overline{n}}{C\rho c_p}\right)_2\cos\theta+\left(\frac{\overline{n}}{C\rho c_p}\right)_1\cos\delta\right] \tag{3-21}$$

We introduce a dimensionless parameter TD, which is defined as

$$TD=\frac{\left(C\rho c_p\right)_1}{\left(C\rho c_p\right)_2} \tag{3-22}$$

This parameter can be interpreted as the comparison of the capacity for heat transfer for the two materials. Substituting the above equation into Eq. (3-21), we find that Eq. (3-21) can be written as

$$\frac{q_{rM}}{q_{iM}}=\frac{TD\cdot\cos\theta-\frac{\overline{n}_1}{\overline{n}_2}\cos\delta}{TD\cdot\cos\theta+\frac{\overline{n}_1}{\overline{n}_2}\cos\delta} \tag{3-23}$$

Then the reflectivity of the thermal wave can be defined as the ratio of the reflected energy to the incident energy

$$\rho_{\lambda r}=\frac{Q_r}{Q_i}=\frac{q_{rM}}{q_{iM}} \tag{3-24a}$$

therefore

$$\rho_{\lambda r}=\frac{TD\cdot\cos\theta-\frac{\overline{n}_1}{\overline{n}_2}\cos\delta}{TD\cdot\cos\theta+\frac{\overline{n}_1}{\overline{n}_2}\cos\delta} \tag{3-24b}$$

This is the reflectivity of a single wavelength thermal wave. If the thermal wave is normal to the interface ($\theta = \delta = 0$, one-dimensional wave), then the above equation can be simplified to

$$\rho_{\lambda r}=\frac{TD-\frac{\overline{n}_1}{\overline{n}_2}}{TD+\frac{\overline{n}_1}{\overline{n}_2}} \tag{3-25}$$

Equation (3-24) is the general formula for reflectivity of a single wavelength thermal wave. Tzou (1993) also developed a similar equation for the reflection at an interface of two materials with the same relaxation time. However, he did not discuss the reflection processes presented by Eq. (3-25) in detail, for example, the physical meaning of positive and negative reflectivity given by Eq. (3-25). For one-dimensional heat conduction, Eq. (3-25) should be used to calculate the reflectivity of a single wavelength thermal wave. In engineering, the reflection of a thermal wave at the boundaries of the materials is also very important. The most often encountered boundary is the convective boundary at which convective heat transfer takes place. Assume that the convection heat transfer coefficient is h, then the heat transfer at the boundary is

$$q_{\lambda t} = hT_{\lambda t} \tag{3-26}$$

For an adiabatic boundary, the convective heat transfer coefficient h is zero. Similar to the derivation of reflectivity in the previous section, we can obtain the reflectivity for a convective boundary condition as follows:

$$\rho_{\lambda r} = \frac{1-h\dfrac{\overline{n}}{C\rho c_p}}{1+h\dfrac{\overline{n}}{C\rho c_p}} = \frac{1-Bi\cdot\Gamma^{1/2}\overline{n}}{1+Bi\cdot\Gamma^{1/2}\overline{n}}, \quad Bi = \frac{hL}{K}, \ \Gamma = \frac{\alpha\tau}{L^2} \tag{3-27}$$

If we define TD_B as

$$TD_B = \frac{h}{C\rho c_p} = Bi\cdot\Gamma^{1/2} \tag{3-28}$$

where the subscript B denotes boundary. Then Eq. (3-27) can be rewritten as

$$\rho_{\lambda r} = \frac{1-\overline{n}\cdot TD_B}{1+\overline{n}\cdot TD_B} \tag{3-29}$$

The reflectivities given by Eqs. (3-25) and (3-29) are complex. This is because the incident wave (Eqs. (3-12a,d)) is a complex thermal wave. However, in practical applications, thermal waves are always real, and therefore, the reflectivity is real. We need

to define the real reflectivity which can be used to calculate the reflection of a real thermal wave. The complex incident wave and reflected wave are written as

$$q_{\lambda i} = (q_{iR} + iq_{iI})e^{i\omega(t-\frac{n_1}{C}x)}, \quad q_{\lambda r} = (q_{rR} + iq_{rI})e^{i\omega(t+\frac{n_1}{C}x)} \tag{3-30}$$

Then a real thermal wave can be superposed by the following thermal wave of a single wavelength using a Fourier transform

$$\mathrm{Re}(q_{\lambda i}) = q_{iR}\cos(\omega t - \omega\frac{n_1}{C_1}x) - q_{iI}\sin(\omega t - \omega\frac{n_1}{C_1}x)\exp(-\omega\frac{k_1}{C_1}x) \tag{3-31}$$

The magnitudes q_{iR} and q_{iI} are two arbitrary real constants for the given frequency. Similar to the incident wave, the reflected wave is

$$\mathrm{Re}(q_{\lambda r}) = q_{rR}\cos(\omega t + \omega\frac{n_1}{C_1}x) - q_{rI}\sin(\omega t + \omega\frac{n_1}{C_1}x)\exp(\omega\frac{k_1}{C_1}x) \tag{3-32}$$

Then at the interface (x=0), from Eq. (3-24a), we have

$$\begin{aligned} q_{\lambda r} = \rho_{\lambda r} q_{\lambda i} &= \rho_R[q_{iR}\cos(\omega t) - q_{iI}\sin(\omega t)] - \rho_I[q_{iR}\sin(\omega t) + q_{iI}\cos(\omega t)] \\ &+ i\rho_R[q_{iR}\sin(\omega t) + q_{iI}\cos(\omega t)] + i\rho_I[q_{iR}\cos(\omega t) - q_{iI}\sin(\omega t)] \end{aligned} \tag{3-33}$$

where
$$\rho_{\lambda r} = \rho_R + i\rho_I = \frac{TD - (\hat{n} - i\hat{k})}{TD - (\hat{n} - i\hat{k})} \tag{3-34}$$

and

$$\hat{n} = \frac{n_1 n_2 + k_1 k_2}{n_2^2 + k_2^2}, \text{ and } \hat{k} = \frac{k_1 n_2 - n_1 k_2}{n_2^2 + k_2^2} \tag{3-35}$$

we can solve for ρ_R and ρ_I as

$$\rho_R = \frac{TD^2 - \hat{n}^2 - \hat{k}^2}{(TD + \hat{n})^2 + \hat{k}^2}, \text{ and } \rho_I = \frac{2TD\cdot\hat{k}}{(TD + \hat{n})^2 + \hat{k}^2} \tag{3-36}$$

The real parts of the incident and reflected waves at the interface x = 0 are

$$\begin{aligned} \mathrm{Re}(q_{\lambda i}) &= [q_{iR}\cos(\omega t) - q_{iI}\sin(\omega t)] \\ \mathrm{Re}(q_{\lambda r}) &= \rho_R[q_{iR}\cos(\omega t) - q_{iI}\sin(\omega t)] - \rho_I[q_{iR}\sin(\omega t) + q_{iI}\cos(\omega t)] \end{aligned} \tag{3-37}$$

Therefore, the real reflectivity for the real thermal wave is

$$\hat{\rho}_\lambda = \frac{\mathrm{Re}(q_{\lambda r})}{\mathrm{Re}(q_{\lambda i})} = \rho_R - \rho_I \frac{[q_{iI}\cos(\omega t) + q_{iR}\sin(\omega t)]}{[q_{iR}\cos(\omega t) - q_{iI}\sin(\omega t)]} \tag{3-38}$$

If we introduce

$$\tan(\psi) = \frac{q_{iI}}{q_{iR}} \tag{3-39}$$

then we have

$$\hat{\rho}_\lambda = \rho_R - \rho_I \tan(\omega t + \psi) \tag{3-40}$$

This equation shows that the reflectivity of a real thermal wave is time dependent. When q_{iI} is zero, the incident thermal wave is a cosine wave, and Eq. (3-40) is

$$\hat{\rho}_\lambda = \rho_R - \rho_I \tan(\omega t) \tag{3-41}$$

When q_{iR} is zero, the incident wave is a sine wave, and Eq. (3-40) becomes

$$\hat{\rho}_\lambda = \rho_R - \rho_I \tan(\omega t + \pi/2) \tag{3-42}$$

The total reflectivity can be defined as the ratio of the reflected energy for all wavelengths to the incident energy for all wavelengths

$$\tilde{\rho} = \frac{\int_0^\infty \mathrm{Re}(q_{\lambda r})d\lambda}{\int_0^\infty \mathrm{Re}(q_{\lambda i})d\lambda} = \frac{\int_0^\infty \hat{\rho}_\lambda \mathrm{Re}(q_{\lambda i})d\lambda}{\int_0^\infty \mathrm{Re}(q_{\lambda i})d\lambda} \tag{3-43}$$

This is the general equation for calculating the reflectivity of a given thermal wave. There are several special cases for which the above equation can be simplified.

(1). Reflectivity of a step change thermal wave.

A step change thermal wave is the wave of which the temperature and heat flux have a step change at the front of the wave as shown in Fig. 3-3. For such a wave, the frequency is infinite at the wave front, and very small behind the wave front. Therefore, we have $\bar{n} = n - ik = 1$ at the wave front. From Eqs. (3-35), (3-36), (3-40) and (3-43) we have

$$\tilde{\rho} = \hat{\rho}_\lambda = \frac{TD-1}{TD+1} \tag{3-44}$$

where TD is defined by Eq. (3-22).

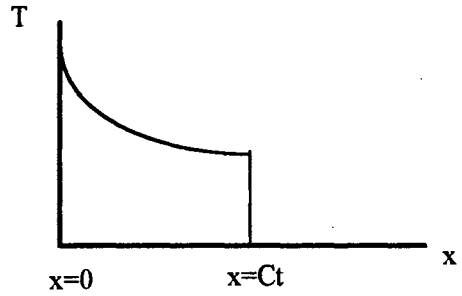

Fig. 3-3 Step Change Thermal Wave

(2). Two materials have the same relaxation time.

If two materials have the same relaxation time, then their refractive indexes and the extinction coefficients are also the same, as shown by Eqs. (3-7) and (3-8). So we have the following relationships from Eqs. (3-35) and (3-36)

$$\rho_R = \frac{TD-1}{TD+1} \quad \text{and} \quad \rho_I = 0 \tag{3-45}$$

Therefore, from Eqs. (3-40) and (3-43), the reflectivity can be derived as

$$\tilde{\rho} = \frac{TD-1}{TD+1} \tag{3-46}$$

(3). Time-averaged reflectivity for thermal waves with high frequency.

Since the thermal wave is usually important for heat conduction with high frequency temperature and heat flux changes (Chester, 1963), the reflectivity for this case will be more practical for engineering application than the reflectivity given by Eq. (3-40). From Eq. (3-40) we notice that the reflectivity is time dependent. However, the time-averaged reflectivity

$$\hat{\rho}_{\lambda m} = \lim_{t\to\infty} \frac{1}{t} \int_0^t \hat{\rho}_\lambda(t')dt' = \rho_R \tag{3-47}$$

is not a function of time. Because only the high frequency thermal waves contribute to reflection, while the low frequency waves are diffusive and they do not contribute to reflection, the above equation can be written as

$$\hat{\rho}_{\lambda m} = \frac{TD-1}{TD+1} \tag{3-48}$$

We substitute this reflectivity into Eq. (3-43), then we obtain

$$\tilde{\rho}_m = \frac{TD-1}{TD+1} \tag{3-49}$$

Therefore, this equation is independent of time and can be used to predict the reflectivity for most types of thermal wave reflection.

For convective boundaries, combining Eq. (3-47) with Eqs. (3-29), and (3-43), we can obtain

$$\tilde{\rho}_m = \frac{1-TD_B}{1+TD_B} \tag{3-50}$$

where TD_B is defined by Eq. (3-28).

From Eqs. (3-49) and (3-50), we find that the reflectivity can be negative when TD < 1 for media interfaces and when $TD_B > 1$ for convective boundaries. The explanation of this very significant phenomena will be given by the numerical study of the wave propagation process in Chapter VI.

CHAPTER IV

TWO-DIMENSIONAL HYPERBOLIC THERMAL WAVES

Two-dimensional thermal waves are much more complicated than one-dimensional thermal waves because of the interaction and multi-dimensional reflection as well as transmission of such waves. In this chapter, we will discuss the theory for two-dimensional thermal waves.

4.1 Thermal Wave Equations

The energy conservation equation and the hyperbolic model for multi-dimensional heat conduction are given as

$$\rho c_p \frac{\partial T}{\partial t} + \nabla \cdot \vec{q} = 0 \tag{4-1}$$

$$\vec{q} + \tau \frac{\partial \vec{q}}{\partial t} = -K \nabla T \tag{4-2}$$

From the above equations, we can derive the following wave equations for temperature and heat flux

$$\tau \frac{\partial^2 T}{\partial t^2} + \frac{\partial T}{\partial t} = \nabla(\alpha \nabla T) \tag{4-3}$$

$$\tau \frac{\partial^2 \vec{q}}{\partial t^2} + \frac{\partial \vec{q}}{\partial t} = \alpha \nabla^2 \vec{q} + \nabla \times (\nabla \times \vec{q}) \tag{4-4}$$

and

$$\nabla \times \vec{q} + \tau \frac{\partial}{\partial t}(\nabla \times \vec{q}) = 0 \tag{4-5}$$

where $\nabla^2 (= \nabla \cdot \nabla)$ is the Laplace operator. From Eq. (4-5), the curl of the heat flux can be solved as an exponential function of time $\nabla \times \vec{q} = (\nabla \times \vec{q})_{t=0} e^{-t/\tau}$. Therefore, it will be zero if it is initially zero. This means that temperature is the potential function of heat flux, and

heat transfer is parallel to the gradient of temperature. However, $\nabla \times \bar{q}$ does not have to be initially zero, at least mathematically. Physically, this can happen in a very short time period at the beginning of heat transfer because of the delay between formation of a temperature gradient and the response of heat transfer due to the relaxation time. However, heat flux finally will be in the direction of temperature since the curl of heat flux will decay quickly according to Eq. (4-5). If the curl of the heat flux is initially zero, Eq. (4-4) can also be written as

$$\tau \frac{\partial^2 \bar{q}}{\partial t^2} + \frac{\partial \bar{q}}{\partial t} = \alpha \nabla^2 \bar{q} \tag{4-6}$$

So Eqs. (4-3) and (4-6) are the wave equations for multi-dimensional thermal waves. The heat flux and temperature are not independent of each other. Actually, the heat flux is an induced wave of temperature. A two-dimensional harmonic wave of a given frequency can be written as

$$T = T_M \exp\left[i\omega(t - \frac{\bar{n}_x}{C}x - \frac{\bar{n}_y}{C}y) \right] \tag{4-7}$$

where $\bar{n}_x$ and $\bar{n}_y$ are the refractive indexes along x and y coordinates. They satisfy the following equation

$$\bar{n}_x^2 + \bar{n}_y^2 = \bar{n}^2 \tag{4-8}$$

The heat fluxes along the x and y coordinates are obtained from Eqs. (4-2) and (4-7)

$$q_x = \frac{\bar{n}_x}{\bar{n}^2} \rho c_p C T_M \exp\left[i\omega(t - \frac{\bar{n}_x x}{C} - \frac{\bar{n}_y y}{C}) \right] \tag{4-9}$$

and

$$q_y = \frac{\bar{n}_y}{\bar{n}^2} \rho c_p C T_M \exp\left[i\omega(t - \frac{\bar{n}_x x}{C} - \frac{\bar{n}_y y}{C}) \right] \tag{4-10}$$

where, subscript x represents the x component and y represents the y component.

Assume that the amplitude of the heat flux wave is q_M, then we obtain from the above equations the relationship between the amplitude of heat flux and the amplitude of temperature

$$q_{Mx} = \frac{\bar{n}_x}{\bar{n}} \frac{C\rho c_p}{\bar{n}} T_M \tag{4-11}$$

$$q_{My} = \frac{\bar{n}_y}{\bar{n}} \frac{C\rho c_p}{\bar{n}} T_M \tag{4-12}$$

and

$$\|\vec{q}_M\| = \frac{C\rho c_p}{\bar{n}} T_M \tag{4-13}$$

where $\| \ \|$ represents the magnitude of a vector. We introduce an angle ε which is defined as

$$\tan\varepsilon = \frac{\bar{n}_y}{\bar{n}_x} \tag{4-14}$$

This angle can be real or complex. When it is a real angle, the wave is called a homogeneous wave because the plane of its constant amplitude is parallel to the plane of its constant phase. When the angle is a complex angle, the wave is inhomogeneous and the plane of its constant amplitude is not parallel to the plane of its constant phase. A homogeneous wave can become an inhomogeneous wave and vise versa. Inhomogeneous thermal waves will be discussed in the following section.

4.2 Reflection and Transmission of a Two-Dimensional Thermal Wave

In section 3.2 we have derived the reflection of a plane thermal wave striking an interface at angle θ. We obtained two important relationships Eqs. (3-18) and (3-24). From Eq. (3-18)

$$\sin\theta = \sin\varphi = \frac{\bar{n}_2}{\bar{n}_1} \frac{C_1}{C_2} \sin\delta \tag{3-18}$$

we find that the transmission angle δ is always a complex angle because the refractive indexes are complex. Therefore, this angle is not the angle along which a real thermal wave propagates. Because the transmission angle is complex, the transmitted thermal wave is an inhomogeneous thermal wave. The transmitted thermal wave can be written as

$$\bar{q}_t = \bar{q}_{Mt} \exp\left[i\omega(t - \frac{\bar{n}_2}{C_2} x\cos\delta - \frac{\bar{n}_1}{C_1} y\sin\theta) \right] \tag{4-15}$$

From Eqs. (3-6), (3-18), and (3-35), we can derive

$$\cos\delta = \left[1 - (\hat{n}^2 - \hat{k}^2)\left(\frac{C_2}{C_1}\right)^2 \sin^2\theta + i2\hat{n}\hat{k}\left(\frac{C_2}{C_1}\right)^2 \sin^2\theta \right]^{1/2} \tag{4-16}$$

where $\hat{n}$ and $\hat{k}$ are given by Eq. (3-35). Now we introduce a angle ϕ which is defined by

$$\tan(2\phi) = \left(\frac{C_2}{C_1}\right)^2 \frac{2\hat{n}\hat{k}\sin^2\theta}{\left[1 - (\hat{n}^2 - \hat{k}^2)\left(\frac{C_2}{C_1}\right)^2 \sin^2\theta\right]} \tag{4-17}$$

Then we can obtain

$$\cos\delta = |\eta|^{1/2} e^{i\phi} = |\eta|^{1/2}\left[\cos\phi + i\sin\phi\right] \tag{4-18}$$

where η is

$$\eta^2 = \left[1 - (\hat{n}^2 - \hat{k}^2)\left(\frac{C_2}{C_1}\right)^2 \sin^2\theta \right]^2 + \left[2\hat{n}\hat{k}\left(\frac{C_2}{C_1}\right)^2 \sin^2\theta \right]^2 \tag{4-19}$$

Using Eq. (4-18), it can be shown that

$$\begin{aligned} &\frac{\bar{n}_2}{C_2} x\cos\delta + \frac{\bar{n}_1}{C_1} y\sin\theta \\ &= \frac{n_2\cos\phi + k_2\sin\phi}{C_2} |\eta|^{1/2} x + \frac{n_1}{C_1} y\sin\theta \\ &+ i\left[\frac{n_2\sin\phi - k_2\cos\phi}{C_2} |\eta|^{1/2} x - \frac{k_1}{C_1} y\sin\theta \right] \end{aligned} \tag{4-20}$$

Therefore, the transmitted thermal wave (Eq. (4-15)) has a constant amplitude plane and a constant phase plane, respectively

$$\frac{n_2 \sin\phi - k_2 \cos\phi}{C_2}|\eta|^{1/2} x - \frac{k_1}{C_1} y \sin\theta = \text{constant} \tag{4-21}$$

$$\frac{n_2 \cos\phi + k_2 \sin\phi}{C_2}|\eta|^{1/2} x + \frac{n_1}{C_1} y \sin\theta = \text{constant} \tag{4-22}$$

We can see that these planes are not parallel to each other. Therefore, the transmission thermal wave is an inhomogeneous wave. The thermal wave propagates along the direction normal to the constant phase plane. From Eq. (4-22), we can derive the actual or physical transmission angle as

$$\tan\delta_o = \frac{\frac{n_1}{C_1}\sin\theta}{\left[\frac{n_2\cos\phi + k_2\sin\phi}{C_2}|\eta|^{1/2}\right]} \tag{4-23}$$

Also from Eq. (4-23), we can write the refraction law in the form

$$\frac{\sin\delta_o}{\sin\theta} = \frac{\frac{n_1}{C_1}}{\sqrt{\left[\frac{n_2\cos\phi + k_2\sin\phi}{C_2}\right]^2 |\eta| + \left[\frac{n_1}{C_1}\sin\theta\right]^2}} \tag{4-24}$$

Note that this is not quite a "Snell-like law", since sinθ also appears in the right side of the equation. Comparing Eq. (4-24) with Eq. (3-18), we can introduce the effective refractive index of the second material defined as

$$n_2' = C_2\sqrt{\left[\frac{n_2\cos\phi + k_2\sin\phi}{C_2}\right]^2 |\eta| + \left[\frac{n_1}{C_1}\sin\theta\right]^2} \tag{4-25}$$

We can see from the above equation that the effective refractive index is dependent upon the physical properties of the two materials as well as the incident angle.

The reflectivity of a plane wave was given in the previous chapter Eq. (3-24b) as

$$\rho_{\lambda r} = \frac{TD\cdot\cos\theta - \frac{\bar{n}_1}{\bar{n}_2}\cos\delta}{TD\cdot\cos\theta + \frac{\bar{n}_1}{\bar{n}_2}\cos\delta} \tag{3-24b}$$

Similar to Eq. (3-36), this equation can be rearranged in the following form by using Eqs. (3-35) and (4-18)

$$\rho_{\lambda r} = \rho_R + i\rho_I \tag{4-26}$$

where

$$\rho_R = \frac{(TD\cos\theta)^2 - \tilde{n}^2 - \tilde{k}^2}{(TD\cos\theta + \tilde{n})^2 + \tilde{k}^2}, \quad \rho_I = \frac{2TD\cos\theta \cdot \tilde{k}}{(TD\cos\theta + \tilde{n})^2 + \tilde{k}^2} \tag{4-27}$$

and

$$\tilde{n} = |\eta|^{1/2}(\hat{n}\cos\phi + \hat{k}\sin\phi) \qquad \tilde{k} = |\eta|^{1/2}(\hat{k}\cos\phi - \hat{n}\sin\phi) \tag{4-28}$$

Then, similar to the development of Eqs. (3-30) to (3-40), a real incident thermal wave such as (see Eq. (3-31))

$$\mathrm{Re}(\bar{q}_{\lambda i}) = e^{-\omega\frac{k_1}{C_1}(x\cos\theta + y\sin\theta)}\left[\bar{q}_{iR}\cos[\omega\cdot t - \omega\frac{n_1}{C_1}(x\cos\theta + y\sin\theta)] - \bar{q}_{il}\sin[\omega\cdot t - \omega\frac{n_1}{C_1}(x\cos\theta + y\sin\theta)\right] \tag{4-29}$$

is reflected with a real reflectivity

$$\hat{\rho}_\lambda = \rho_R - \rho_I \tan(\omega\cdot t - \omega\tfrac{n_1}{C_1} y\sin\theta + \psi) \tag{4-30}$$

where

$$\tan\psi = \frac{|\bar{q}_{il}|}{|\bar{q}_{iR}|} \tag{4-31}$$

Equations (4-27)-(4-30) reduce to Eqs. (3-35)-(3-40) when the thermal wave is one-dimensional where $\theta = 0$.

From Eq. (4-30), we can see that the reflectivity of a real thermal wave is a function of time, the position on the interface and the incident angle. The reflectivity consists of two terms, the term ρ_R and term ρ_I. The reflected wave can be considered as the combination of two waves, one is the wave from the term ρ_R and the other wave is from the term ρ_I. Since the reflectivity is a function of time and frequency, the phase of the reflected wave is different from that of the incident wave. The term ρ_R represents the direct reflection of the incident thermal wave, the term ρ_I represents the "induction" of the incident thermal wave, this term contributes to the phase change of the reflected wave. The term "induction"

stands for the reflected wave from the term ρ_I. Because this wave is not the direction of the incident wave, it is a wave that is induced by the incident wave. When the wave frequency is very large, or the two materials have the same relaxation time, the term ρ_I disappears and the reflectivity is independent of time and location for one-dimensional reflection.

In order to discuss Eq. (4-30), let us consider an ideal plane wave and an interface of two materials. The extinction coefficient of the ideal incident wave is zero

$$\hat{n} = 1 \text{ and } \hat{k} = 0 \tag{4-32}$$

From Eq. (4-19), we obtain

$$\eta = 1 - \left(\frac{C_2}{C_1}\right)^2 \sin^2\theta \tag{4-33}$$

The angle ϕ now depends on η according to Eq. (4-17). There are two situations for the above equation:

(1) $0 < \eta < 1$. Since η is positive, from Eq. (4-17), we can see that the angle ϕ is zero, the transmission angle is real and it is found as (Eq. (4-18))

$$\cos\delta = \eta^{1/2} \tag{4-34}$$

In this case, the limits on $\sin\theta$ are from 0 to C_1/C_2 or to 1.0, whichever is smaller. Then, from Eqs. (4-26, 27, 28), we obtain the reflectivity which is independent of time and location on the interface

$$\hat{\rho}_\lambda = \frac{TD\cos\theta - \eta^{1/2}}{TD\cos\theta + \eta^{1/2}} = \frac{TD\cos\theta - \cos\delta}{TD\cos\theta + \cos\delta} \tag{4-35}$$

This equation shows that the reflectivity now is a function of TD, the incident angle, and the transmission angle. From Eqs. (4-33) and (4-35), the reflectivity is zero when TD is unity and the propagation speeds in the two materials are the same. However, this is not a

necessary condition for no reflection. When the incident angle satisfies the following equation

$$TD^2 \cos^2\theta = 1 - \left(\frac{C_2}{C_1}\right)^2 \sin^2\theta = \cos^2\delta \qquad (4\text{-}36)$$

the reflectivity will also be zero. This result is completely different from the one-dimensional thermal wave (Eq. (3-25) for which the reflectivity is a function of TD only. Equation (4-35) is plotted in Fig. 4-1. We can see from the figure that when $C_2 / C_1 < 1.0$, the reflectivity decreases with the increase of the incident angle. When $C_2 / C_1 > 1.0$, the reflectivity increases, and tends to unity with the increase of the incident angle. This is the so called total reflection phenomenon.

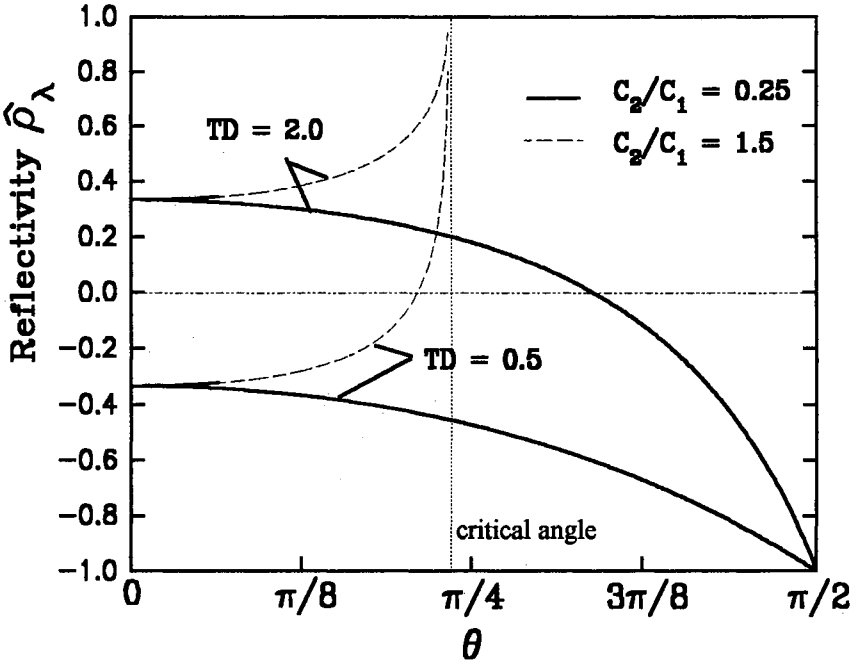

Fig. 4-1 Reflectivity as a Function of TD and θ ($\eta > 0$)

In Eq. (4-35), the parameter TD represents the comparison of heat conduction abilities of the two materials along the thermal wave propagation direction. In a one-dimensional situation, since the incident wave and the transmitted wave are always normal to the interface, therefore, the comparison of heat transfer abilities of the two materials is

based on TD alone. However, in a two-dimensional situation, the wave propagation speed normal to the interface depends on the actual wave propagation direction. For the incident wave, the propagation speed normal to the interface is $C_1\cos\theta$. For the transmitted wave, the speed normal to the interface is $C_2\cos\delta$. Therefore, in this case, the comparison in heat transfer of the two materials is

$$\frac{(\rho c_p)_1}{(\rho c_p)_2}\frac{C_1\cos\theta}{C_2\cos\delta} = TD\frac{\cos\theta}{\cos\delta} \tag{4-37}$$

When $C_2 < C_1$, the transmission angle (δ) is always real. As the incident angle is increased, Eq. (4-37) decreases, that means the heat transfer in material 2 becomes large compared to the heat transfer in material 1. For this reason, the reflectivity decreases with an increase in the incident angle, and tends to be negative when Eq. (4-37) is less than 1. This situation is similar to the situation of TD < 1 for one-dimensional heat transfer that is discussed in Chapter III.

When $C_2 > C_1$, the transmission angle δ increases quickly with an increase in the incident angle θ. This makes Eq. (4-37) increase. In this case, the heat transfer in material 2 becomes small compared to the heat transfer in material 2. Therefore, the energy from the incident wave is reflected, and the reflectivity increases with the increase of incident angle. When Eq. (4-37) is infinite ($\delta = \pi/2$), the reflectivity is 1, so the energy is totally reflected because in this case the heat transfer in material 2 normal to the interface is zero. Note that in this case, $\sin\theta$ is limited from 0 to C_1 / C_2 in order to keep the transmission angle real. Therefore, the dashed curves shown in Fig. 4-1 are only half of the whole story.

(2) $\eta < 0$. In this situation, $C_2 > C_1$, and $\sin\theta > C_1 / C_2$. From Eqs. (4-17, 18, 33, 34) we can see that the transmission angle now is a complex value, and $\phi = \pi/2$

$$\cos\delta = |\eta|^{1/2} i \tag{4-38}$$

The reflectivity derived from the Eqs. (4-27), (4-28), and (4-30) is

$$\rho_R = \frac{(TD\cos\theta)^2}{(TD\cos\theta+\tilde{n})^2+\tilde{k}^2}, \quad \text{and} \quad \rho_I = \frac{2TD\cos\theta\cdot\tilde{k}}{(TD\cos\theta+\tilde{n})^2+\tilde{k}^2} \tag{4-39}$$

where, from Eq. (4-28),

$$\tilde{n}=0 \ \text{ and } \ \tilde{k}=-|\eta|^{1/2} \tag{4-40}$$

$$\hat{\rho}_\lambda = \rho_R - \rho_I \tan(\omega\cdot t - \omega\tfrac{n_1}{C_1} y\sin\theta+\psi) \tag{4-41}$$

and where

$$\tan\psi = \frac{|\tilde{q}_{iI}|}{|\tilde{q}_{iR}|} \tag{4-42}$$

Now the reflectivity again is dependent upon time and location on the interface. It consists of two terms ρ_R and ρ_I. These two terms are shown in Fig. 4-2. This figure actually is the other half of the situation shown in Fig. 4-1 by the dashed curves. We see from the figure, ρ_R and ρ_I change very quickly in the region near the critical angle when TD is small (e.g. TD = 0.25). The total reflection is not very stable because of this resaon. A little shift of incident angle may cause a significant change in reflection. On the other hand, with the increase of incident angle, the term ρ_R decreases, and both ρ_R and ρ_I tend to zero with the increase of incident angle. Because of these two terms, the reflection in this situation consists of two waves, one is because of ρ_R, and the other is because of ρ_I. The first wave can be considered as the direct reflection of the incident wave. The second wave is not directly caused by the reflection of the incident wave, but caused by the transmitted wave component parallel to the interface. This wave works like an incident wave from material 2, and its reflection is similar to the previous situation of $\eta > 0$ discussed before. This is the reason that we call the second wave an induced wave. However, the transmitted wave that causes the second wave is related to the incident wave and the direct reflection of ρ_R. Therefore, this situation is complicated. We will present some numerical results to show the physical processes of two-dimensional reflection in Chapter VI.

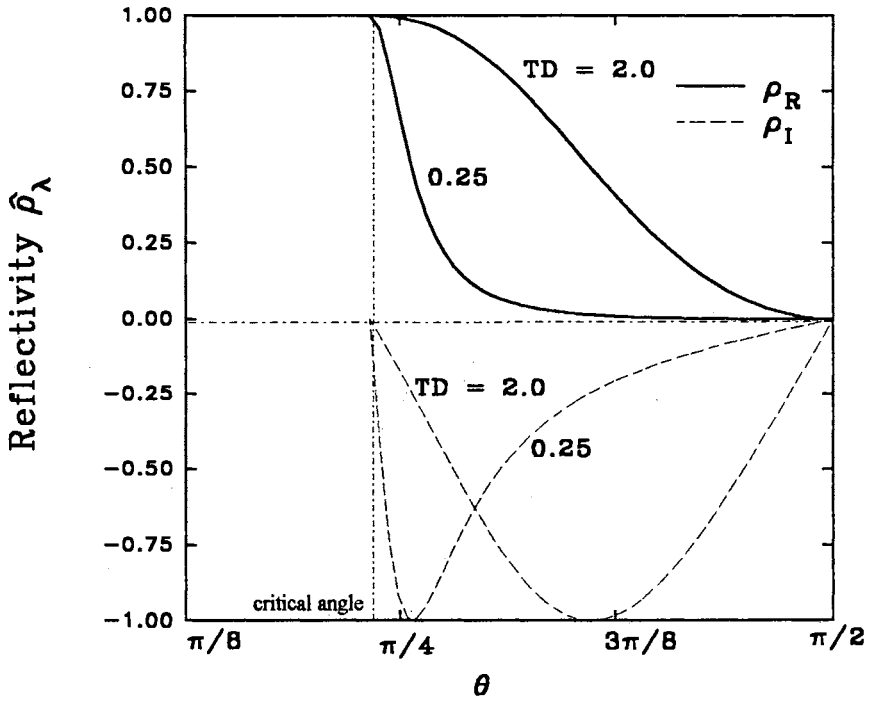

Fig. 4- 2 Reflectivity for $C_2/C_1 = 1.5$ and $\eta < 0$

4.3 Analysis of Wave Front

The analysis of the previous section is valid for an ideal plane wave. However, an ideal plane thermal wave actually does not exist in a two-dimensional heat conduction process because of the interaction of thermal waves. Therefore, the actual situation may not agree with the theory exactly.

As we have mentioned before, a thermal wave is actually composed of two waves; a temperature wave which represents the internal energy propagation, and a heat flux wave which represents the heat flow. These two waves exchange energy with each other during the propagation. At any point in a material, when the temperature at this point is stimulated by an incident thermal wave, there will be a spherical wave (if the material is three-dimensional) or a circular wave (if the material is two-dimensional) emitted by the material at that point. A plane wave is the composition of many spherical waves or circular waves.

Suppose, in a two-dimensional situation, that a plane wave strikes an interface at an angle θ. We are interested in the propagation of the wave fronts of the reflected wave and the transmitted wave. Since the incident wave is not normal to the interface, the front of the incident wave arrives at the interface at different times for different positions along the interface. When the incident thermal wave arrives at the interface, there will be two circular waves at the interface as shown in Fig. 4-3. One circular wave, which is the solid circle in the figure, propagates in material 1 with propagation speed C_1, and another, which is the dashed circle in the figure, propagates in material 2 with propagation speed C_2. Since the propagation speeds of these two waves are different, the diameters of the circles corresponding to the same center are different.

There are two different situations for the wave reflection process. One case is $C_1 > C_2$. In this case, we can see from Fig. 4-1 that there are obvious tangential lines for the two circular waves. In the figure, the solid tangential line represents the wave front of the reflected wave, and the dashed tangential line represents the wave front of the transmission wave. Therefore, the direction normal to these tangential lines are the directions of propagation for the reflected wave and the transmission wave. If we assume that the refractive indexes of the two materials are approximately unity, then from the geometric relation of the tangential lines, we can easily derive the relationship between the incident angle, the reflection angle and the transmission angle (see Eq. (3-18)).

$$\sin\theta = \sin\varphi = \frac{C_1}{C_2}\sin\delta \qquad (3\text{-}18)$$

Note that in this case, δ must be real (not complex). This equation agrees with the results derived in the previous section for the waves of very high frequency, e.g. the step change thermal wave.

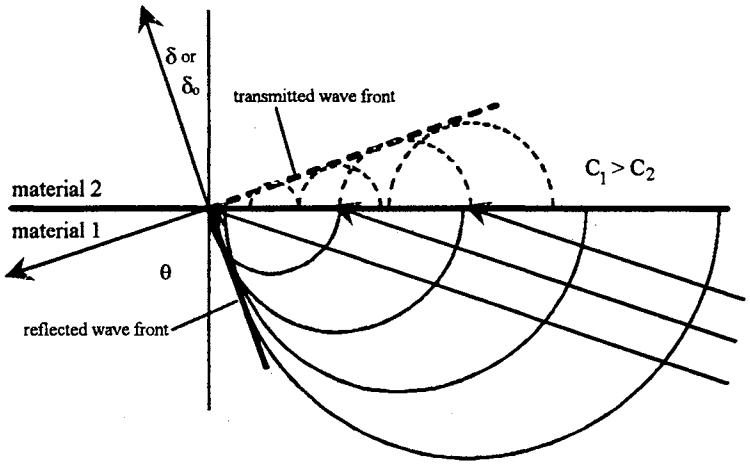

Fig. 4-3 Wave Fronts for $C_1 > C_2$

Another case is that the wave propagation speed of material 2 is larger than that of material 1. This situation is shown in Fig. 4-4. We can see from the figure that the wave fronts are completely different from the previous situation. Since $C_1 < C_2$, the circular wave in material 2 propagates faster than the waves in material 1.

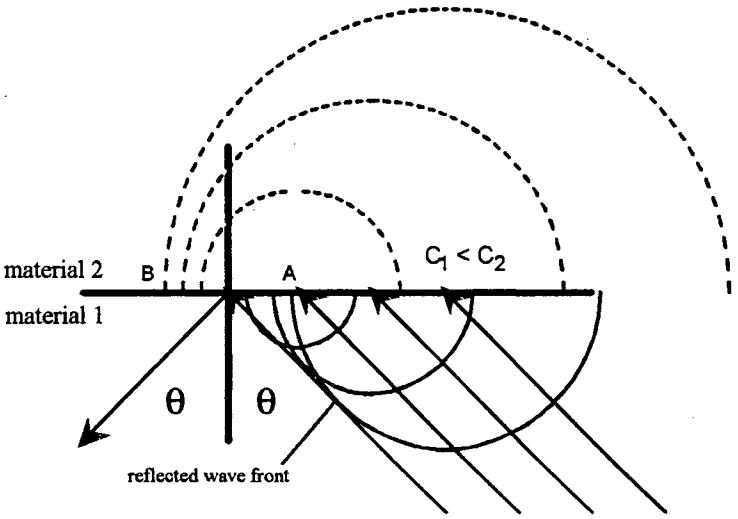

Fig. 4-4 Wave Fronts for $C_1 < C_2$

In material 2, the circular wave originating from point A arrives at point B before the incident wave arrives at this point because the transmitted wave has a larger propagation speed. Therefore, the transmitted wave emitted earlier by the interface will

affect the transmitted waves emitted later. On the other hand, the transmitted wave will also affect the wave pattern in material 1, actually producing an incident wave from material 2 to material 1. Because of this interaction, the wave front of the transmitted wave will diverge, and that means that there is not an obvious thermal wave front in material 2. The wave front which can be observed will be a circular wave front which is actually the wave front of the circular transmitted wave emitted at the earliest time. There is an obvious reflection wave front. However, in some situations, such as the incident angle being close to $\pi/2$, this wave front will not be obvious because of the interaction with the transmitted wave. According to the above two types of reflection, we can see that total reflection, which is true for electromagnetic waves, is not really true for thermal waves since in this case, there is still energy passing through the interface. Because of the interchange between internal energy and the heat flux, the reflection process in the case that $\sin\delta = \frac{C_2}{C_1}\sin\theta > 1$ is an interesting process. In this case, the angle δ is complex (not real), and δ_o is $\pi/2$. Unfortunately, this special situation cannot be easily illustrated by using numerical solution of the hyperbolic heat conduction equation. This is because the total reflection is very sensitive to the incident angle, and can be affected significantly by the interaction of waves.

CHAPTER V

NUMERICAL METHODS

Numerical methods for solving thermal wave phenomenon are very limited. Difficulties encountered in numerical solution are the numerical oscillations and the representation of sharp discontinuities with good resolution at the wave front. When the thermal wave is in a composite material, the discontinuity in the physical properties of the different components of the composite material also causes difficulties in numerical solution. Therefore, there is not a single method which is general for different problems.

Although there are many finite difference schemes available for one-dimensional thermal waves, most of them cannot be used for solving heat conduction problems in composite materials except the characteristic method. The reason for this is that the discontinuity in the physical properties at the interface between two materials cannot be handled by these methods. The characteristic method is the basic and the most accurate method.

There is only one method available for two-dimensional thermal waves, it is the characteristic-based TVD method (Yang, 1992). This method also cannot be used to solve thermal wave problems in composite materials for the same reason as that of the methods for one-dimensional problems (we will explain later). Therefore, in this research, we have developed a finite difference method which is applicable to one-, two- and three-dimensional thermal wave problems, either in homogeneous materials or in non-homogeneous materials.

5.1 Numerical Method for Solving One-Dimensional Thermal Waves

In the previous chapter, we have analyzed the reflectivity. To validate the theory, we will solve the thermal wave equation by using numerical methods. The method of

characteristics will be used in this study. This method has been proven accurate by Wiggert (1977). The governing equations of the thermal wave are

$$\tau_i \frac{\partial q}{\partial t} + q + K_i \frac{\partial T}{\partial x} = 0$$
$$(\rho c_p)_i \frac{\partial T}{\partial t} + \frac{\partial q}{\partial x} = 0 \tag{5-1}$$

where subscript i stands for different materials. Now we introduce the following variables

$$\hat{q} = \frac{q\tau}{(\rho c_p)_1 L},\ \bar{t} = \frac{t}{\tau},\ \bar{x} = \frac{x}{L},\ \tau = \sum_{i=1}^{2} \tau_i,\ \Gamma_i = \frac{\alpha_i \tau}{L^2},\ \gamma_i = \frac{\tau_i}{\tau} \tag{5-2}$$

where L is the reference length which can be the thickness of the composite material. Then Eq. (5-1) becomes

$$\gamma_1 \frac{\partial \hat{q}}{\partial \bar{t}} + \hat{q} + \Gamma_1 \frac{\partial T}{\partial \bar{x}} = 0$$
$$\frac{\partial T}{\partial \bar{t}} + \frac{\partial \hat{q}}{\partial \bar{x}} = 0 \tag{5-3a}$$

$$\gamma_2 \frac{\partial \hat{q}}{\partial \bar{t}} + \hat{q} + \Gamma_2 \beta \frac{\partial T}{\partial \bar{x}} = 0$$
$$\beta \frac{\partial T}{\partial \bar{t}} + \frac{\partial \hat{q}}{\partial \bar{x}} = 0 \tag{5-3b}$$

where $\beta = (\rho c_p)_2 / (\rho c_p)_1$ or the equation for material 1 can also be written as

$$\begin{bmatrix} \gamma_i & 0 \\ 0 & 1 \end{bmatrix} \begin{bmatrix} \hat{q} \\ T \end{bmatrix}_{\bar{t}} + \begin{bmatrix} 0 & \Gamma_i \\ 1 & 0 \end{bmatrix} \begin{bmatrix} \hat{q} \\ T \end{bmatrix}_{\bar{x}} + \begin{bmatrix} \hat{q} \\ 0 \end{bmatrix} = 0 \tag{5-4}$$

where, the subscripts $\bar{t}$ and $\bar{x}$ represent the derivative respect to time and coordinate $\bar{x}$. The eigenvalues are determined by

$$\det \begin{bmatrix} -\tilde{\lambda}\gamma_i & \Gamma_i \\ 1 & -\tilde{\lambda} \end{bmatrix} = 0,\ \tilde{\lambda} = \pm \left(\frac{\Gamma_i}{\gamma_i} \right)^{1/2} \tag{5-5}$$

Therefore, we have

$$d\bar{x} = \pm\left(\frac{\Gamma_1}{\gamma_1}\right)^{1/2} d\bar{t} \tag{5-6a}$$

Similarly, we can derive the relationship between $d\bar{x}$ and $d\bar{t}$ for material 2 as

$$d\bar{x} = \pm\left(\frac{\Gamma_2}{\gamma_2}\right)^{1/2} d\bar{t} \tag{5-6b}$$

Now the discrete grid is shown in Fig. 5-1

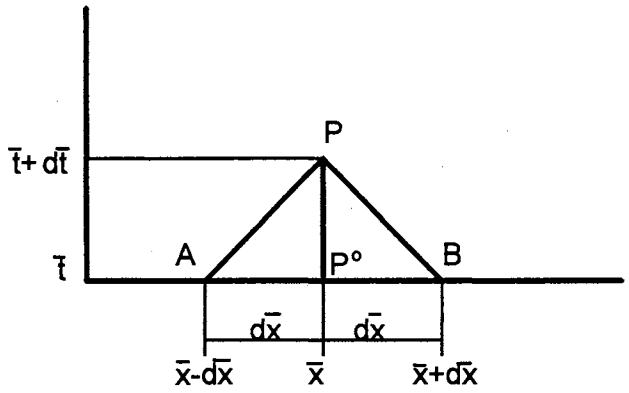

Fig. 5-1 The Grid System

Then Eq. (5-3) can be written as

$$\gamma_1 \frac{\partial \hat{q}}{\partial \bar{t}} \pm (\Gamma\gamma)_1^{1/2} \frac{\partial T}{\partial \bar{t}} + \hat{q} = 0 \tag{5-7a}$$

$$\gamma_2 \frac{\partial \hat{q}}{\partial \bar{t}} \pm (\Gamma\gamma)_2^{1/2} \beta \frac{\partial T}{\partial \bar{t}} + \hat{q} = 0 \tag{5-7b}$$

Performing the integration over $\bar{t}$ we have

$$\gamma_1(\hat{q}_P - \hat{q}_A) + (\Gamma\gamma)_1^{1/2}(T_P - T_A) + \frac{1}{2}(\hat{q}_A + \hat{q}_P)\Delta\bar{t} = 0 \tag{5-8a}$$

$$\gamma_1(\hat{q}_P - \hat{q}_B) - (\Gamma\gamma)_1^{1/2}(T_P - T_B) + \frac{1}{2}(\hat{q}_B + \hat{q}_P)\Delta\bar{t} = 0 \tag{5-8b}$$

for material 1, and

$$\gamma_2(\hat{q}_P - \hat{q}_A) + (\Gamma\gamma)_2^{1/2}\beta(T_P - T_A) + \frac{1}{2}(\hat{q}_A + \hat{q}_P)\Delta\bar{t} = 0 \tag{5-8c}$$

$$\gamma_2(\hat{q}_P - \hat{q}_B) - (\Gamma\gamma)_2^{1/2}\beta(T_P - T_B) + \frac{1}{2}(\hat{q}_B + \hat{q}_P)\Delta\bar{t} = 0 \tag{5-8d}$$

for material 2, where the time step and the discrete distance is chosen according to Eqs. (5-6). Notice that the discrete distance is different in different materials because of the differences in physical properties of the materials. The above equation causes difficulty when we use the characteristic method to solve for the thermal waves in composite materials. However, if the composite material is a two layer material, and we are only interested in the reflection of the thermal waves at the interface of the two layer, then we can set the thickness of one layer of the composite material according to Eqs. (5-6). From Eqs. (5-8), we can solve for the heat flux and temperature as

$$T_P = \frac{1}{2}[(T_A + T_B) + (\hat{q}_A - \hat{q}_B)\frac{\gamma_1 - 0.5\Delta\bar{t}}{(\Gamma\gamma)_1^{1/2}}] \tag{5-9a}$$

$$\hat{q}_P = \frac{(\hat{q}_A + \hat{q}_B)(\gamma_1 - 0.5\Delta\bar{t}) + (\Gamma\gamma)_1^{1/2}(T_A - T_B)}{2(\gamma_1 + 0.5\Delta\bar{t})} \tag{5-9b}$$

for material 1, and

$$T_P = \frac{1}{2}[(T_A + T_B) + (\hat{q}_A - \hat{q}_B)\frac{\gamma_2 - 0.5\Delta\bar{t}}{\beta(\Gamma\gamma)_2^{1/2}}] \tag{5-10a}$$

$$\hat{q}_P = \frac{(\hat{q}_A + \hat{q}_B)(\gamma_2 - 0.5\Delta\bar{t}) + \beta(\Gamma\gamma)_2^{1/2}(T_A - T_B)}{2(\gamma_2 + 0.5\Delta\bar{t})} \tag{5-10b}$$

for material 2. At the interface, from Eqs. (5-8a) and (5-8d), we obtain

$$\hat{q}_P = \frac{\left(\frac{\Gamma}{\gamma}\right)_1^{1/2}(T_A - T_B) + \left(1 - \frac{\Delta\bar{t}}{2\gamma_1}\right)\hat{q}_A + TD\left(1 - \frac{\Delta\bar{t}}{2\gamma_2}\right)\hat{q}_B}{\left(1 + \frac{\Delta\bar{t}}{2\gamma_1}\right) + \left(1 + \frac{\Delta\bar{t}}{2\gamma_2}\right)TD} \tag{5-11}$$

$$T_P = \frac{TD\left(1 + \frac{\Delta\bar{t}}{2\gamma_2}\right)T_A + \left(1 + \frac{\Delta\bar{t}}{2\gamma_1}\right)T_B + \left(\frac{\Gamma}{\gamma}\right)_1^{-1/2} TD\left[\hat{q}_A\left(1 - \frac{\Delta\bar{t}}{2\gamma_1}\right)\left(1 + \frac{\Delta\bar{t}}{2\gamma_2}\right) - \hat{q}_B\left(1 + \frac{\Delta\bar{t}}{2\gamma_1}\right)\left(1 - \frac{\Delta\bar{t}}{2\gamma_2}\right)\right]}{\left(1 + \frac{\Delta\bar{t}}{2\gamma_1}\right) + \left(1 + \frac{\Delta\bar{t}}{2\gamma_2}\right)TD} \tag{5-12}$$

where TD is given by Eq. (3-22).

The boundary conditions are derived from Eqs. (5-8). At $\bar{x} = 0$, we have $T_P = f(\bar{t})$; then we obtain the heat flux from Eq. (5-8b)

$$\hat{q}_P = \frac{\hat{q}_B\left(1 - \frac{\Delta\bar{t}}{2\gamma_1}\right) + \left(\frac{\Gamma}{\gamma}\right)_1^{1/2}(f(\bar{t}) - T_B)}{1 + \frac{\Delta\bar{t}}{2\gamma_1}} \tag{5-13}$$

At $\bar{x} = 1$, the heat flux is given as convective boundary condition $\hat{q}_p = hT_p$, so we have the temperature from Eq. (5-8c)

$$T_P = \frac{\beta\left(\frac{\Gamma}{\gamma}\right)_2^{1/2} T_A + \left(1 - \frac{\Delta\bar{t}}{2\gamma_2}\right)\hat{q}_A}{\beta\left(\frac{\Gamma}{\gamma}\right)_2^{1/2} + \beta\Gamma_2 Bi\left(1 + \frac{\Delta\bar{t}}{2\gamma_2}\right)} \tag{5-14}$$

where Γ is defined in Eq. (5-2), and β is the same as that after Eq. (5-3b).

Therefore, the thermal wave propagation can be simulated using the above equations. From the above discussion, we can see that the characteristic method is an implicit method. The temperature and heat flux at the current moment $(\bar{t}+d\bar{t})$ can be solved easily using to the values from the previous moment $\bar{t}$. The most important feature of this method is that it provides two implicit equations for determining the temperature and heat flux at the interface between two materials. These interface equations make it possible to apply this method to thermal wave problems in composite materials. However, since the time step $d\bar{t}$ and the space increment $d\bar{x}$ are related by Eqs. (5-6), we have to use different space increments for different materials in a composite material. It is impossible to satisfy Eqs. (5-6) if the thickness of the composite material is fixed. This is the reason that this method cannot be used for all kinds of problems. However, it is a good idea to combine this method with other methods which are only applicable to the heat conduction in homogeneous materials. For example, we can use the interface equations given by Eqs. (5-12) to solve for the temperature and heat flux at the interface, then use the other methods to solve for the temperature inside the substances of a composite material.

5.2 Numerical Method for Solving Two-Dimensional Thermal Waves

The numerical methods for solving two-dimensional thermal wave problems are based on the methods for one-dimensional thermal wave problems. We first introduce the TVD method, then will develop the control volume finite difference method.

5.2.1 TVD Method

Numerical study of two-dimensional hyperbolic heat conduction is very limited. The only study available is Yang's (1992) numerical solution for two-dimensional thermal shocks. In his study, the time-splitting technique was used to split a two-dimensional heat conduction problem into two one-dimensional heat conduction problems. The TVD (Total Variational Diminishing) method was then used to solve the finite difference equations. The same method is used in our study.

Two-dimensional hyperbolic heat conduction is described by the following governing equations

$$\begin{aligned} \rho c_p \frac{\partial T}{\partial t} + \nabla \cdot \vec{q} &= 0 \\ \tau \frac{\partial \vec{q}}{\partial t} + K\nabla T + \vec{q} &= 0 \end{aligned} \tag{5-15}$$

For two-dimensional processes, we can introduce the following vectors

$$\vec{F} = \begin{bmatrix} T \\ q_x \\ q_y \end{bmatrix} \quad \text{and} \quad \vec{S} = \begin{bmatrix} 0 \\ q_x \\ q_y \end{bmatrix} \tag{5-16}$$

where subscripts x and y represent the components in x and y directions. Then Eqs. (5-15) can be written as

$$[A]\frac{\partial \vec{F}}{\partial t} + [\tilde{B}]_x \frac{\partial \vec{F}}{\partial x} + [\tilde{B}]_y \frac{\partial \vec{F}}{\partial y} + \vec{S} = 0 \tag{5-17}$$

where

$$[A] = \begin{bmatrix} \rho c_p & 0 & 0 \\ 0 & \tau & 0 \\ 0 & 0 & \tau \end{bmatrix}, \quad [\tilde{B}]_x = \begin{bmatrix} 0 & 1 & 0 \\ K & 0 & 0 \\ 0 & 0 & 0 \end{bmatrix}, \quad [\tilde{B}]_y = \begin{bmatrix} 0 & 0 & 1 \\ 0 & 0 & 0 \\ K & 0 & 0 \end{bmatrix} \tag{5-18}$$

Now we define

$$[B]_x = [A]^{-1}[\tilde{B}]_x = \begin{bmatrix} 0 & 1/\rho c_p & 0 \\ K/\tau & 0 & 0 \\ 0 & 0 & 0 \end{bmatrix}, \quad [B]_y = [A]^{-1}[\tilde{B}]_y = \begin{bmatrix} 0 & 0 & 1/\rho c_p \\ 0 & 0 & 0 \\ K/\tau & 0 & 0 \end{bmatrix} \tag{5-19}$$

Then Eq. (5-17) can be written as

$$\frac{\partial \vec{F}}{\partial t}+[B]_x\frac{\partial \vec{F}}{\partial x}+[B]_y\frac{\partial \vec{F}}{\partial y}+\frac{1}{\tau}\vec{S}=0 \tag{5-20}$$

This is the governing equation that we will use for hyperbolic heat conduction.

To solve Eq. (5-20) numerically, we will first use the time-splitting method. The time step is split into two sub-steps, the first half step from t to t+dt, and the second step is from t+dt to t+2dt. The first step only estimates the change along the x axis, the second step estimates the change along the y-axis. So Eq. (5-20) can be split into two equations

$$\frac{\partial \vec{F}^*}{\partial t}+[B]_x\frac{\partial \vec{F}^o}{\partial x}+\frac{1}{\tau}\vec{S}^o=0 \tag{5-21}$$

and

$$\frac{\partial \vec{F}}{\partial t}+[B]_y\frac{\partial \vec{F}^*}{\partial y}+\frac{1}{\tau}\vec{S}^*=0 \tag{5-22}$$

where "o" represents the data at time t, "*" represents the data at time t+dt.

The eigen equation for Eq. (5-21) is

$$\left\{[B]_x-\tilde{\lambda}[I]\right\}[R]=0 \tag{5-23}$$

where [I] represents the unit matrix. Then the eigenvalues and eigenvectors are found as

$$\mathrm{diag}\left(\tilde{\lambda}\right)_x=\begin{bmatrix} C & 0 & 0\\ 0 & -C & 0\\ 0 & 0 & 0\end{bmatrix},\quad [R]_x=\begin{bmatrix} 1/C & -1/C & 0\\ \rho c_p & \rho c_p & 0\\ 0 & 0 & 1\end{bmatrix} \tag{5-24}$$

Thus Eq. (5-21) is written as

$$\frac{\partial \vec{F}^*}{\partial t}+[R]_x\,\mathrm{diag}\left(\tilde{\lambda}\right)_x[R]_x^{-1}\frac{\partial \vec{F}^o}{\partial x}+\frac{1}{\tau}\vec{S}^o=0 \tag{5-25}$$

We define

$$\vec{G}_x=2[R]_x^{-1}\vec{F}=\begin{bmatrix} CT+q_x/\rho c_p\\ -CT+q_x/\rho c_p\\ 2q_y\end{bmatrix},\ \textit{and}\ \vec{S}_x=2[R]_x^{-1}\vec{S}=\begin{bmatrix} q_x/\rho c_p\\ q_x/\rho c_p\\ 2q_y\end{bmatrix} \tag{5-26}$$

So Eq. (5-25) can be rearranged to become

$$\frac{\partial \bar{G}_x^*}{\partial t} + \mathrm{diag}\left(\tilde{\lambda}\right)_x \frac{\partial \bar{G}_x^o}{\partial x} + \frac{1}{\tau}\bar{S}_x^o = 0 \tag{5-27}$$

Similarly, we can get the following equation from Eq. (5-22)

$$\frac{\partial \bar{G}_y}{\partial t} + \mathrm{diag}\left(\tilde{\lambda}\right)_y \frac{\partial \bar{G}_y^*}{\partial y} + \frac{1}{\tau}\bar{S}_y^* = 0 \tag{5-28}$$

where

$$\bar{G}_y = 2[R]_y^{-1}\bar{F} = \begin{bmatrix} CT + {}^{q_y}/_{\rho c_p} \\ -CT + {}^{q_y}/_{\rho c_p} \\ 2q_x \end{bmatrix}, \text{ and } \bar{S}_y = 2[R]_y^{-1}\bar{S} = \begin{bmatrix} {}^{q_y}/_{\rho c_p} \\ {}^{q_y}/_{\rho c_p} \\ 2q_x \end{bmatrix} \tag{5-29a}$$

and

$$\mathrm{diag}\left(\tilde{\lambda}\right)_y = \begin{bmatrix} C & 0 & 0 \\ 0 & 0 & 0 \\ 0 & 0 & -C \end{bmatrix}, \quad [R]_y = \begin{bmatrix} {}^{1}/_{C} & 0 & {}^{-1}/_{C} \\ 0 & 1 & 0 \\ \rho c_p & 0 & \rho c_p \end{bmatrix} \tag{5-29b}$$

Now we will discuss the numerical method for solving Eq. (5-27). We will omit the subscript x and superscripts "*" and "o" in the following equations, and use superscripts n to represent current time, and n+1 to represent the next time step. The equation can be written as a finite difference equation

$$\bar{G}_i^{n+1} = \bar{G}_i^n - \frac{\Delta t}{\Delta x}(P_{i+1/2} - P_{i-1/2}) - \frac{\Delta t}{\tau}\bar{S}_i^n \tag{5-30}$$

The variable P here can be calculated by using the following method (Yang, 1992):

1. Upwind Scheme

$$P_{i+1/2}^{UP} = \frac{\tilde{\lambda}}{2}(\bar{G}_{i+1}^n + \bar{G}_i^n) - \frac{|\tilde{\lambda}|}{2}(\bar{G}_{i+1}^n - \bar{G}_i^n) \tag{5-31}$$

2. Lax-Wendroff Scheme

$$P_{i+1/2}^{LW} = \frac{\tilde{\lambda}}{2}(\bar{G}_{i+1}^n + \bar{G}_i^n) - \frac{\Delta t\tilde{\lambda}^2}{2\Delta x}(\bar{G}_{i+1}^n - \bar{G}_i^n) \tag{5-32}$$

3. TVD Scheme

$$P_{i+1/2}^{TVD} = P_{i+1/2}^{UP} + \chi(\varsigma)(P_{i+1/2}^{LW} - P_{i+1/2}^{UP})$$
$$\varsigma = \frac{\Delta_{i+1/2-\hat{\sigma}}}{\Delta_{i+1/2}}, \quad \text{and} \quad \hat{\sigma} = \text{sign}(\tilde{\lambda}) \tag{5-33}$$

where
$$\chi(\varsigma) = \max[0, \min(2\varsigma, 1), \min(\varsigma, 2)] \tag{5-34}$$

$$\Delta_{i+1/2} = \bar{G}_{i+1}^{n} - \bar{G}_{i}^{n} \tag{5-35}$$

Therefore, the temperature and heat flux can be solved using the above equations with an explicit time marching technique.

This method has been proven accurate for solving one- and two-dimensional thermal waves in homogeneous materials (Yang, 1990, 1992). However, it is difficult to use this method for solving thermal wave problems in non-homogeneous materials. The reason is that there are not interface equations, like Eqs. (5-12a,b) for the characteristic method, to describe the relationship between of temperature and heat flux at the interface. The interface equations given by the characteristic method cannot be used here because the increments in the x direction, dx, and in the y direction, dy, are both different for different materials. An idea to improve this method is to consider the variation of the physical properties in the equations in the aboved derived equations. However, the vector $\vec{G}$ will be discontinuous at the interface because of the discontinuity of the physical properties at the interface. This will cause other numerical problems such as oscillation. Therefore, we cannot use it to study the reflection of the thermal waves at the interface between two different materials.

5.2.2 Control Volume Finite Difference Method

Since the TVD method and the characteristic method cannot be used to solve the two-dimensional reflection process, we have developed the another method to meet our requirements. This alternate method, a control volume finite difference method, is described in this section.

The governing equations for two-dimensional hyperbolic heat conduction are

$$\rho c_p \frac{\partial T}{\partial t} + \frac{\partial q_x}{\partial x} + \frac{\partial q_y}{\partial y} = 0 \tag{5-36}$$

$$q_x + \tau \frac{\partial q_x}{\partial t} + K \frac{\partial T}{\partial x} = 0 \tag{5-37}$$

$$q_y + \tau \frac{\partial q_y}{\partial t} + K \frac{\partial T}{\partial y} = 0 \tag{5-38}$$

Taking the derivatives of Eqs. (5-37) and (5-38) with respect to x and y, respectively, we obtain

$$\frac{\partial q_x}{\partial x} + \tau \frac{\partial^2 q_x}{\partial t \partial x} + \frac{\partial}{\partial x}\left(K \frac{\partial T}{\partial x}\right) = 0 \tag{5-39}$$

$$\frac{\partial q_y}{\partial y} + \tau \frac{\partial^2 q_y}{\partial t \partial y} + \frac{\partial}{\partial y}\left(K \frac{\partial T}{\partial y}\right) = 0 \tag{5-40}$$

Substituting Eqs. (5-39) and (5-40) into Eq. (5-36), we obtain

$$\rho c_p \frac{\partial T}{\partial t} = \frac{\partial}{\partial x}\left(K \frac{\partial T}{\partial x}\right) + \frac{\partial}{\partial y}\left(K \frac{\partial T}{\partial y}\right) - \tau \frac{\partial^2 q_x}{\partial t \partial x} - \tau \frac{\partial^2 q_y}{\partial t \partial y} + S \tag{5-41}$$

To obtain the finite difference equations for numerical solution, we use the hybrid grid system as shown in Fig. 5-2.

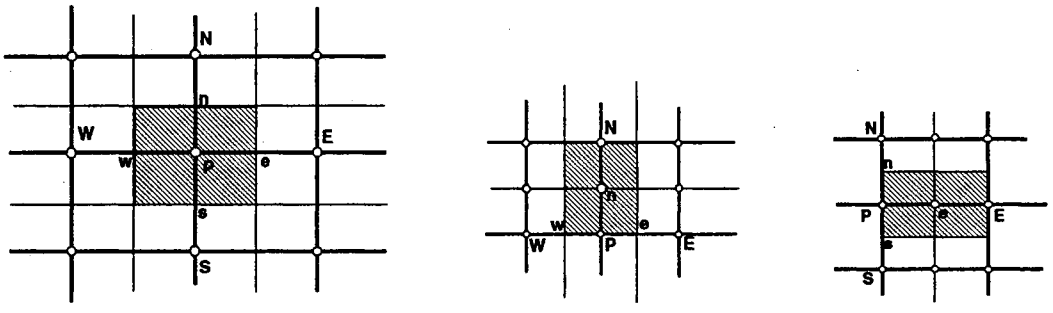

a. main grid for T b. grid for q_y c. grid for q_x

Fig. 5-2(a) The Hybrid Grid System for T and q

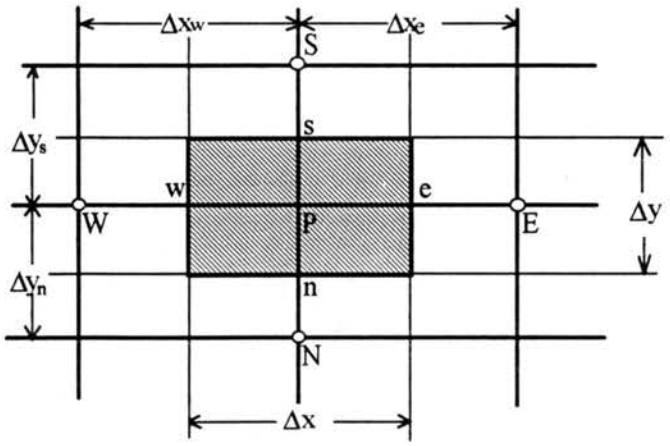

Fig. 5-2(b) The Geometric Definitions of the Grid System

If Eq. (5-41) is integrated over the control volume of the main grid, we can obtain the difference equation for T at the node P

$$\begin{aligned}\rho c_p(T_P - T_P^o)\Delta V = {} & \Delta y(\tau_e q_e - \tau_w q_w) + \Delta x(\tau_n q_n - \tau_s q_s) \\ & -\Delta y(\tau_e q_e^o - \tau_w q_w^o) + \Delta x(\tau_n q_n^o - \tau_s q_s^o) \\ & + \frac{K_e \Delta t}{\Delta x_e}\Delta y(T_E - T_P) - \frac{K_w \Delta t}{\Delta x_w}\Delta y(T_P - T_W) \\ & + \frac{K_n \Delta t}{\Delta y_n}\Delta x(T_N - T_P) - \frac{K_s \Delta t}{\Delta y_s}\Delta x(T_P - T_S) + S_P \Delta V \end{aligned} \tag{5-42}$$

where superscript o means the data at previous time step, and subscripts represent the data at the nodes corresponding to Figs. 5-2. Now we need the heat fluxes at the interfaces of the control volume ΔV (= ΔxΔy). The heat fluxes given by Eqs. (5-37) and (5-38) are integrated over the control volumes shown in Figs. 5-2 (b) and (c), yielding the finite difference equations for heat fluxes

$$(\xi q_n + \varsigma q_n^o)\Delta x \Delta y_n \Delta t + \tau_n \Delta x \Delta y_n (q_n - q_n^o) + K_n \Delta x \Delta t (T_N - T_P) = 0 \tag{5-43}$$

and

$$(\xi q_e + \varsigma q_e^o)\Delta y \Delta x_e \Delta t + \tau_e \Delta y \Delta x_e (q_e - q_e^o) + K_e \Delta y \Delta t (T_E - T_P) = 0 \tag{5-44}$$

where ξ and ζ are numerical parameters determining the implicit/explicit weighting.

$$0 < \xi < 1, \quad \varsigma = 1 - \xi \tag{5-45}$$

From Eqs. (5-43) and (5-44), we can obtain the heat fluxes at the interfaces e and n

$$q_e = \frac{\tau_e - \varsigma\Delta t}{\tau_e + \xi\Delta t} q_e^\circ + \frac{\Delta t K_e}{\Delta x_e(\tau_e + \xi\Delta t)}(T_P - T_E) \tag{5-46}$$

$$q_n = \frac{\tau_n - \varsigma\Delta t}{\tau_n + \xi\Delta t} q_n^\circ + \frac{\Delta t K_n}{\Delta y_n(\tau_n + \xi\Delta t)}(T_P - T_N) \tag{5-47}$$

Similarly, we can derive

$$q_w = \frac{\tau_w - \varsigma\Delta t}{\tau_w + \xi\Delta t} q_w^\circ + \frac{\Delta t K_w}{\Delta x_w(\tau_w + \xi\Delta t)}(T_W - T_P) \tag{5-48}$$

$$q_s = \frac{\tau_s - \varsigma\Delta t}{\tau_s + \xi\Delta t} q_s^\circ + \frac{\Delta t K_s}{\Delta y_s(\tau_s + \xi\Delta t)}(T_S - T_P) \tag{5-49}$$

If we substitute Eqs. (5-46)-(5-49) into Eq. (5-42), then we obtain the difference equation for temperature

$$A_P T_P = A_E T_E + A_W T_W + A_N T_N + A_S T_S + B_P \tag{5-50}$$

where

$$A_E = \frac{\Delta y \Delta t^2 K_e \xi}{\Delta x_e(\tau_e + \xi\Delta t)} \tag{5-51}$$

$$A_W = \frac{\Delta y \Delta t^2 K_W \xi}{\Delta x_w(\tau_w + \xi\Delta t)} \tag{5-52}$$

$$A_N = \frac{\Delta x \Delta t^2 K_n \xi}{\Delta y_n(\tau_n + \xi\Delta t)} \tag{5-53}$$

$$A_S = \frac{\Delta x \Delta t^2 K_S \xi}{\Delta y_s(\tau_s + \xi\Delta t)} \tag{5-54}$$

$$A_p = A_E + A_W + A_N + A_S + \rho c_P \Delta V \tag{5-55}$$

$$B_P = \rho c_p \Delta V T_P^\circ + \frac{\tau_p \Delta t \Delta y}{\tau_p + \xi\Delta t}(q_w^\circ - q_e^\circ) + \frac{\tau_p \Delta x \Delta t}{\tau_p + \xi\Delta t}(q_s^\circ - q_n^\circ) + S_P \Delta V \Delta t \tag{5-56}$$

Notice that the temperature is stored at the main grid nodes W, E, N, S, and P, and the heat fluxes are stored at the interface nodes w, e, n, and s. This is similar to one of the techniques used in computational fluid mechanics (Patankar, 1981).

This is an implicit-explicit-mixed scheme. If ξ is 1, then it is an implicit scheme; if ξ is zero, it is an explicit scheme. In most calculations, we will choose ξ to be 0.5. The scheme can be used to calculate parabolic heat conduction easily by setting the relaxation time τ to zero. This method is absolutely stable for $\xi = 0.5$. The boundary conditions can be specified by giving the temperature or heat flux. The grid at the boundary is shown in Fig. 5-3. The first node (main grid) has zero control volume.

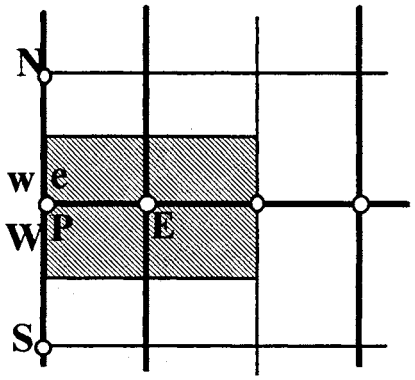

Fig. 5-3 The Boundary Grid and Control Volume

If the temperature at the boundary is given, then it can be directly used in Eq. (5-46). Once the temperature distribution is found, the heat flux can be updated by using Eqs. (5-46)-(5-49). If the heat flux is given, we can use the heat flux in Eqs. (5-37) and (5-38) directly. When we have solved for the temperature at the inner nodes, then the temperature at the boundary nodes can be found using Eqs. (5-46)-(5-49). This scheme can produce stable, non-oscillatory solutions. However, the wave front is not very sharp.

The finite difference scheme given above is stable and convergent. It has many advantages over the other methods:

1. The difference equation is the discretization of a conservation equation (5-36);

therefore, the numerical solution should be always conservative.

2. In addition to two-dimensional problems, the method can be easily used for one-dimensional and three-dimensional problems; and the finite difference equation keeps its basic form as in Eq. (5-55).
3. The effects of varying properties can be considered by using appropriate interpolation methods.
4. Since the scheme is partially implicit, the time step can be large as compared to the explicit scheme. For the explicit scheme, the time step should be very small to ensure the stability and convergency of the solution.

A numerical example is a one-dimensional heat conduction problem shown in Fig. 5-4. The initial conditions are given by

$$t = 0,\ T = T_o,\ and\ q = 0 \tag{5-57a}$$

where T_o is the initial temperature, it is set to be equal to 1.0 for our problem solved below. Two situations are considered, one situation is that the material is homogeneous, another situation is that the material is composed by two substances (see Fig. 5-4). The boundary conditions are given by

$$\begin{aligned} x &= 0 \quad T = 2.0 \\ x &= 1.0 \quad q = 0 \end{aligned} \tag{5-57b}$$

The wave speed in substance A is assumed to be 1, and in substance B it is assumed to be 0.5

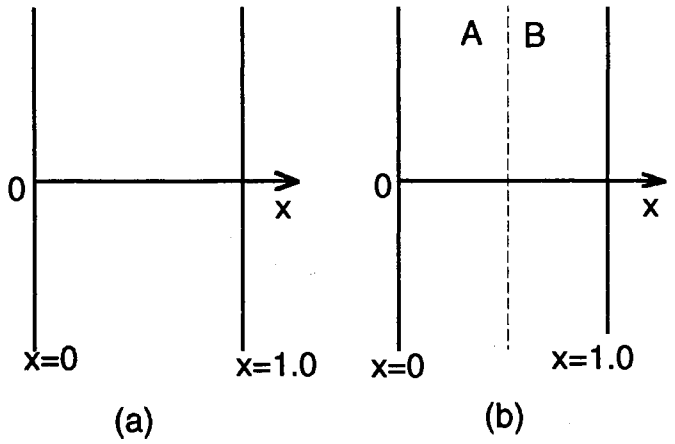

Fig. 5-4 One-Dimensional Example Problem

The comparison of the current method with the characteristic method is shown in Figs. 5-5a and 5-5b. Figure 5-5a shows the temperature waves with reflection and without reflection (i.e., with or without an interface at x = 0.5). Figure 5-5b shows the temperature at the interface as a function of time. From the figures, we can see that the current method can "catch" the wave front and the reflection. However, the wave front is not as sharp as that found by the characteristic method. In this calculation for Figs. 5-5a and b, we have used 100 grid nodes, and the relaxation times of two materials were set the same. We can increase the accuracy of the current method by increasing the grid number. The effect of grid number on the accuracy is shown in Fig. 5-6. It can be seen that the accuracy is improved when the grid number is larger and the time step is smaller. For different TDs and other x/x_0 and $\Delta t/\tau$ values, the accuracy can be improved by using the same technique.

In the next chapter, we will present the numerical solutions of both one-dimensional thermal waves and two-dimensional thermal waves. The numerical solutions for reflectivity will be compared to the closed form solutions of Chapters III and IV.

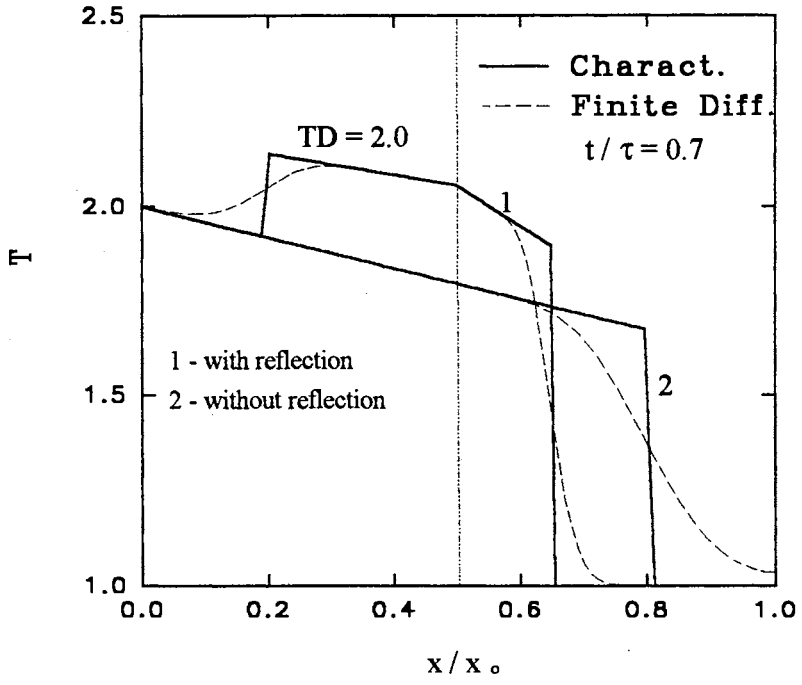

Fig. 5-5a Comparison of Current Method with Characteristic Method for a Composite Material

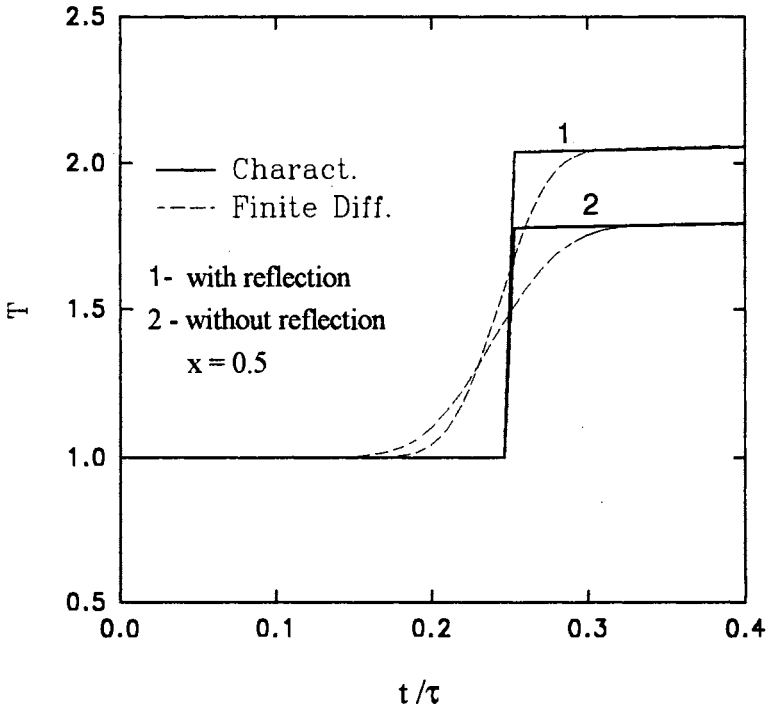

Fig. 5-5b Comparison of Current Method with Characteristic Method for a Homogeneous Material

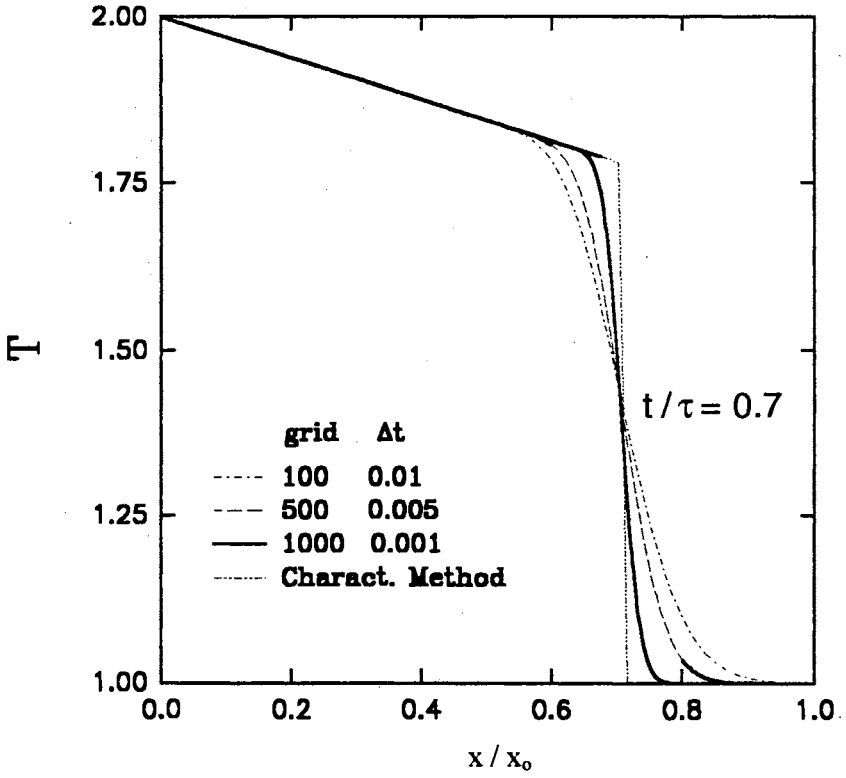

Fig. 5-6 The Effect of Grid Number on the Accuracy of Solution

CHAPTER VI

RESULTS OF HYPERBOLIC HEAT CONDUCTION

The reflectivity determined from the numerical solution of the thermal wave equations (in Chapter V) is compared with that obtained by theoretical formulas derived in previous chapters. The comparison is not only a verification of the theory, but also an explanation of the theory.

6.1 One-Dimensional Thermal Waves

The characteristics method has been used to get the numerical solutions discussed in this section. The grid number was 150, the time step was determined by Eqs. (5-6). First, we will consider thermal waves caused by a step change in temperature, then we will consider thermal waves caused by sinusoidally varying temperature.

6.1.1 Step Change Thermal Waves

The reflection of a step change thermal wave is given by Eq. (3-44). The comparison of numerical results of Chapter V with the theory is shown in Fig. 6-1. Since TD is related to the properties of the two materials, we have studied the effect of each property on the reflectivity. The reason for doing this is because the dimensionless parameter TD cannot be obtained naturally by normalizing the thermal wave equations. We can see that the numerical results which are given by the symbols agree exactly with the theory which is the solid line in the figure. The reflectivity is positive when TD is greater than unity. Therefore, part of energy will be reflected at the interface. The reflectivity is actually negative when the TD is less than unity. Because the transmissivity is

$$\tilde{\tau}_m = 1 - \tilde{\rho}_m$$

it is greater than unity in this case. This means that the energy passing through the interface is greater than the incident energy. From the fiugre 6-1, we can see that we can

change the value of TD by changing any one of the physical properties related to TD, and obtain the same result of reflectivity. TD is the only parameter to determine the reflectivity. Therefore, in the following discussion, we will not study the effect of each physical property on the reflectivity, but the effect of TD. This is similar to the Reynold's number in fluid dynamics, in that, we do not pay much attention on viscosity and velocity, but we concentrate on Reynold's number.

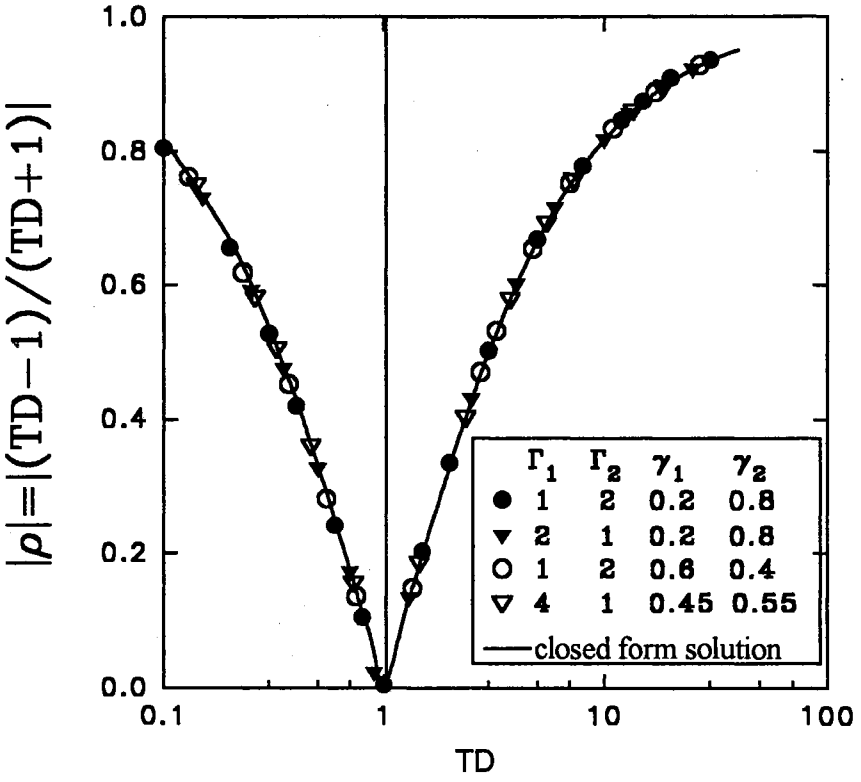

Fig. 6-1 The Reflectivity at an Interface Inside the Medium

The result shown in Fig. 6-1 raises a question when TD < 1 as to where the extra energy comes from. The parameter $C\rho c_p$ is a measure of the ability for the material to propagate the thermal wave. If the propagation speed C is zero, the material cannot transfer thermal energy, and it has no heat transfer ability . If ρc_p of the material is zero, there will be no temperature change because the material does not absorb any energy, therefore, heat transfer cannot take place in such a material. TD is a comparison of the

abilities of the two materials to transfer thermal energy. When TD is less than one, the second material has greater ability for heat transfer; therefore, to transfer a specified amount of thermal energy, the temperature gradient in the second material is smaller than that in the first material. For this reason, the temperature at the interface will not be as large as the value of the incident temperature wave after reflection. This means that the temperature of the first material is forced to decrease when the incident wave is reflected. Therefore, the material is forced to give up its internal energy to increase the heat transfer through the interface.

This process is shown in Figs. 6-2(a) and 6-2(b). In these figures, the temperature and heat flux distribution are presented at different times. Figure 6-2a is the temperature and heat flux distribution after the first reflection at the interface ($\bar{x} = 0.5$). The parameters Γ, γ, heat flux, and TD are defined in Eq. (5-2) and Eq. (3-22). In our solution, parameters Γ and γ are also set according to the chosen TD. This is because TD is an non-dimensional parameter which is only for the reflection at an interface. For either material A or material B, TD does not exist, therefore, we have to give parameters Γ and γ for both material A and material B. However, the reflection is affected by TD only. So as long as TD is given, the values of Γ and γ are not important. The temperature and heat flux are initially zero, and the temperature at the left boundary changes to unity suddenly at the begineering of the process. The right boundary is adiabatic, so heat flux at this boundary is always zero.

We can see from Fig. 6-2(a) that the actual temperature T is less than the temperature T_s which is the temperature before the reflection. The temperature decrease T_s - T is a reflected wave propagating backward to the left boundary. Because of the temperature decrease, the internal energy of material A has to be converted to heat transferred to material B. So the heat flux $\hat{q}$ is larger than the incident heat flux $\hat{q}_s$. From the figure, we can see that the energy passing through the interface is larger than the

incident energy. The energy increase comes from the decrease of internal energy in material A.

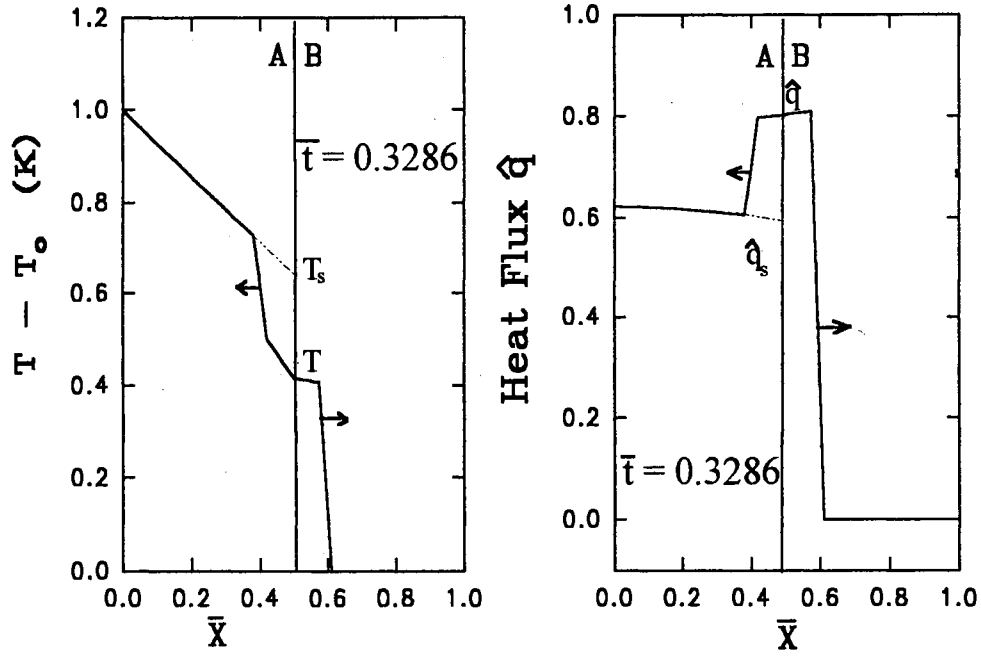

$\Gamma_1=1.0,\ \Gamma_2=2.0,\ \gamma_1=0.3,\ \gamma_2=0.7,\ TD=0.5$

Fig. 6-2(a) Thermal Wave for TD < 1.0 at $\bar{t}$ = 0.3286

Figure 6-2(b) shows the thermal wave propagation at different times in the medium. We can see that the waves are reflected many times by the interface and the boundaries. An interesting phenomenon shown in the figure is that the temperature inside the medium can be larger than the left boundary temperature, for example, the temperature shown by curve 3. However, there is no heat generation insider the medium. Does this conflict with the second law of thermodynamics? It seems not. Actually, the heat transfer is always along the direction of decreasing temperature gradient. Inside the medium, heat transfer is strongly irreversible. In the figure, the heat flux propagation directions shown by the arrows are not always the same as the heat transfer direction, sometimes they are opposite. Tzou (1993) discussed the entropy production of hyperbolic heat conduction

processes. He claimed that hyperbolic heat conduction satisfies the second law of thermodynamics. However, for the case that TD > 1.0, we still do not believe that the process can happen. A discussion of the entropy production is given in Appendix II. From the discussion, we will see that reflection is conditional. The process with TD > 1.0 cannot be true because it does not satisfy the second law of thermodynamics. Here, we will only discuss the reflection processes based on the energy conservation law.

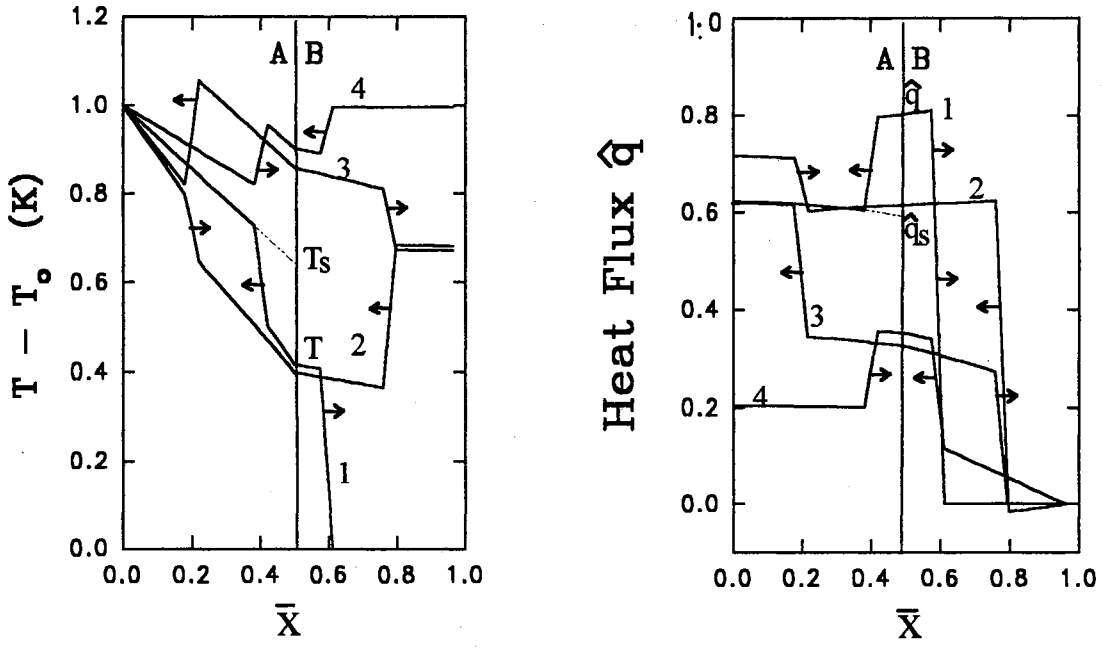

Fig. 6-2(b) Thermal Wave for TD < 1.0 at Different Times

The temperature and heat flux distribution for TD greater than unity are shown in Figs. 6-3(a). In this case, material B does not have the ability to transfer the total incident heat flux, so a larger temperature gradient is needed, and the temperature T at the interface is larger than the incident temperature T_S. Thus, material A has to absorb more

energy to increase its temperature, causing the heat transfer through the interface to decrease ($\hat{q} < \hat{q}_s$).

Comparing to the situation shown in Fig. 6-2(a), the reflectivity in this situation is positive. Because the reflected heat transfer is in the opposite direction of the incident heat transfer, the total heat transfer which is equal to the incident heat transfer plus the reflected heat flux (it is negative in this situation) will decrease. The temperature then increases because of less heat transfer. This is the physical mechanism shown in Fig. 6-3a.

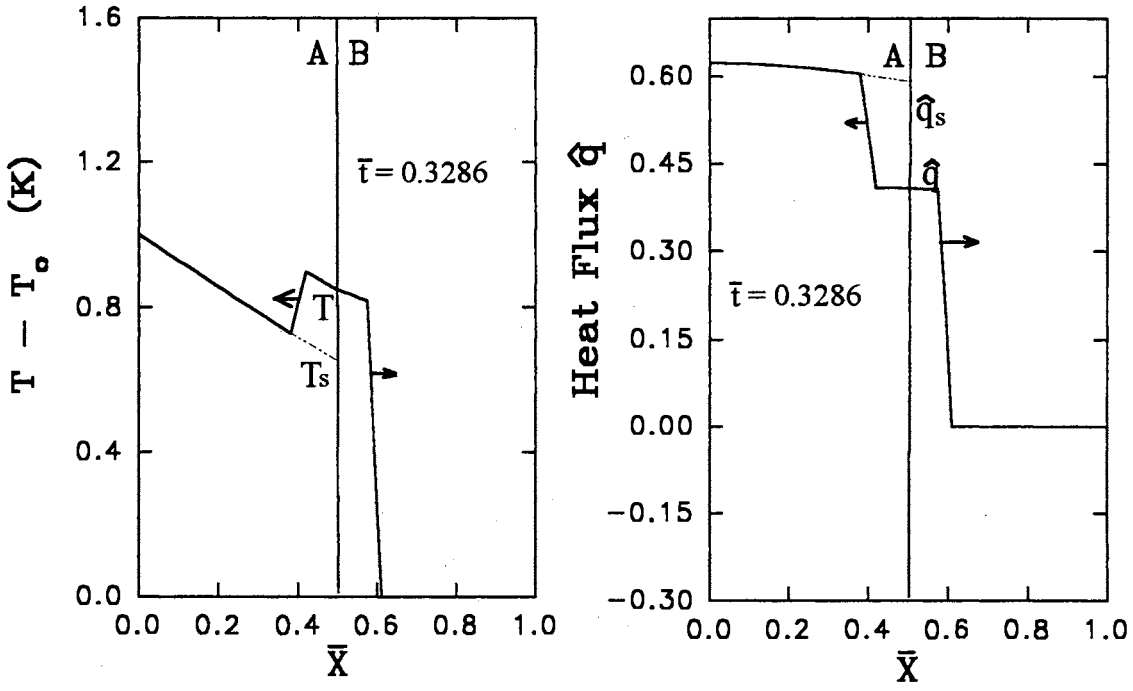

$\Gamma_1 = 1.0,\ \Gamma_2 = 2.0,\ \gamma_1 = 0.3,\ \gamma_2 = 0.7,\ \mathrm{TD} = 2.0$

Fig. 6-3(a) Thermal Wave for TD > 1.0 at $\bar{t}$ = 0.3286

Fig. 6-3(b) shows the wave propagation in the medium. In this figure, the waves are reflected by the interface and boundaries. As time increases, the magnitude of heat transfer decreases, and it will become zero when the process becomes steady. As we have discussed before, the heat transfer is always in the direction of decreasing temperature gradient, and it may not in the same direction as the wave propagation shown by the arrows in the figure. Curve 4 in Fig. 6-3(b) is an example. We can see that the

temperature shown by curve 4 increases in the region from $\bar{x} = 0$ to $\bar{x} = 0.4$. The corresponding heat transfer in this region is negative, although the wave front at $\bar{x} = 0.4$ is moving along the positive direction. So don't confuse the wave propagation direction with the heat transfer direction; they are not always (or necessarily) the same.

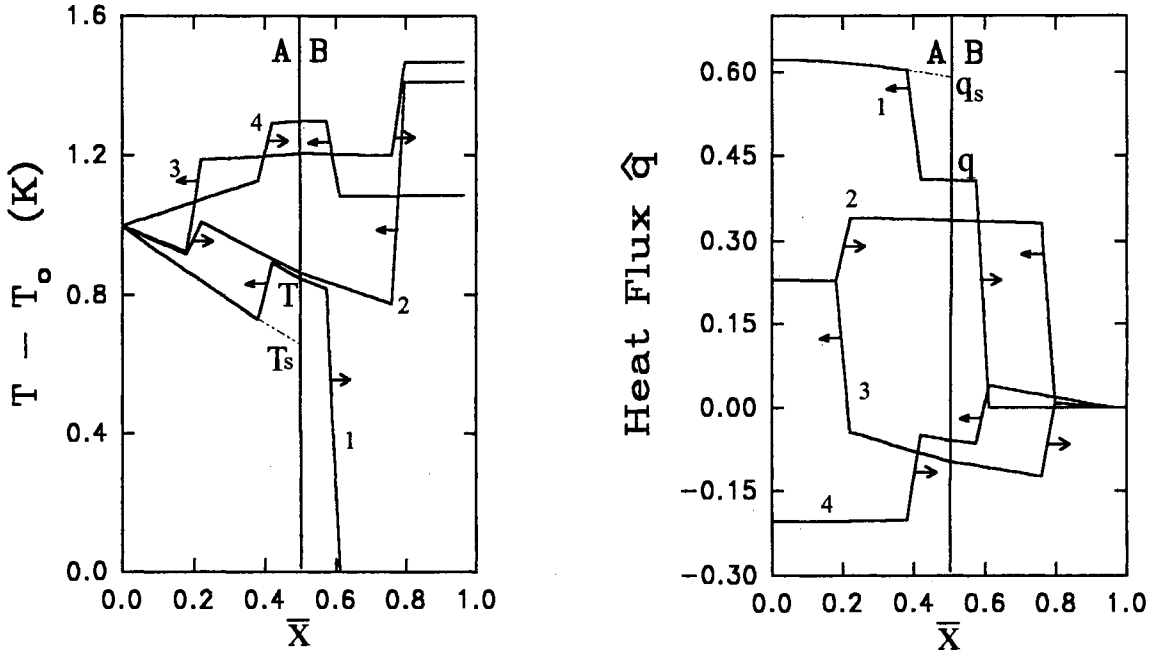

1 —— $\bar{t}$=0.3286, 2 —— $\bar{t}$=0.6573

3 —— $\bar{t}$=0.9858, 4 —— $\bar{t}$=1.3144

Γ_1=1.0, Γ_2=2.0, γ_1=0.3, γ_2=0.7, TD = 2.0

Fig. 6-3(b) Thermal Wave for TD > 1.0 at Different Times

From Figs. (6-2) and (6-3), we also find that reflectivity from material A to material B is different from the reflectivity from material B to material A. When an incident wave is from material A, the parameter is TD (it is 0.5 in Fig. 6-2a). However, when the same incident wave is from material B, now the parameter TD is the inverse of the previous TD (it will be 2.0 as shown in Fig. 6-3a). From Eq. (3-44), the reflectivity from B to A is the negative of the reflectivity from A to B.

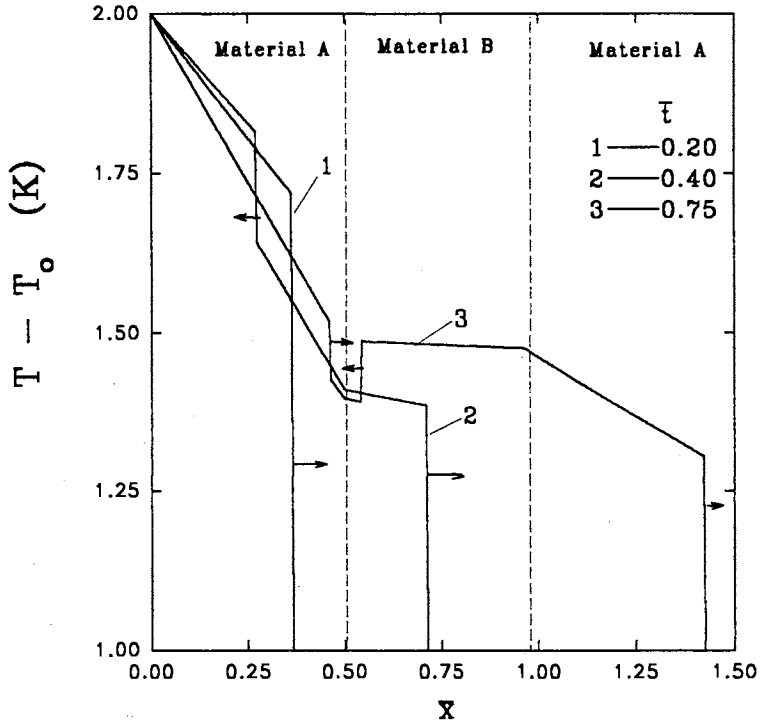

$\Gamma_1=1.0,\ \Gamma_2=2.0,\ \gamma_1=0.3,\ \gamma_2=0.7,\ TD_{A\text{-}B}=0.5$

Fig. 6-4 Wave Propagation in a Three-Layer Composite Medium

In Fig. 6-4, we show the wave propagation process in a three-layer composite material. In this case, there are two interfaces. The incident wave starts from the left boundary and propagates in the material. Curve 1 is the temperature distribution before the wave arrives at the first interface between material A and material B. Since parameter TD is 0.5 for this interface, after reflection, temperature decreases as we have discussed before. Curve 2 is the result after the reflection at the first interface. It is similar to the situation shown in Fig. 6-2a. Now the wave in material B is an incident wave for the interface between material B and material A, the second interface. For this interface, the parameter TD is the inverse of the parameter TD for the first interface; so it is 2.0 rather than 0.5. Since now the parameter TD for the second interface is larger than unity, the reflection will increase temperature as for the situation shown in Fig. 6-3a. Curve 3 in Fig. 6-4 is the temperature distribution after the reflection at the second interface.

The reflectivity of a step change thermal wave at a convective boundary is shown in Fig. 6-5. The theoretical results are solved by using Eq. (3-50). When $TD_B < 1.0$, the reflectivity is positive, and when $TD_B > 1.0$, the reflectivity is negative. The physical meaning of TD_B is similar to Bi, which represents the comparison of the heat transfer ability of the environment to the heat transfer ability of the material. So a negative reflectivity indicates that the heat transfer ability of the environment is larger than the heat transfer ability of the material. From the results, we conclude that the reflectivities given by Eqs. (3-49) and (3-50) are exact for the step change thermal waves. As we have seen, a significant difference between thermal waves and other kinds of waves, such as sound and electromagnetic waves, is that the reflectivity of a thermal wave can be negative. But the other kinds of waves always have positive reflectivity, even though the electromagnetic formulation has the same form for its one-dimensional wave equations as that of the thermal formulation.

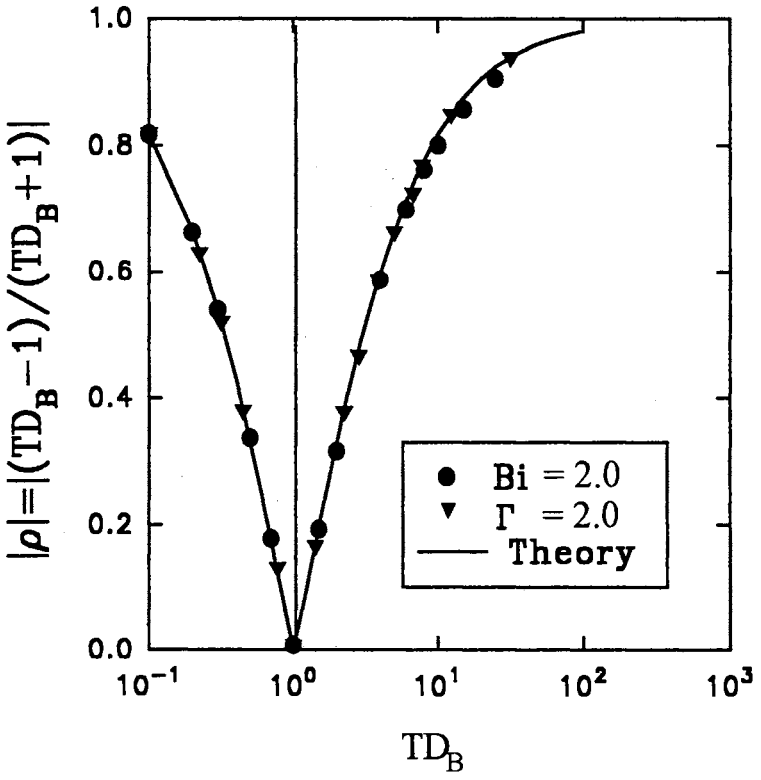

Fig. 6-5 Reflectivity of a Thermal Wave at a Convective Boundary

From thermal wave Eqs. (3-1) and (3-2), we know that a thermal wave consists of two energy waves: one is the internal energy and the other is the heat flux. Both waves are damping waves during propagation. The extinction of the internal energy contributes to the heat flow, and the extinction of the heat flow contributes to the internal energy. However, the total energy is conserved. Since the reflectivity is based only on the heat flow without considering internal energy, it is reasonable that thermal reflectivity can be negative in some cases, such as cases when TD < 1.0.

6.1.2 Monochromatic Thermal Wave

A monochromatic thermal wave is a wave of a single frequency or wavelength. Two types of monochromatic waves are discussed in this section. They are the sine wave and the cosine wave. The reflectivities of these waves are given by Eqs. (3-41) and (3-42). From these equations, we can see that the reflectivity consists of two parts. The first part is independent of time, and it can be calculated by

$$\rho_{\lambda R} = \frac{TD-1}{TD+1}$$

for large frequency. The second part is a tangent function of time. Numerical solution of the thermal wave equations demonstrates this fact.

The reflectivity of a cosine wave with frequency $\omega = 50$ is shown in Fig. 6-6(a). The top plot presents the numerical solutions of the reflectivities for different TDs, and the bottom plot is a closer view of the reflectivity for TD = 2.0. The theoretical results for reflectivity are also presented in the bottom plot. We can see that the numerical results agree with the theory very well. The reflectivity is zero when time is less than 0.42. This is because that the thermal wave has not reached the interface (x = 0.5) before time is 0.42; so during this time period, there is no reflection. When time is greater than 0.42, the reflectivities are time dependent. From the bottom plot, we can see that the reflectivity fluctuates around ρ_R (= 0.3333) which is a function of TD and independent of time (see

Eq. (3-40)). The fluctuating part is a tangent function of time. The peaks of the theoretical results in the figure do not tend to $\pm\infty$ periodically because the theoretical results were calculated according to the discrete time steps of the numerical solution, and these time steps are not continuous. Since the fluctuation is a periodic function of time, the average value of the fluctuation in the period is zero. We also found that there is an offset between the theoretical solution and the numerical solution. This is caused by the error of numerical solution. We found that the numerical solution is always one step ($\Delta\bar{t}$) ahead the theoretical solution. This may be caused by the boundary condition we set in the numerical solution. At $\bar{t}=0$, we set the left boundary temperature or heat flux to be the given conditions. However, it actually should be the conditions at $\bar{t}=\Delta\bar{t}$.

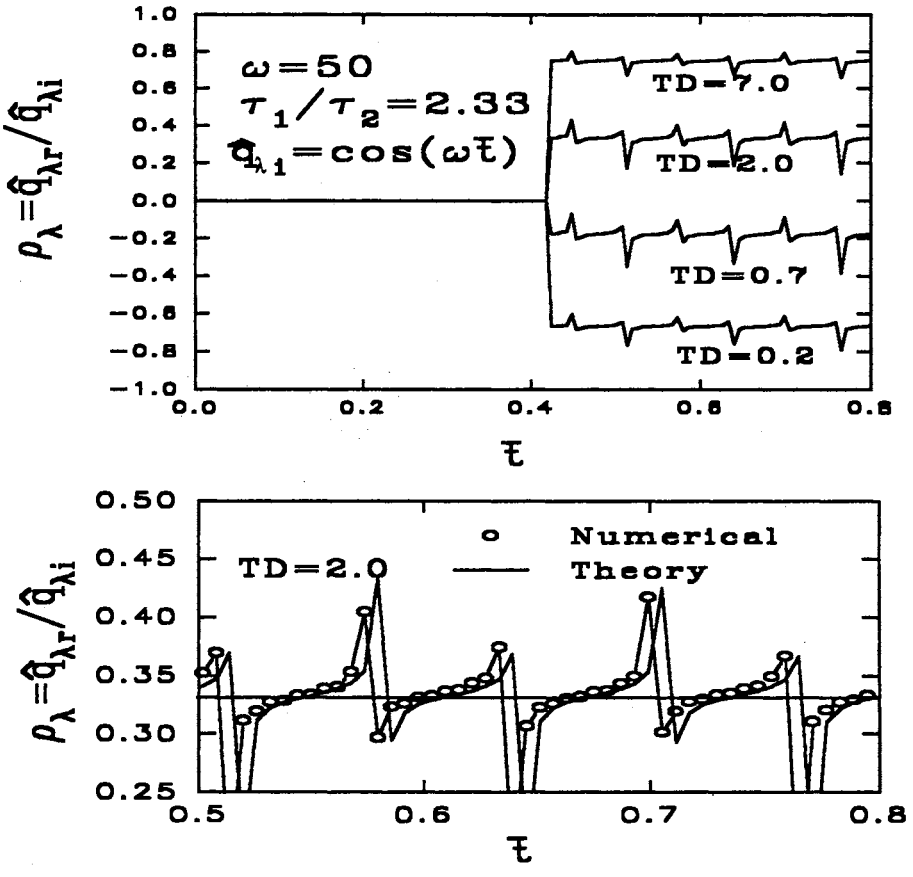

Fig. 6-6(a) Reflectivity of a Cosine Thermal Wave as a Function of Time ($\bar{x}=0.5$)

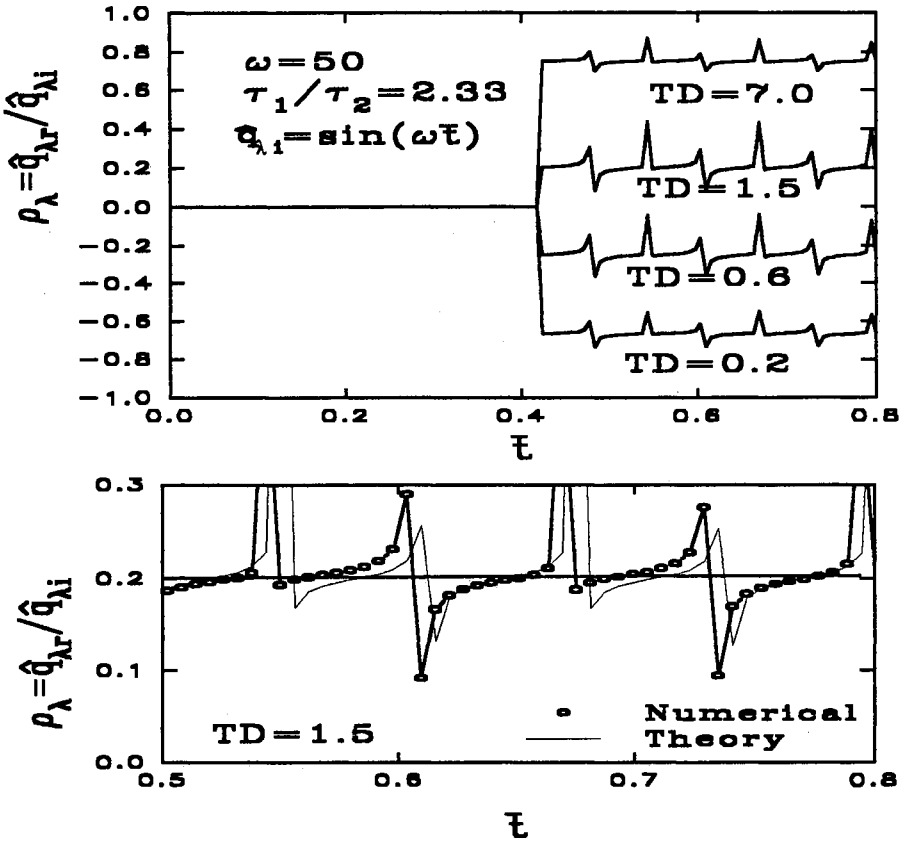

Fig. 6-6(b) Reflectivity of a Sine Thermal Wave as a Function of Time ($\bar{x}$ = 0.5)

The numerical results for the sine wave are presented in Fig. 6-6(b). Similar to the cosine wave, the reflectivity of a sine wave is also a function of time, and it has similar properties to those of the cosine wave. The difference between the reflectivities of the sine wave and the cosine wave is that their fluctuations are different in phase. According to the theory, this phase difference is $\pi/2$. The numerical results also show this fact.

In Fig. 6-7, we compare the reflectivities of the sine wave and the cosine wave for another set of parameters. From the figure, we can see that the fluctuations of the reflectivities of both sine and cosine waves are based on the same constant $\rho_{\lambda R}$ (=0.5). The phases of those fluctuations are different by $\pi/2$. This result agrees with the theoretical relationships from Eqs. (3-41) and (3-42) for the cosine wave and the sine wave.

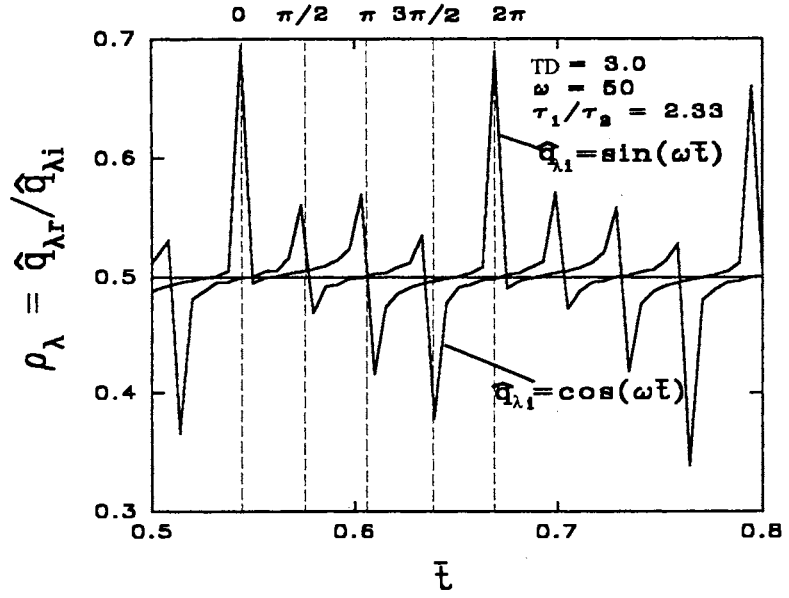

Fig. 6-7 Comparison of Reflectivities of the Sine Wave and Cosine Wave ($\bar{x} = 0.5$)

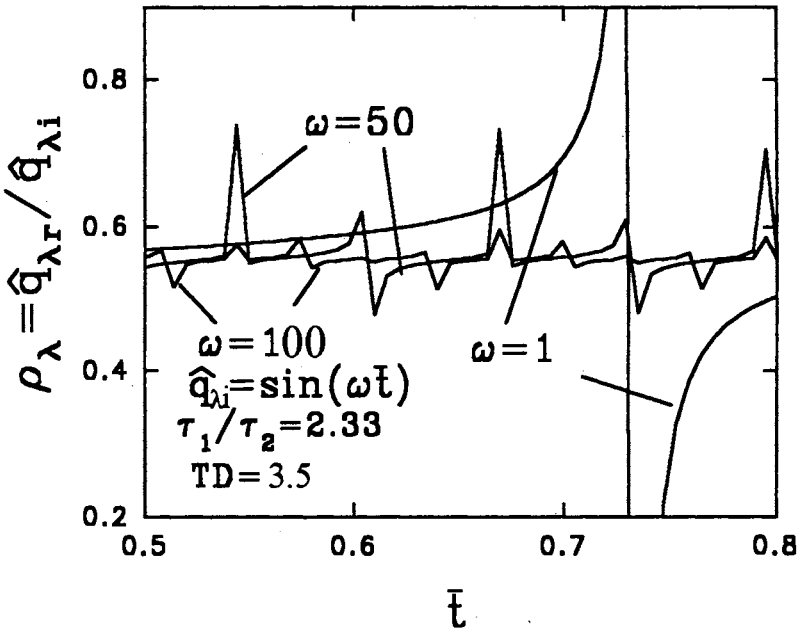

Fig. 6-8 Effect of Frequency on Reflectivity ($\bar{x} = 0.5$)

The effect of frequency on reflectivity is presented in Fig. 6-8 according to the numerical solution. From the figure, it is clearly shown that the larger the frequency, the shorter the period of fluctuation. This result also agrees with Eq. (3-42).

When the two materials have the same relaxation time, according to the theory presented Chapter III, the reflectivity is independent of time and can be calculated using Eq. (3-45). Verification of this is shown in Fig. 6-9. In this figure, the numerical solutions of the reflectivities of a sine wave and cosine wave are presented for two materials having the same relaxation time.

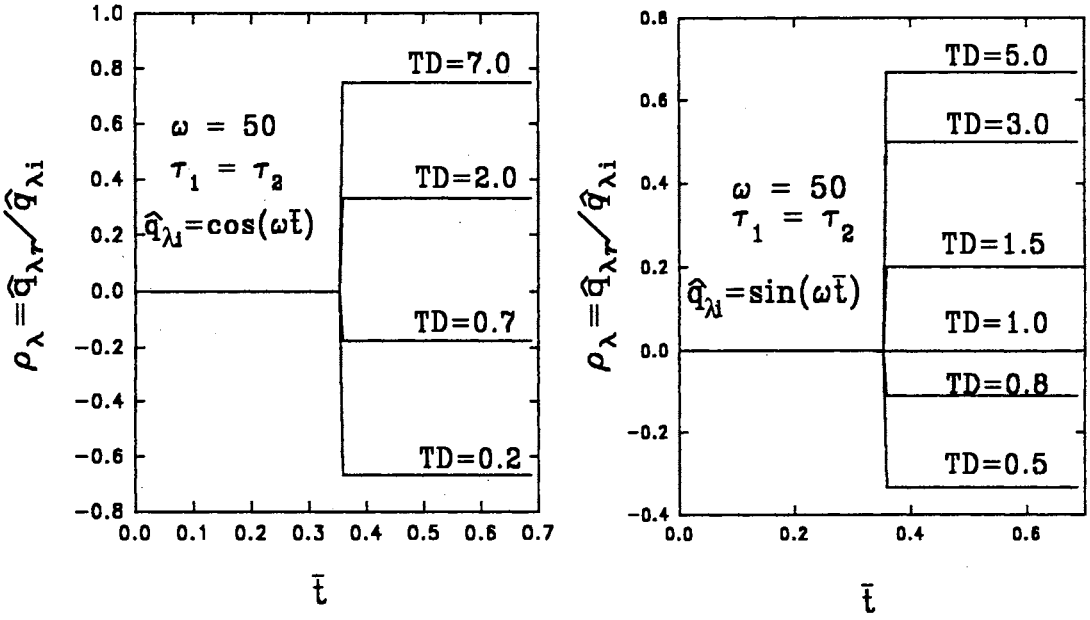

Fig. 6-9 Reflectivities of Sine and Cosine Waves for Two Materials Having the Same Relaxation Time ($\bar{x} = 0.5$)

The theoretical results according to Eq. (3-45) are also presented in the figure. However, the difference cannot be seen from the figure because the numerical results agree with the theoretical results very well (the error is less than 1%).

From the figure, we can see that the reflectivity is independent of time. It is only a function of TD and its value almost exactly agrees with Eq. (3-45). The fluctuations have disappeared. Frequency does not have effect on the reflectivity in this case. Since sine and cosine waves are the basic components which can be used to construct almost any kind of wave, the characteristics presented in Figs. 6-7 to 6-9 are common to any other kind of thermal wave.

6.2 Two-Dimensional Thermal Waves

Two-dimensional thermal waves are much more complicated than one-dimensional thermal waves because of the complex reflection, transmission and interaction. This section presents the numerical solution of two-dimensional thermal waves and comparison with the theory discussed in the Chapter IV. We will first look at thermal waves propagating in a homogeneous medium and then at thermal waves propagating in a two layer medium.

6.2.1 Two-Dimensional Wave Interaction

To show the complex interaction in two-dimensional wave propagation, we solved a heat conduction process in the two-dimensional material shown in Fig. 6-10 by using the TVD method. The boundary conditions are also shown in the figure. In the numerical solution, 100 × 100 grid nodes were used, and the dimensionless time step was 0.001.

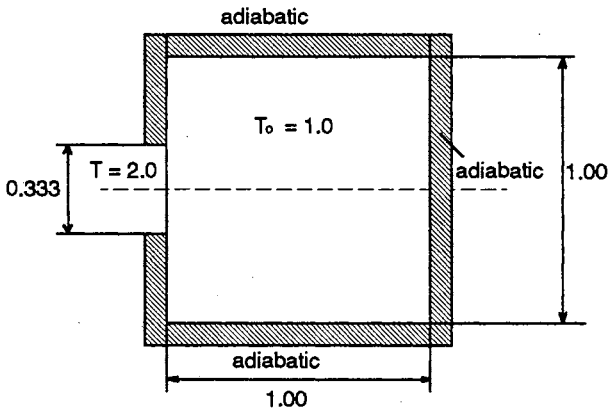

Fig. 6-10 Initial and Boundary Conditions for Two-Dimensional Hyperbolic Heat Conduction in a Rectangular Region

In Fig. 6-11, the two-dimensional temperature distribution and temperature contours with time are presented. The temperature difference between two adjacent contours is 0.025. From Fig. 6-11(a), we can see that the front of the thermal wave is a circularly shaped curve. Along the symmetric line y = 0.5, the wave front is relatively flat. This result shows that the thermal wave emitted from a certain point is a circular

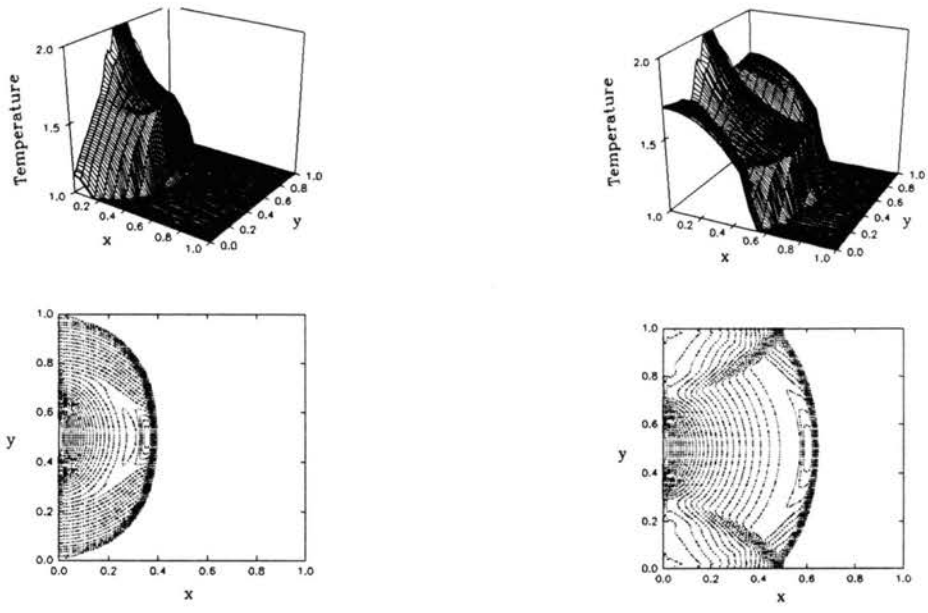

a. $\bar{t} = 0.188$ b. $\bar{t} = 0.313$

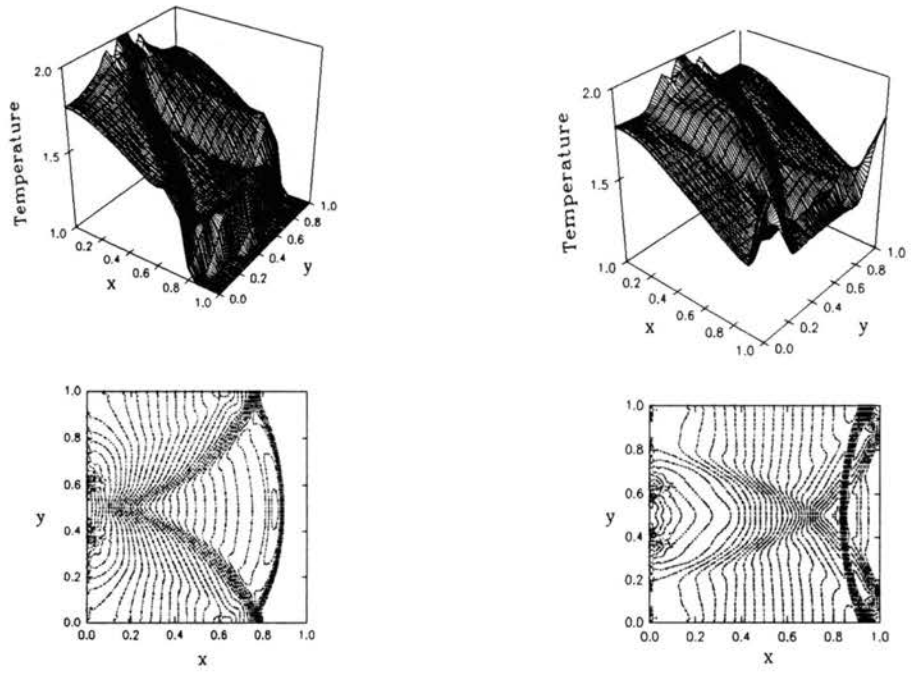

c. $\bar{t} = 0.438$ d. $\bar{t} = 0.562$

Fig. 6-11 Three-Dimensional Temperature Distribution and Temperature Contours

wave, and the plane wave is the composition of many circular waves emitted by each point on a constant temperature line. Figure 6-11(b) clearly shows the reflection of the thermal wave by the top and bottom sides. From the figure, we can see that the reflection angle is equal to the incident angle. This agrees with the theory. This fact is also shown by Fig. 6-11(c). The interaction of the incident wave and the waves reflected by the boundaries are shown in Fig. 6-11(d). From this figure, we can see that the waves reflected by the top and bottom boundaries cross each other, and they interact with the reflected wave from the right boundary.

6.2.2 Reflection and Transmission

It is difficult to calculate the reflection and transmission of two-dimensional thermal waves. First, the reflectivity in this case is much more complicated than that of one-dimensional thermal waves. It has been shown in Chapter IV that the reflectivity at an interface will be a function of both time and position. The formula for transmission angle (the real angle, Eq. (4-24)) is very complicated. Secondly, most of thermal waves in actual situations are not plane waves. The reflections from all of the boundaries and the interaction of waves make the actual thermal waves complex. Therefore, the theory presented in Chapter IV cannot handle such complicated waves. However, basic properties of reflection still can be shown by numerical solutions of two-dimensional thermal waves in some special situations. One example is two-dimensional heat conduction in a composite material shown in Fig. 6-12. The left boundary has a given uniform temperature which can be a constant or a sine function of time. Since the upper and the bottom boundaries are adiabatic, the thermal wave is one-dimensional before it arrives the interface of the two-materials. Although this is a good approximation of the heat conduction required by the theory in Chapter IV, it is still very rough because it is impossible to avoid the reflection from the top and bottom boundaries when the thermal wave strikes the interface. Therefore, the numerical results will not agree very well with the theory.

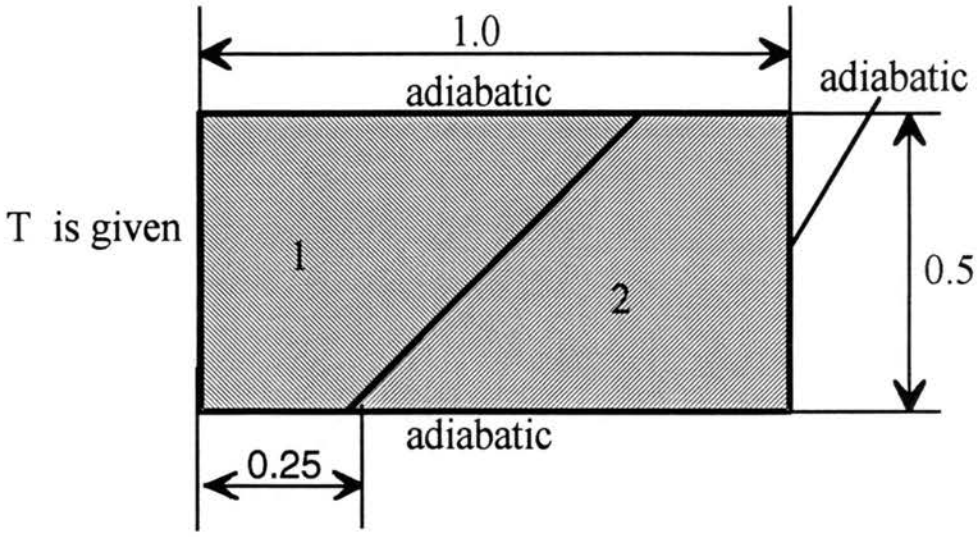

Fig. 6-12 Geometry of Composite Material and Boundary Conditions

The numerical method used here is the control volume finite difference method developed in Chapter V, section 5.2.2. The grid was 100 by 50, and the dimensionless time step was 0.001. The contours of temperature are shown in Fig. 6-13. The propagation of thermal waves for two different situations is shown in the figure, and the wave fronts of the incident waves, the reflected waves and the transmitted waves can be seen clearly. From the figure, we can see that the transmitted wave does not have an obvious wave front when the propagation speed in material 2 is larger than that in the material 1. As we have analyzed in Chapter IV, in this situation, the transmitted waves are a series of circular waves with circular wave fronts (see Fig. 4-2). The very front wave is a circular wave emitted by the point which is the first point that receives the incident wave. In Fig. 6-13(b), both the reflected wave and the transmitted wave have very clear wave fronts as in Fig. 4-1, and the propagation direction of the reflected wave is normal to the x-axis, and the propagation direction of the transmitted wave is parallel to the interface in Fig. 6-13(a), and it is 18.9°. Compared to the theoretical result from Eq. 4-32, which is 20°, the accuracy is satisfactory.

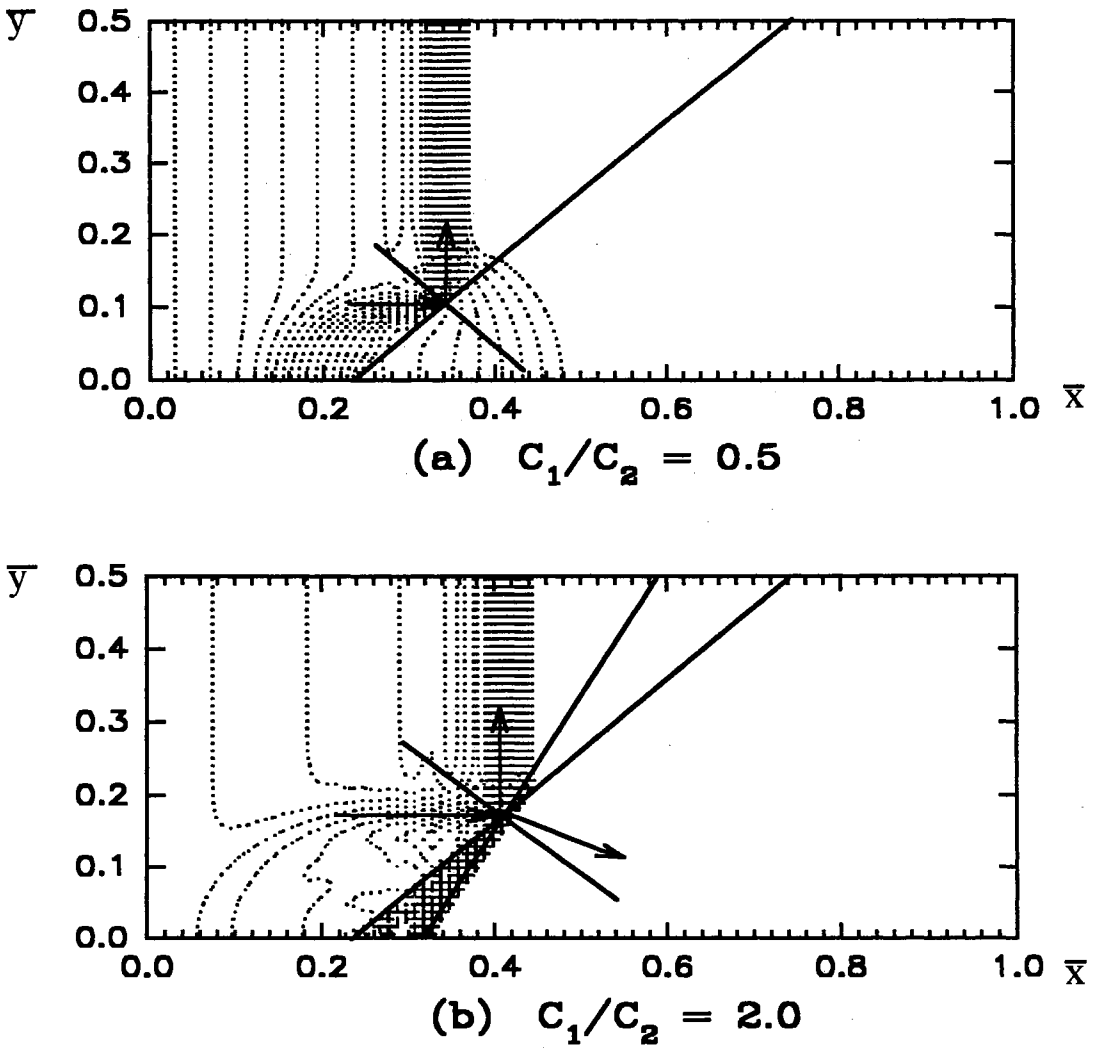

Fig. 6-13 Contour Plots of Wave Fronts of Reflected Wave and Transmitted Wave (TD = C_1 / C_2).

The reflectivity is shown in Fig. 6-14. From the figure we see that the reflectivity is a function of time and its trend basically agrees with the theoretical result Eq. (4-30). However, because of the effects of the interaction between the reflected waves from the bottom boundary and the incident wave, the reflectivity does not agree with the theory very well in its magnitude.

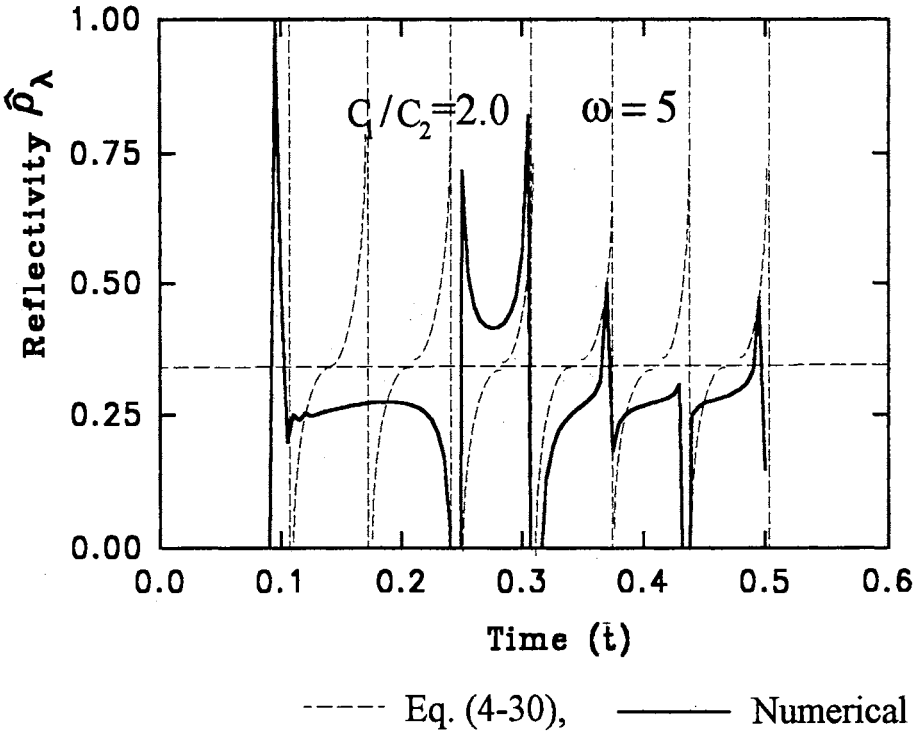

Fig. 6-14 Reflectivity of an Incident Sine Wave as a Function of Time with $TD = C_1 / C_2$, $\bar{y} = 0.25$, $\bar{x} = 0.5$

There are several reasons that reduce the accuracy of the theory in this conduction process. The most important one is that, in the actual situation such as the heat conduction of this example, the incident thermal wave is not really collimated but a directionally diffuse wave. As we have seen from Fig. 6-11, the thermal wave at a given position is actually a wave composed of many circular waves. Therefore, the incident wave at the interface is actually distributed in all the directions in a semi-spherical space above the interface. When the incident wave is normal to the interface (one-dimensional), the wave can be treated as a collimated wave, so the theory of Chapter III can be applied. For a two-dimensional thermal wave, this is no longer true. Therefore, the theory is only strictly accurate for the directional reflection but not for the total energy reflection.

Because of this reason, in actual situations, total internal reflection cannot happen. However, at the moment when the incident plane wave just arrives at the interface, the

reflectivity can be approximated by the theory because at this moment, the incident wave is almost collimated, because at this moment the incident wave has not been affected by the waves reflected by the other boundaries. Figure 6-15 shows the reflectivities when the incident angle is $\pi/8$. The left plot shows the incident temperature wave and the reflected temperature waves as a function of time at the interface. The right plot shows the reflectivities. In this plot, the dashed lines are the reflectivities for $\theta = 0$, and the solid straight lines (0.461, 0.217) are the theoretical results for $\pi/8$. We can see that at the moment when the incident wave just arrives at the interface, the reflectivity agrees well with the theory. With the increase of time, the reflectivity changes, and it does not agree with the theory any more. Now the question is how can a two-dimensional thermal wave be a directionally diffuse wave?

To explain this question, we need to introduce a new concept: heat conduction intensity. The heat conduction intensity is related to Debye's phonon theory. It is discussed in the next chapter.

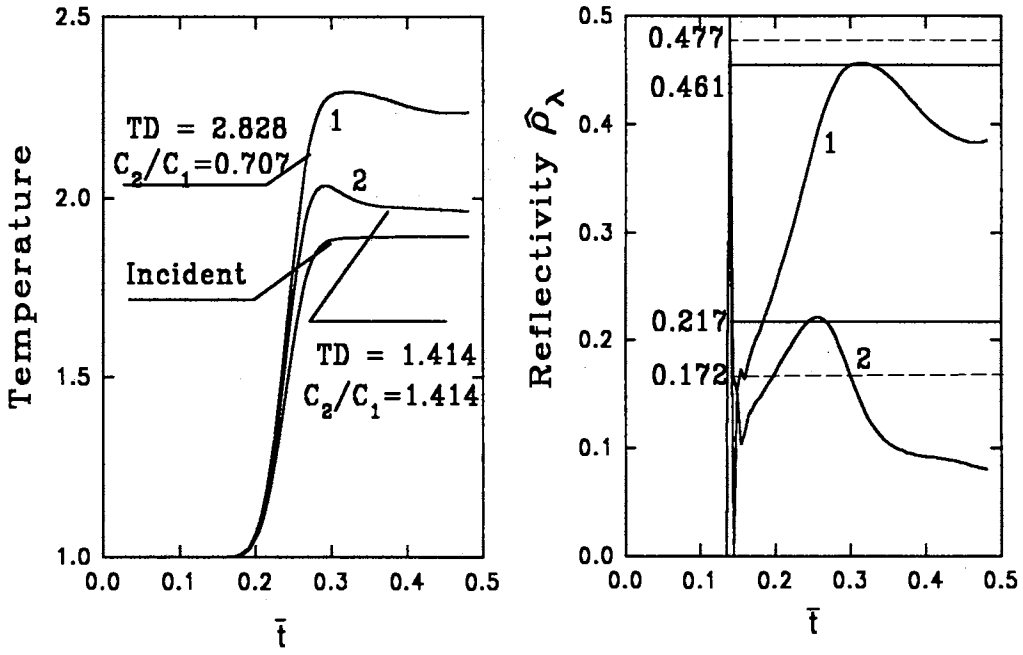

Fig. 6-15 Reflectivity for $\theta = \pi/8$

Another example is the heat conduction shown in Fig. 6-16. In this case, the incident wave is parallel to the interface of two layers, therefore, the incident angle is $\pi/2$. In our numerical solution, we assumed that the two layers have the same relaxation time, both equal to unity. However, their wave speeds are different. The grid was 100 by 50 in this numerical solution, and the dimensionless time step was 0.001.

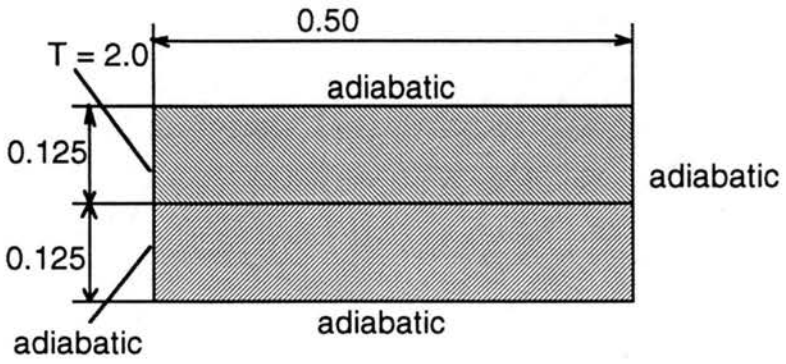

Fig. 6-16 Geometry of Two-Layer Composite Material

The temperature distribution for $C_1 / C_2 = 2.0$ is shown in Fig. 6-17. In this case, according to Eq. (4-32), the transmission angle is real, and it should be 30°. From the temperature contours, we can see three wave fronts; one is in the top layer, and the other two are in the bottom layer. The wave front in the top layer is the wave front of the incident wave. At $\bar{t} = 0.2$, it is at $\bar{x} = 0.4$ since C_1 is 2.0. The wave front around the left bottom corner of the bottom layer represents the wave reflected by the bottom boundary. The other wave front which is a straight line starting at the interface is the wave front of the transmitted wave. The numerical solution clearly shows the transmitted wave and its direction. The result is the same as the theory. On the other hand, compared to Fig. 6-13(b), we find that we can not see the reflected wave in this figure. Actually, the reflected wave is parallel to the interface, as predicted by the theory in Chapter IV. We also find that the contours in the top layer are almost straight lines perpendicular to the interface. From the three-dimensional view of the temperature, we find that the temperature in the top layer is fairly one-dimensional, or it does not change very much in the $\bar{y}$ direction.

This is because the reflectivity is minus one according to the theoretical solution shown in Fig. 4-1. Since the reflected wave is parallel to the interface, the reflection does not change the one-dimensional feature of the incident wave.

The situation of $C_1 / C_2 = 0.5$ is shown in Fig. 6-18. In this figure, there are only two obvious wave fronts; one is in the bottom layer, and the other is in the top layer. The wave front in the top layer now is not parallel to the interface, but in the direction shown by the arrow. This front is ahead the wave front of the incident wave, and it represents the transmitted wave caused by the wave from the bottom layer. Because the wave in the bottom layer is parallel to the interface, the direction of the wave in the top layer is 30°. A large peak is observed in the top layer, and this peak is around the wave front of the original incident wave front. Its magnitude is even larger than the boundary temperature which is equal to 2.0. The mechanism is that the incident wave in the top layer first causes a transmitted wave in the bottom layer, then the transmitted wave again works as an incident wave in the bottom layer, and causes a transmitted wave in the top layer. Then this transmitted wave accumulates arround the original incident wave front in the top layer, and forms a large peak in the temperature. There is also a reflected wave in the bottom layer. However, this wave is parallel to the interface, just as we have shown in Fig. 6-19; therefore, we cannot see an obvious wave front.

These results agree with the theory that we have developed in Chapter IV. However, as we have said before, the quantitative comparison of numerical solution and theory is not very satisfactory. The reason is that the numerical model does not simulate the exact situation of theory.

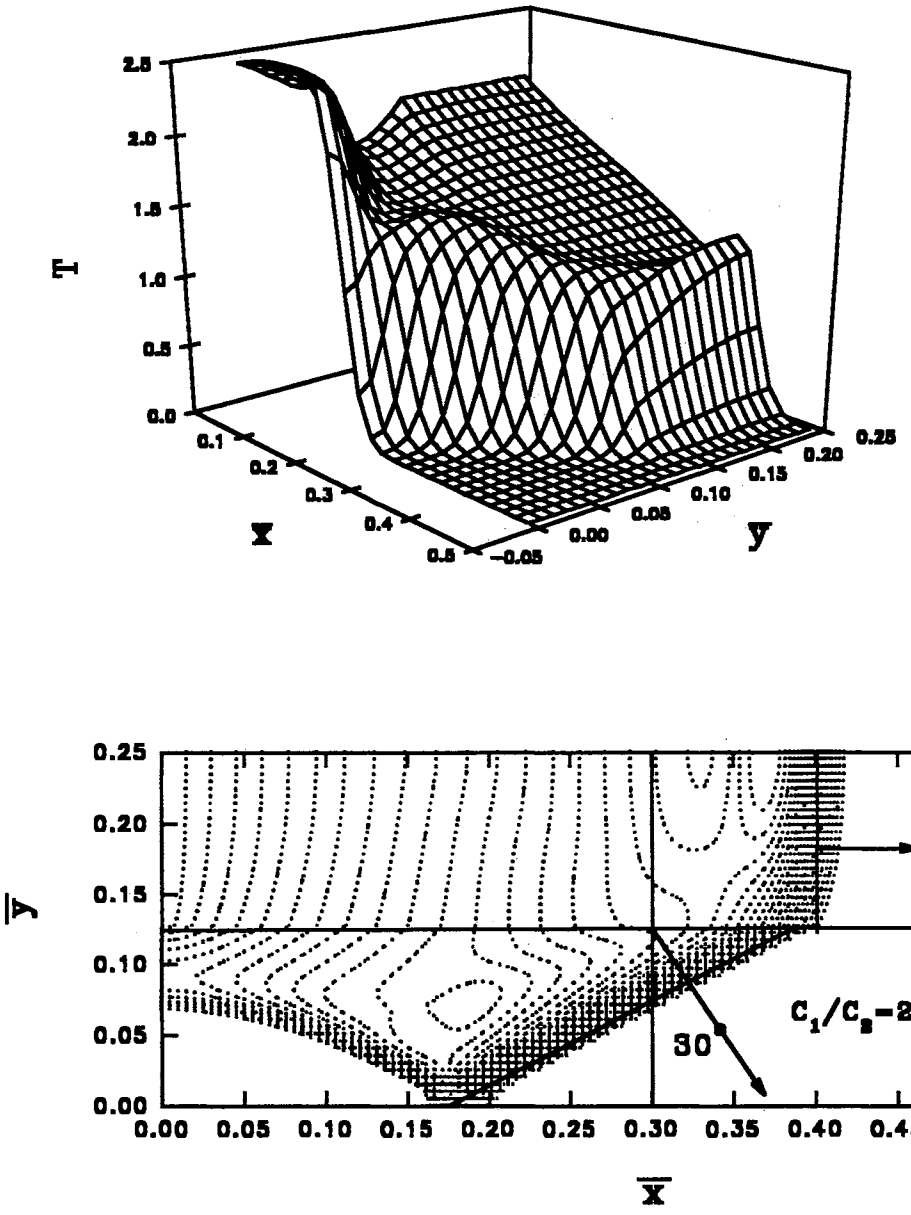

Fig. 6-19 Two-Dimensional Wave Propagation in a Two-Layer Medium with $C_1 > C_2$ and $\bar{t} = 0.2$

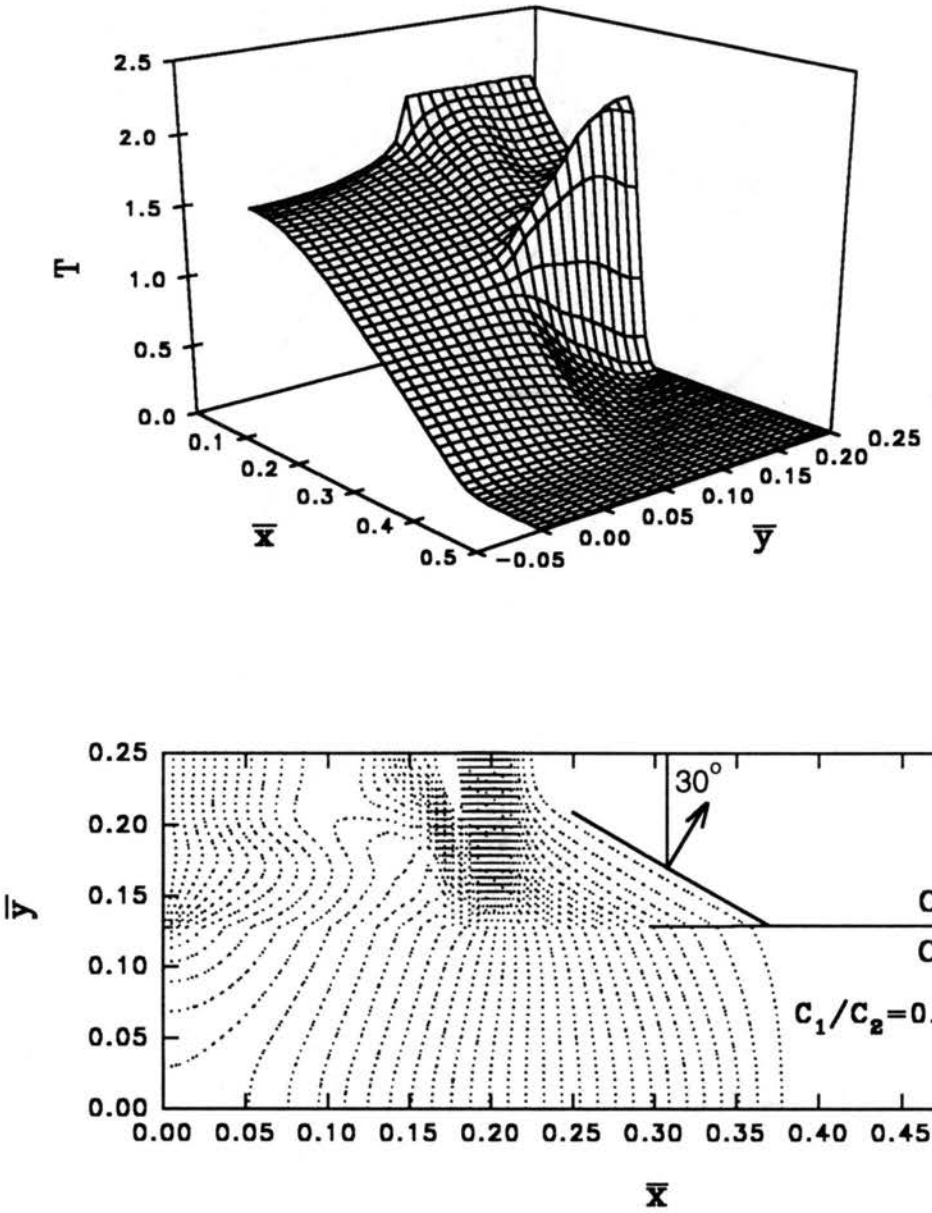

Fig. 6-20 Two-Dimensional Wave Propagation in a Two-Layer Medium with $C_1 < C_2$ and $\bar{t} = 0.2$

CHAPTER VII

PHONON TRANSPORT THEORY

In the previous chapters, we have studied hyperbolic thermal waves theoretically and numerically. We did not discuss the mechanism for hyperbolic heat conduction (HHC) behind the macroscopic hyperbolic equation (Eq. (1-4)). As we have stated in Chapter II, the hyperbolic model is still a approximate model for heat conduction, and its accuracy is very questionable. In this chapter, we are going to study the heat conduction mechanism based on phonon theory. We will explain the hyperbolic model and parabolic model based on phonon transport theory. We will also study the relationships among the phonon transport theory and the HHC and PHC models.

We know that heat conduction in solid materials is based on two mechanisms; one is lattice vibration, and the other is the motion of electrons. In conductors such as metals, the electrons carry most of the heat flow. In dielectric materials, lattice vibration is the dominant contribution to heat transfer. In alloys and semiconductors, lattice vibration and electrons have comparable effects on heat transfer. In this chapter, we will show that thermal waves actually are acoustic waves in dielectric materials. We will discuss heat conduction from the view point of particle motion. Lattice vibration is characterictized by a particle called a phonon, which is a quantum of energy in an elastic wave. From the discussion on these particles, we will derive the transport equation for phonons, and we will explain the thermal wave in more detail.

7. 1 The Phonon and Its Properties

Let's first review the physics of phonons, the theory that was first developed by Debye, and later enriched by many other physicists. In this section, we will just use the conclusions of physics that are to be employed in the following sections, but we will not discuss how these conclusions were achieved. We will introduce some new concepts such

as phonon intensity, and the relationships between heat transfer, internal energy, and phonon intensity.

The quantum of energy in an elastic wave is called a phonon. The term phonon has been created as an analogy with the photon in order to underline the similarities which exist, not only between the classical wave theories of sound and light, but also between the corresponding quantum theories. Similar to photons, phonons are also Bose particles without rest mass and without conservation of particle number. Under thermodynamic equilibrium, phonons are distributed over the possible states (frequency or wavelength) according to Planck's law which is the same distribution law for photons under thermodynamic equilibrium. Therefore, phonons are particularly useful for the treatment of transport processes in solids.

The physical states of phonons are determined by the polarization modes p and the wave frequency or wave vector **q** of the elastic waves. In this chapter, we will use **q** to represent wave vector, and **J** to represent heat flux. This is because **q** and **J** are commonly used this way in physics. Therefore, phonons are distributed in a p-**q** space according to their thermal equilibrium states. There are three polarization modes (Ziman,1960), two transverse modes and one longitudinal mode. The wave vector **q** is a vector in a space called reciprocal space. The modulus, q, of wave vector **q** is related to the motion of the wave in a crystal; in a distance $2\pi/q$ along the direction of **q** we pass a complete cycle. Thus the wavelength is given by

$$\lambda = 2\pi / q \tag{7-1}$$

Therefore, the modulus q represents the 'distance' in reciprocal space. 'Distances' in reciprocal space are measured in m^{-1} and 'volume' in m^{-3}. The vibration frequency for a given polarization mode is $\nu_{p,q}$, and the energy of a phonon is $\hbar\nu_{p,q}$. If we consider a small volume **dq**, which is a small volume around **q** in reciprocal space, and the polarization mode is p, then the energy at a given state (p, **q**) is (Ziman, 1960)

$$E_p = \sum_{\vec{q}} \hbar \nu_{p,q} (n^o_{p,q} + \tfrac{1}{2}) \tag{7-2a}$$

where, $n^o_{p,q}$ is the average number of phonons in this state (i.e. "o" indicates equilibrium state). The energy for $n^o_{p,q} = 0$ is called the zero state energy. If we choose the reference state carefully, for example, we choose the zero state energy as the origin, the phonons' energy can be written as (Ziman, 1960)

$$E_p = \sum_{\vec{q}} \hbar \nu_{p,q} n^o_{p,q} \tag{7-2b}$$

The average number of phonons is given by a distribution function as (Ziman, 1960)

$$n^o_{p,q} = \frac{1}{\exp(\hbar \nu_{p,q} / kT) - 1} \tag{7-3}$$

where k is the Boltzmann constant.

Since phonons are due to lattice vibrations, which are acoustic waves of different frequencies, the wave propagation speed or the group velocity of phonons is defined by

$$\bar{v}_{p,q} = \frac{\partial \nu_{p,q}}{\partial \vec{q}} \tag{7-4}$$

The frequency of a phonon is related to the wave vector **q**, for a one-dimensional transverse wave (p is fixed), we have (Ziman, 1960, Kittel, 1986)

$$\nu_q \propto \left| \sin \tfrac{1}{2} q \right| \tag{7-5}$$

This equation shows that the frequency is a periodic function of q, and its maximum value is equal to the frequency when $q = \pi$. For the one-dimensional situation, q is defined in a range from $-\pi$ to π, so the maximum frequency is called the cut-off frequency. In the three-dimensional situation, the wave vector **q** is limited to a volume which is called the first Brillouin zone. Therefore, the first Brillouin zone represents the zone in which the phonon's energy is included.

We can also define the phase velocity of phonons as (Ziman, 1960, Kittel, 1986)

$$s_{p,q} = \nu_{p,q} / q \tag{7-6}$$

where q is the modulus of **q**. The phase velocity usually is directionally-dependent for most crystals because of their anisotropic structure.

The flux of energy carried by phonons is (Ziman, 1960, Bak, 1964)

$$\vec{J}_p = \sum_{\vec{q}} \hbar \nu_{p,q} n^{o}_{p,q} \bar{v}_{p,q} \tag{7-7}$$

To simplify the above equations, we introduce Debye's theory (Ziman, 1960). According to Debye's theory, we assume:

1. The first Brillouin zone is approximated by a spherical zone which is called a Debye sphere with radius R (m^{-1}). Ignore small deviations of the sphere from the actual shapes.
2. The modulus of the wave vector is a function of frequency, and the direction of the wave vector is in the spherical-polar coordinates in **q**-space.
3. The phase velocity of phonons is independent of the modulus of the wave vector, so we have

$$s_p = \nu_{p,q} / q \tag{7-8}$$

Now we consider a crystal which has volume V. A unit cell is a cell which contains one atom in the crystal. The density of the unit cells in a crystal is N, which is the number of unit cells (atoms) contained in a unit volume of crystal. These unit cells correspond to different values of **q** in reciprocal space. Usually, the density of the unit cells is very high. If we are dealing with a large enough volume of crystal, then we can use $\int_{\vec{q}} .. d\vec{q}$ to represent the summation $\sum_{\vec{q}} ..$ in the previous equations. Based on these assumptions, each given frequency corresponds to a sphere of radius q. The phonons' energy is limited to a small volume $q^2 dq d\Omega$, where $d\Omega$ is the solid angle along the

direction (θ, ϕ) as shown in Fig. 7-1. Notice that we use θ to represent the angle between **q** direction and x-axis rather than z-axis.

Since the number of phonons in a unit solid angle along (θ, ϕ), of unit radius q is $n^{o}_{p,q}$, we introduce the phonons' intensity (or energy density) at the equilibrium state along the direction (θ, ϕ) that is defined as the energy per unit volume in a unit solid angle

$$I^{o}_{p,\Omega} = \frac{V}{8\pi^3}\int_0^R \hbar\nu_{p,q} n^{o}_{p,q} q^2 dq = \frac{V}{8\pi^3} s_p(\theta,\phi)\int_o^R \hbar q^3 n^{o}_{p,q} dq \qquad (7\text{-}9)$$

where $V/8\pi^3$ is dimensionless and is introduced to take account of the density of the unit cells allowed in reciprocal space (Ziman, 1960), and R is the Debye radius. Then the total energy is the summation of the energy intensity over all of the directions, from Eqs. (7-2) and (7-9), we obtain

$$E_p = \int_{4\pi} I^{o}_{p,\Omega} d\Omega \qquad (7\text{-}10)$$

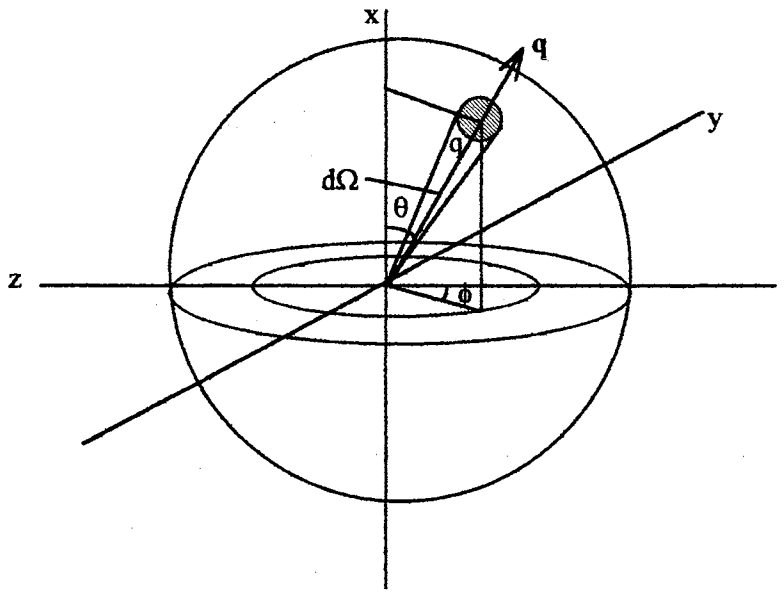

Fig. 7-1 The Geometry of **q**-Space

Usually, the intensity given by Eq. (7-9) is directionally dependent because the phase speed is directionally dependent for most crystals. However, if, in addition to our first assumptions on the previous page, we add:

4. The crystal anisotropy is ignored, so the phase velocity or the frequency is independent of direction. Then we can use Eq. (7-3) and a change of integration variable ($\xi = \hbar\nu_{p,q} / kT$) in Eq. (7-10) to derive (Ziman, 1960, Roberts and Miller, 1960)

$$E_p = 3NkT\left(\frac{T}{\Theta_p}\right)^3 \int_0^{\Theta_p/T} \frac{\xi^3}{e^{\xi}-1} d\xi \tag{7-11}$$

where $\Theta_p = \frac{\hbar s_p R}{k}$, and the Debye's radius R is related to N and V by $R^3 = 24\pi^3 N / V$. This is the result of Debye's theory, and Θ_p is Debye's temperature. When the temperature is very low, say $\Theta_p >> T$, the above equation becomes

$$E_p = \frac{1}{5}\frac{Nk\pi^4}{\Theta_p^{\ 3}} T^4 \tag{7-12a}$$

and when $T >> \Theta_p$, Eq. (7-11) is

$$E_p = NkT = \frac{1}{3}\bar{c}_v T \tag{7-12b}$$

where N is Avogadro's number (the same as N on the previous pages), and c_v is constant volume specific heat.

From the above discussion, we would like to describe the phonons as a kind of energy transfer in space. In a dielectric material, for a given temperature T, the intensity (energy in a solid angle $d\Omega$) emitted by the material is given by Eq. (7-9). The energy propagates in space with a velocity given by Eq. (7-4). At very low temperature, much smaller than the Debye's temperature (Θ_p), the phonon emission Eq. (7-12a) is the same as the photon emission law (Boltzmann law or the T^4 law) (Siegel and Howell, 1981). Based on this reduction, the energy transfer by phonons at very low temperatures is similar to the energy transfer by photons, except that the phonons cannot propagate in a vacuum.

7. 2 The Boltzmann Equation and Thermal Waves

When a system has external thermodynamic forces acting on it, for example, a temperature gradient or an electric field, the system will not be at an equilibrium state and heat conduction will take place, because of the flow and scattering of phonons and electrons. Lets take phonons as an example to derive the transport equation. The idea can also be directly applied to electrons (Ziman, 1960). The distribution of the particle number density can be found at a local point from the solution of the Boltzmann transport equation for the distribution function (Ziman, 1960)

$$\frac{\partial n_{p,q}}{\partial t} + \bar{v}_{p,q} \cdot \nabla n_{p,q} + \left[\dot{n}_{p,q}\right]_{field} = \Xi_{scatt}\, n_{p,q} \tag{7-18}$$

where $\dot{n}_{p,q}$ represents the rate of phonon distribution caused by external forces. This is the general form of the Boltzmann equation which is applicable to phonons and electrons, where $\Xi_{scatt}\, n_{p,q}$ is an integration operator on the distribution function, which represents the effects of scattering processes between phonons, electrons, and phonon-electrons as well as the scattering between particles and impurities and lattice deformations. This equation is an integro-differential equation which cannot be easily solved.

If $n^{\circ}_{p,q}$ is the local distribution function at thermal equilibrium, then

$$\Xi_{scatt}\, n^{\circ}_{p,q} = 0 \tag{7-19}$$

However, if external thermodynamic forces act on the particles, then the distribution function is not $n^{\circ}_{p,q}$ any more, and the scattering term will be significant to heat transfer. Heat current (or heat flux), which is the energy carried by phonons passing a unit normal area in a unit time, can be determined from the distribution function as (Ziman, 1960, Bak, 1964)

$$\bar{J}_p = \frac{V}{8\pi^3} \int_{4\pi} \int_{q} (\hbar_{p,q} v_{p,q}) \bar{v}_{p,q} n_{p,q} q^2 dq d\Omega \tag{7-20a}$$

Similar to Eq. (7-9), the phonon's energy in a unit solid angle, and in a unit radius can be defined as the phonon's energy intensity under non-equilibrium

$$I_{p,q,\Omega} = \frac{\partial I_{p,\Omega}}{\partial q} = \frac{V}{8\pi^3}\hbar\nu_{p,q}n_{p,q}q^2 \tag{7-20b}$$

and the energy in a unit volume is

$$E_p = \int\int_{4\pi\, q} I_{p,q,\Omega}\, dq d\Omega \tag{7-21a}$$

the heat flux is

$$\vec{J}_p = \int\int_{4\pi\, q} \vec{v}_{p,q} I_{p,q,\Omega}\, dq d\Omega \tag{7-21b}$$

Now, we can derive the intensity's integro-differential equation by multiplying Eq. (7-18) by $\frac{V}{8\pi^3}\hbar\nu_{p,q}q^2$, and neglecting the acceleration term (i.e., the rate of phonon distribution by external forces)

$$\frac{\partial I_{p,q,\Omega}}{\partial t} + \vec{v}_{p,q}\cdot\nabla I_{p,q,\Omega} = \frac{V}{8\pi^3}\hbar\nu_{p,q}q^2\Xi_{scatt}n_{p,q} \tag{7-22}$$

Statistically, the phonon speeds in all the directions are the same and are equal to the mean speed. Therefore, the velocity vector can be written as

$$\vec{v}_{p,q} = \bar{v}_{p,q}\vec{r}, \quad |\vec{r}| = 1 \tag{7-23}$$

where $\bar{v}_{p,q}$ is the average velocity of the phonons at the state p-q; and we will assume that it is a constant. So Eq. (7-22) is written as

$$\frac{1}{\bar{v}_{p,q}}\frac{\partial I_{p,q,\Omega}}{\partial t} + \vec{r}\cdot\nabla I_{p,q,\Omega} = \frac{1}{\bar{v}_{p,q}}\frac{V}{8\pi^3}\hbar\nu_{p,q}q^2\Xi_{scatt}n_{p,q} \tag{7-24}$$

This is the general form of the energy transport equation. The total heat flux is obtained from Eq. (7-21b) and by adding the heat fluxes of the three polarization modes

$$\vec{J} = \sum_p \int_q \int_{4\pi} \vec{v}_{p,q} I_{p,q,\Omega}\, d\Omega dq \tag{7-25}$$

We see that the difficulty in solving the transport equation is the evaluation of the scattering term, which is basically an integral operator. The scattering of phonons from "collisions" with phonons, electrons, and impurities has been discussed by Ziman (1960), Bak (1964), and Roberts and Miller (1960). It was shown that the scattering process is very complicated, and so far there is no simple method to calculate this process accurately.

However, there is an approximate method called the relaxation time approximation available to simplify the transport equation (Ziman, 1960, Bak, 1964, Kittel, 1986, Majumdar, 1993). In this simple model, only absorption and emission effects in the collision term of the transport equation are considered. Consider the atoms of the material as the basic material particles. The collision of a phonon with an atom will cause a change in the potential energy of the atom. This process can cause the atom to absorb the phonon or emit a phonon. The reaction (collision) can be expressed as

$$A(E)+\hbar v \leftrightarrow A(E') \tag{7-26}$$

where A(E) refers to an atom at energy level E.

Actually the absorption and emission of phonons can also take place in collisions between phonons and electrons or between photons and phonons. Here we will only consider the phonon-phonon process. Equation (7-26) indicates that the scattering process may create phonons, and also phonons may be absorbed during a collision between a phonon and an atom at energy state E, which then changes the atom to another energy state E'. Therefore, the scattering term in Eq. (7-24) can be split into two terms, the creative term and the destructive term, corresponding to destruction and creation of phonons. Based on this idea, the transport Eq. (7-24) now may be written as

$$\frac{1}{\bar{v}_{p,q}}\frac{\partial I_{p,q,\Omega}}{\partial t}+\vec{r}\cdot\nabla I_{p,q,\Omega}=\frac{1}{\bar{v}_{p,q}}\left[\frac{\delta I_{p,q,\Omega}}{\delta t}\right]_{+}-\frac{1}{\bar{v}_{p,q}}\left[\frac{\delta I_{p,q,\Omega}}{\delta t}\right]_{-} \tag{7-27}$$

where $\frac{1}{\bar{v}_{p,q}}\left[\frac{\delta I_{p,q,\Omega}}{\delta t}\right]_{+}$ and $\frac{1}{\bar{v}_{p,q}}\left[\frac{\delta I_{p,q,\Omega}}{\delta t}\right]_{-}$ are the creative and destructive operators, respectively. In this scattering term, $\left[\frac{\delta I_{p,q,\Omega}}{\delta t}\right]$ represents the rate of intensity change during a collision time δt, and the subscripts + and - stand for the creative and destructive change. Suppose the mean free path that a phonon can travel before it collides with an

atom is $\Lambda_{p,q} = \bar{v}_{p,q}\tau_{p,q}$, and the relaxation time, which is the time between two collisions, is $\tau_{p,q}$. Then the creation (emission) and destruction (absorption) can be approximated by

$$\frac{1}{\bar{v}_{p,q}}\left[\frac{\delta I_{p,q,\Omega}}{\delta t}\right]_{+} - \frac{1}{\bar{v}_{p,q}}\left[\frac{\delta I_{p,q,\Omega}}{\delta t}\right]_{-} \cong \frac{1}{\bar{v}_{p,q}}\left(\frac{I^{o}_{p,q,\Omega} - I_{p,q,\Omega}}{\tau_{p,q}}\right) \tag{7-28}$$

where $I^{o}_{p,q,\Omega}$ is the intensity at the equilibrium state. Therefore, the transport equation can be written as

$$\frac{1}{\bar{v}_{p,q}}\frac{\partial I_{p,q,\Omega}}{\partial t} + \bar{r}\cdot\nabla I_{p,q,\Omega} = \frac{1}{\bar{v}_{p,q}\tau_{p,q}}\left(I^{o}_{p,q,\Omega} - I_{p,q,\Omega}\right) \tag{7-29a}$$

Now the transport equation is greatly simplified. However, it is still not easy to solve Eq. (7-29a) because the phonon speed $\bar{v}_{p,q}$ depends on both polarization and wave vector modulus q (or frequency, see Eq. (7-6)), and because the equilibrium state intensity $I^{o}_{p,q,\Omega}$ is directionally dependent for most crystals. Therefore, more assumptions are needed to make further simplifications. So let's assume that the crystals are spherical. Then the equilibrium state intensity is independent of direction and can be calculated according to Debye's theory. The transport Eq. (7-29a) becomes

$$\frac{1}{\bar{v}_{p,q}}\frac{\partial I_{p,q,\Omega}}{\partial t} + \bar{r}\cdot\nabla I_{p,q,\Omega} = \frac{1}{\bar{v}_{p,q}\tau_{p,q}}\left(I^{o}_{p,q} - I_{p,q,\Omega}\right) \tag{7-29b}$$

Majumdar (1993) also derived the same form of transport equation as Eq. (7-29b) for isotropic crystals. If we multiply Eq. (7-29b) by $\bar{v}_{p,q}$, and integrate over solid angle and q, we obtain

$$\frac{\partial E_p}{\partial t} + \nabla\cdot\vec{J}_p = \frac{1}{\tau_p}\int_{4\pi}\int_{q}(I^{o}_{p,q} - I_{p,q,\Omega})\,dq\,d\Omega \tag{7-30}$$

where we have assumed $\tau_p = \tau_{p,q}$ (independent of q). According to the energy conservation law, the total energy should satisfy

$$\sum_p \left(\frac{\partial E_p}{\partial t} + \nabla \cdot \vec{J}_p\right) = 0 \tag{7-31a}$$

and therefore, comparing Eqs. (7-30) and (7-31), we have

$$\sum_p \frac{1}{\tau_p} \int_{4\pi} \int_q (I^\circ_{p,q} - I_{p,q,\Omega}) dq d\Omega = 0 \tag{7-31b}$$

From the transport equation (Eq. (7-29b), we can derive the thermal conductivity for the macroscopic heat conduction process. The following is the method described by Majumdar (1993) and many other investigators (Ziman, 1960, Bak, 1964, Roberts, 1960).

If the temperature gradient in the material is small and is the only external force, and the deviation of the distribution function ($n_{p,q}$ or $I_{p,q}$) from equilibrium ($n^\circ_{p,q}$ or $I^\circ_{p,q}$) is small, then we can write approximate expressions for the gradient term and the time derivative term of the transport equation as

$$\vec{r} \cdot \nabla I_{p,q,\Omega} \cong \left[\vec{r} \frac{\partial I^\circ_{p,q}}{\partial T}\right] \cdot \nabla T \tag{7-32a}$$

$$\frac{\partial I_{p,q}}{\partial t} = \frac{\partial I^\circ_{p,q}}{\partial T} \frac{\partial T}{\partial t} \tag{7-32b}$$

So the transport equation (Eq. 7-29b) can be written as

$$\frac{1}{\bar{v}_{p,q}} \frac{\partial I^\circ_{p,q}}{\partial T} \frac{\partial T}{\partial t} + \left[\vec{r} \frac{\partial I^\circ_{p,q}}{\partial T}\right] \cdot \nabla T = -\frac{I_{p,q,\Omega} - I^\circ_{p,q}}{\bar{v}_{p,q} \tau_{p,q}} \tag{7-33a}$$

Then, we can obtain Fourier's law by multiplying (dot product of) Eq. (7-33a) by $\bar{v}_{p,q} \tau_{p,q} \bar{v}_{p,q}$, integrating over solid angle, integrating over q space, and summing over all polarizations (Ziman, 1960)

$$\bar{J} = -\left[\sum_p \int_{4\pi} \int_q \vec{v}_{p,q} \cdot \vec{r} (\tau_{p,q} \bar{v}_{p,q}) \frac{\partial I^\circ_{p,q}}{\partial T} dq d\Omega\right] \nabla T \tag{7-33b}$$

If relaxation time is independent of q, then the thermal conductivity can be derived as

$$K = \sum_p \int_{4\pi} \int_q \vec{v}_{p,q} \cdot \vec{r}(\tau_p \bar{v}_{p,q}) \frac{\partial I^\circ_{p,q}}{\partial T} dq d\Omega = \frac{1}{3} \sum_p \bar{c}_v \bar{v}_p \Lambda_p \qquad (7\text{-}33c)$$

where Λ_p is the mean free path, $\bar{v}_p$ is the phonon speed, and c_v is the specific heat. The following relationships (Ziman, 1960, Bak, 1964) were also used in writing Eq. (7-33c)

$$\vec{v}_{p,q} \cdot \vec{r}(\tau_p \bar{v}_{p,q}) = \tau_p \bar{v}^2_{p,q} = \frac{1}{3} \bar{v}_p \Lambda_p$$

$$\Lambda_p = \tau_p \bar{v}_p$$

$$\bar{c}_v = \int_q \int_{4\pi} \frac{\partial I^\circ_{p,q,\Omega}}{\partial T} d\Omega dq$$

Note that we have used the statistical physics equation

$$\bar{v}^2_{p,q} = \frac{1}{3} \bar{v}^2_p$$

The hyperbolic heat conduction equation (Eq. 1-4) can also be derived if we apply Eq. (7-32a) to the second term of the transport equation (Eq. (7-29b)), but keep the first term unchanged (Majumdar,1993), then Eq. (7-29b) becomes

$$\frac{1}{\bar{v}_{p,q}} \frac{\partial I_{p,q,\Omega}}{\partial t} + \vec{r} \cdot \frac{\partial I^\circ_{p,q}}{\partial T} \nabla T = -\frac{I_{p,q,\Omega} - I^\circ_{p,q}}{\bar{v}_{p,q} \tau_{p,q}} \qquad (7\text{-}34)$$

Then, we multiply (dot product) the above equation by $\vec{v}_{p,q} \tau_{p,q} \bar{v}_{p,q}$, integrate over solid angle and wave vector modulus, and sum over all polarization modes (also considering Eqs. (7-32) and (7-33)), we obtain

$$\tau \frac{\partial \bar{J}}{\partial t} + \bar{J} = -K \nabla T \qquad (7\text{-}35)$$

where τ is the average $\tau_{p,q}$, and this average relaxation time is the same as the relaxation time in Eq. (1-4).

The approximations made in deriving Eqs. (7-33) and (7-35) are valid only when the dimensions of the material are much larger than the mean free path of the phonons. In this case, the temperature can be well defined and the deviation of the distribution function from equilibrium can be small. Therefore, theoretically, both Fourier's law and the hyperbolic heat conduction equation (Eq. (7-35)) are valid heat transfer relations in large

dimension materials; and they both neglect boundary scattering effects that may be important when the characteristic dimension of the material is on the order of the mean free path of the phonons. These equations are not very accurate when the boundary scattering is significant, for example, considering heat transfer in very thin films or rods (Klitsner et al., 1990, Ziman, 1960, Goodson and Flik, 1993).

Next, we consider one-dimensional heat conduction in an isotropic material. Assume that the velocity of the thermal waves (acoustic waves) is independent of polarization. In this case, the relaxation time and average wave propagation speed are independent of wave vector and polarization, then the transport equation, Eq. (7-29b), and Eq. (7-31b) can be written as

$$\frac{\partial I(\bar{t},\bar{x},\mu)}{\partial \bar{t}}+\mu\frac{\partial I(\bar{t},\bar{x},\mu)}{\partial \bar{x}}+I(\bar{t},\bar{x},\mu)=\frac{1}{2}\int_{-1}^{1} I(\bar{t},\bar{x},\mu')d\mu' \tag{7-36a}$$

$$I^{\circ}(\bar{t},\bar{x})=\frac{1}{2}\int_{-1}^{+1} I(\bar{t},\bar{x},\mu)d\mu \tag{7-36b}$$

Here, we have used the following relationships to normalize the coordinates

$$\bar{t}=\frac{t}{\tau},\quad \bar{x}=\frac{x}{\bar{v}\tau},\quad \mu=\cos\theta \tag{7-37}$$

where θ is the angle the intensity makes with the x-axis, and $\bar{x}$ is called acoustic thickness since the phonon waves are acoustic waves. Now we introduce the m^{th} moment of intensity

$$U_m(\bar{t},\bar{x})=\int_{-1}^{1}\mu^m I(\bar{t},\bar{x},\mu)d\mu \tag{7-38}$$

Then the 0th and 1st order moments correspond to the internal energy and the heat current (or flux). From multiplying Eq. (7-36a) by μ^m and integrating over μ, we can obtain an equation with these moments

$$\frac{\partial U_m}{\partial \bar{t}}+U_m=-\frac{\partial U_{m+1}}{\partial \bar{x}}+\frac{1-(-1)^{m+1}}{2(m+1)}U_0 \tag{7-39}$$

This wave equation shows that each moment is a wave that is coupled with the other moments during propagation.

Obviously, to solve the above equation exactly, we have to solve all of the moments from 0th order to infinite order. However, we can solve Eq. (7-39) approximately by neglecting the moments of order higher than m+1. Let us consider the second order (m=2) approximation. From Eq. (7-39), we have

$$\frac{\partial U_0}{\partial \bar{t}} = -\frac{\partial U_1}{\partial \bar{x}} \tag{7-40}$$

$$\frac{\partial U_1}{\partial \bar{t}} + U_1 = -\frac{\partial U_2}{\partial \bar{x}} \tag{7-41}$$

$$\frac{\partial U_2}{\partial \bar{t}} + U_2 = -\frac{\partial U_3}{\partial \bar{x}} + \frac{1}{3} U_0 \tag{7-42}$$

Now we neglect the moments of order higher than two and the derivative of the second moment with respect to time. Then in Eq. (7-42), the second order moment reduces to

$$U_2 = \frac{1}{3} U_0 \tag{7-43}$$

Equations (7-40) and (7-41) become

$$\frac{\partial U_0}{\partial \bar{t}} = -\frac{\partial U_1}{\partial \bar{x}}$$

$$\frac{\partial U_1}{\partial \bar{t}} + U_1 = -\frac{1}{3}\frac{\partial U_0}{\partial \bar{x}} \tag{7-44}$$

These are the hyperbolic equations which we have studied in Chapter III. Remember that, in these equations, the $\bar{x}$ coordinate is normalized by $\bar{v}\tau$ (see Eq. (7-37)), so the thermal conductivity is 1/3 (see Eq. (7-33c) for $c_v = 1$). This derivation shows that the hyperbolic Eq. (7-35) is the second order approximation of the intensity transport equation.

We can use higher order approximations. Let m be an odd number. If in Eq. (7-39) we neglect moments higher than m+1 and the derivative of the m+1 moment with respect to time, then we can approximate the moment of order m+1 by

$$U_{m+1} = \frac{1}{m+2} U_0 \tag{7-45}$$

Therefore, substituting Eq. (7-45) into Eq. (7-39) gives the m^{th} order moment

$$\frac{\partial U_m}{\partial \bar{t}} + U_m = -\frac{1}{m+2}\frac{\partial U_0}{\partial \bar{x}} \tag{7-46}$$

If we define the vector of moments as

$$U = [U_0 \;\; U_1 \;\; U_2 \;\; \ldots \;\; U_m]^T \tag{7-47}$$

then we can write the moment equation in the following matrix form

$$\frac{\partial U}{\partial \bar{t}} + U = -A\frac{\partial U}{\partial \bar{x}} + S \tag{7-48}$$

where

$$A = \begin{bmatrix} 0 & 1 & 0 & \ldots & 0 \\ 0 & 0 & 1 & \ldots & 0 \\ 0 & 0 & 0 & \ldots & 0 \\ 0 & 0 & 0 & \ldots & 1 \\ \frac{1}{m+2} & 0 & 0 & \ldots & 0 \end{bmatrix} \quad \text{and} \quad S = \begin{bmatrix} s_0 \\ s_1 \\ s_2 \\ \vdots \\ s_m \end{bmatrix}, \quad s_i = \frac{1-(-1)^{i+1}}{2(i+1)}U_0 \tag{7-49}$$

There are two real eigenvalues of the matrix A that are determined by

$$\begin{vmatrix} -\tilde{\lambda} & 1 & 0 & \ldots & 0 \\ 0 & -\tilde{\lambda} & 1 & \ldots & 0 \\ 0 & 0 & -\tilde{\lambda} & \ldots & 0 \\ 0 & 0 & 0 & \ldots & 1 \\ \frac{1}{m+2} & 0 & 0 & \ldots & -\tilde{\lambda} \end{vmatrix} = 0 \quad \text{and} \quad \tilde{\lambda} = \pm\left(\frac{1}{m+2}\right)^{\frac{1}{m+1}} \tag{7-50}$$

For example, if we choose m = 5, then the real eigenvalues are +0.723, and -0.723. Besides the two real eignevalues, there are m-1 complex eigenvalues, as shown in the following matrices. These complex eigenvalues represent the complicated interaction of the waves that are the components of the intensity wave. When m is very large, the real eigenvalues in Eq. (7-50) tend to the limits +1 and -1, which correspond to the non-dimensional acoustic speed of the material.

$$A := \begin{bmatrix} 0 & 1 & 0 & 0 & 0 & 0 \\ 0 & 0 & 1 & 0 & 0 & 0 \\ 0 & 0 & 0 & 1 & 0 & 0 \\ 0 & 0 & 0 & 0 & 1 & 0 \\ 0 & 0 & 0 & 0 & 0 & 1 \\ \frac{1}{7} & 0 & 0 & 0 & 0 & 0 \end{bmatrix} \qquad e := \text{eigenvals}(A) \qquad e = \begin{bmatrix} -0.723 \\ -0.362 + 0.626i \\ -0.362 - 0.626i \\ 0.723 \\ 0.362 + 0.626i \\ 0.362 - 0.626i \end{bmatrix}$$

where eigenvals( ) is a function of MathCad (Mathsoft Inc. 1986-1994, v.5.0) for solving eigenvalues of a given matrix.

7.3 Numerical Solution of Phonon Transport Equation

The one-dimensional transport equation (Eq. (7-36b)) can be written as (Siegel and Howell, 1981)

$$\frac{\partial I^+(\bar{t},\bar{x},\mu)}{\partial \bar{t}}+\mu\frac{\partial I^+(\bar{t},\bar{x},\mu)}{\partial \bar{x}}+I^+(\bar{t},\bar{x},\mu)=\frac{1}{2}\int_0^1[I^+(\bar{t},\bar{x},\mu')+I^-(\bar{t},\bar{x},\mu')]d\mu' \quad (7\text{-}51)$$

$$\frac{\partial I^-(\bar{t},\bar{x},\mu)}{\partial \bar{t}}-\mu\frac{\partial I^-(\bar{t},\bar{x},\mu)}{\partial \bar{x}}+I^-(\bar{t},\bar{x},\mu)=\frac{1}{2}\int_0^1[I^+(\bar{t},\bar{x},\mu')+I^-(\bar{t},\bar{x},\mu')]d\mu' \quad (7\text{-}52)$$

where I^+ and I^- represent the intensity along the positive and negative directions of the axis $\bar{x}$ (see Fig. 7-2). Since the intensities in the positive and negative directions of the $\bar{x}$-axis can be two series of waves with propagation speeds equal to μ along the $\bar{x}$-axis, these equations are solved numerically by using the TVD method discussed in Chapter V. The boundaries are assumed to be "black", and the temperatures at the boundaries are given. Such boundary conditions are equivalent to the conditions of specifying intensities at the boundaries (see Fig. 7-2).

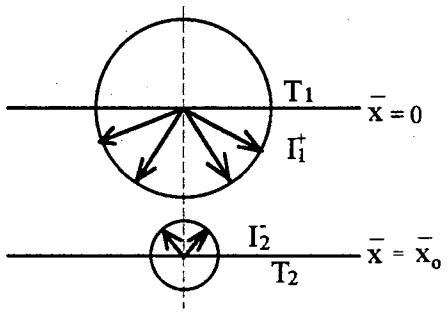

Fig. 7-2 The Boundary Conditions for Thermal Intensities

We introduce two functions, Ψ and Φ, which are defined as

$$\Psi(\bar{t},\bar{x},\mu)=I^+(\bar{t},\bar{x},\mu)+I^-(\bar{t},\bar{x},\mu) \quad (7\text{-}53)$$

$$\Phi(\bar{t},\bar{x},\mu) = I^{+}(\bar{t},\bar{x},\mu) - I^{-}(\bar{t},\bar{x},\mu) \tag{7-54}$$

These two variables are useful because they are related to the internal energy E and heat transfer J. From Eqs. (7-21a,b) we can derive

$$E(T) = 2\pi\int_{0}^{1}\Psi(\bar{t},\bar{x},\mu)d\mu \tag{7-55}$$

$$J = 2\pi\int_{0}^{1}\mu\Phi(\bar{t},\bar{x},\mu)d\mu \tag{7-56}$$

where E is a function of temperature according to Eqs. (7-12a,b), and then temperature is a function of time and location due to Eqs. (7-55) and (7-56). A dimensionless energy can be defined by

$$\overline{E} = \frac{E(T)-E(T_2)}{E(T_1)-E(T_2)} = \frac{\int_{0}^{1}\Psi(\bar{t},\bar{x},\mu)d\mu - I_2^{-}}{I_1^{+}-I_2^{-}} \tag{7-57}$$

When the material of interest is at very low temperature (for example, if the temperature is less than the Debye's temperature), according to Eq. (7-12a), the above equation becomes (Roberts and Miller, 1960, Majumdar, 1993)

$$\overline{E} = \frac{E(T)-E(T_2)}{E(T_1)-E(T_2)} = \frac{T^4-T_2^4}{T_1^4-T_2^4} \tag{7-58a}$$

When temperature is higher, according to Eq. (7-12b), Eq. (7-52) is (Roberts and Miller, 1960)

$$\overline{E} = \frac{E(T)-E(T_2)}{E(T_1)-E(T_2)} = \frac{T-T_2}{T_1-T_2} \tag{7-58b}$$

Therefore, it is convenient to use $\overline{E}$ to express the dimensionless temperature for either case.

The numerical solution of intensity from Eqs. (7-51) and (7-52) in the direction along the $\bar{x}$-axis (μ = 1.0) for the geometry shown in Fig. 7-2 is presented in Fig. 7-3. The boundary conditions and the initial conditions are specified as

$$\begin{aligned} \bar{x} = 0 \quad & I_1^+(\bar{t}, \bar{x}, \mu) = 2.0 \\ \bar{x} = \bar{x}_o \quad & I_2^-(\bar{t}, \bar{x}, \mu) = 1.0 \\ \bar{t} = 0 \quad & I(\bar{t}, \bar{x}, \mu) = 0 \end{aligned} \tag{7-59}$$

From Fig. 7-3, we can see that the intensities along the positive and negative directions of the $\bar{x}$-axis are waves with non-dimensional propagation speed equal to one. The two waves move in opposite directions with time. The propagation is very similar to the thermal waves that are predicted by the hyperbolic heat conduction model (HHC) (see Fig. 6-2).

The obvious difference between the intensity waves and the waves according to the HHC is that the scattering effect is considered for intensity. This difference is clearly shown in Fig. 7-3. At time $\bar{t}$ = 0.5, for example, the wave front of I^+ arrives at $\bar{x}/\bar{x}_o$ = 0.25, and the wave front of I^- arrives at $\bar{x}/\bar{x}_o$ = 0.75. In the region of $\bar{x}/\bar{x}_o$ from 0.25 to 0.75, both I^+ and I^- are zero. However, I^+ is not zero in the region from 0.75 to 1.0, although the wave front has not reached this region. Similarly, I^- is not zero in the region from 0 to 0.25. This is due to the back scattering effect. I^+ scatters to contribute to I^- and vice versa. The scattering effect is the key that couples the positive and negative intensities together. However, this effect is not very strong in this case. This is because the value of the back scattering coefficient times intensity is much smaller than the forward intensity itself.

From the figure, we also see that the two intensity waves cross each other at time $\bar{t}$ = 1.0. It seems that these two waves do not affect each other significantly when they meet each other. This also indicates that the scattering effect is weak. However, the scattering effect is important because it makes the two intensity waves depend upon each other. In the figure, we can see that there exist small oscillations of intensity at the wave fronts. This is numerical error at the wave front. This may be avoided by using smaller time steps in the calculation.

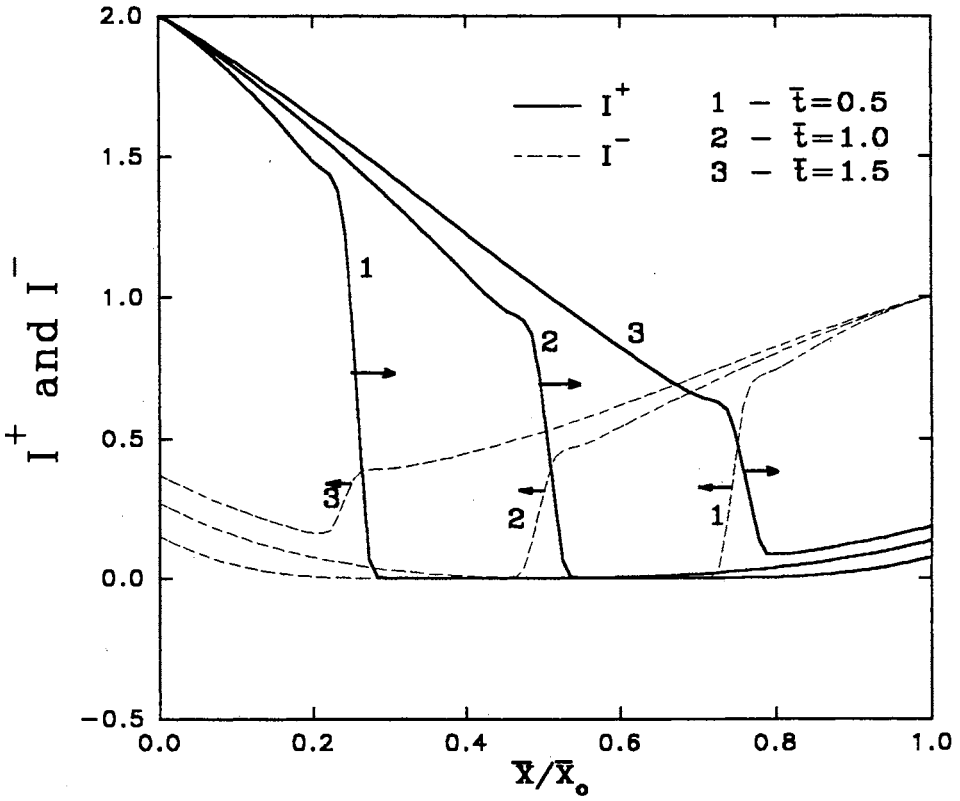

Fig. 7-3 Intensities (μ = 1.0) at Different Times ($\bar{x}_o$ = 2.0)

The intensities at different μ values are similar waves, however, the propagation speeds in the $\bar{x}$-direction are different according to the μ values. Figure 7-4 shows the intensities for three typical μ values at time $\bar{t}$ = 1.5. It is obvious that the wave fronts of these intensities are at different positions. From the transport equations (Eqs. (7-51) and (7-52)), we find that the non-dimensional propagation speed along the $\bar{x}$-axis is μ for the intensity in the μ direction. Actually, the propagation speeds of the intensities are the same, and equal to 1 (dimensionless) along their propagation directions. The different speeds shown in Fig. 7-4 are the $\bar{x}$-axis components of the actual speeds. The dimensionless internal energy is found according to the following equation

$$\bar{E} = \frac{E(T) - E(T_o)}{E(T_1) - E(T_2)} = \frac{\int_0^1 \Psi(\bar{t}, \bar{x}, \mu) d\mu}{I_1^+ - I_2^-} \tag{7-60}$$

and heat flux is found from Eq. (7-56). T_o is the initial temperature which is a constant (here it is zero). From these equations, we can see that the internal energy and heat flux are related to a combination of all of the intensity waves along all of the directions. Because the propagation speeds of these intensity waves are finite, the internal energy and heat flux are also waves with finite propagation speeds. Although these waves have different propagation speeds along the $\bar{x}$-axis, the internal energy and heat flux will have the maximum propagation speed of the intensity waves, and this non-dimensional speed is equal to 1.

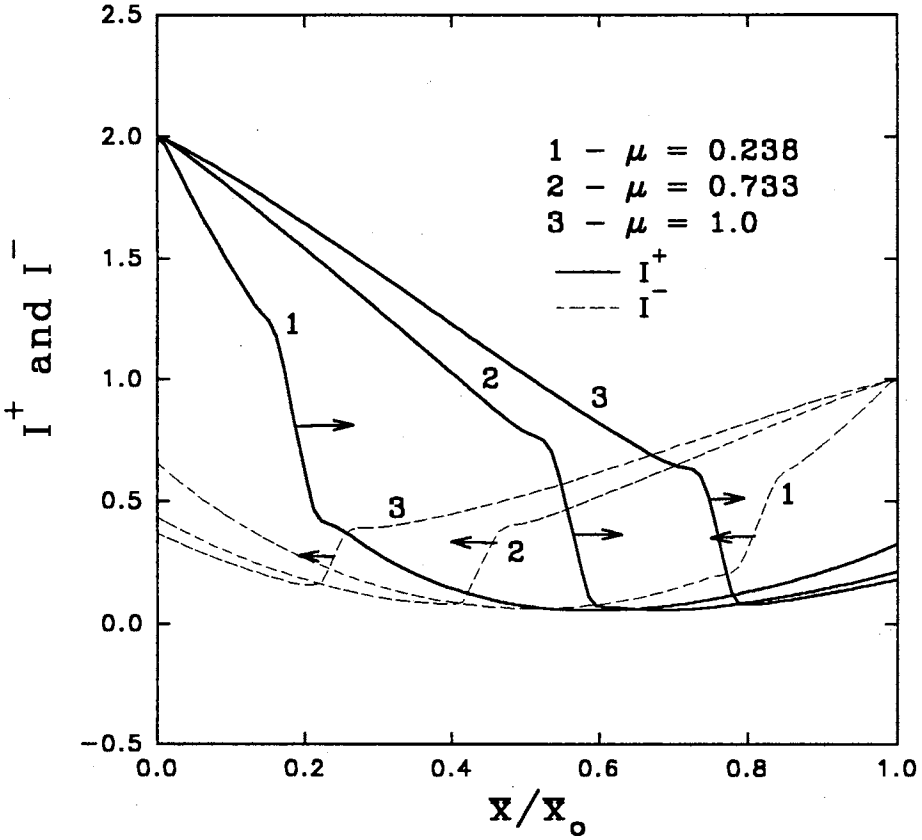

Fig. 7-4 Intensities for Different μ at $\bar{t}$ = 1.5 and $\bar{x}_o$ = 2.0

The results of internal energy and heat flux are shown in Fig. 7-5. The first important fact shown in the figure is that the wave fronts of the internal energy and heat flux do not have obvious discontinuous sharp changes, even at short times such as $\bar{t}$ =

0.5. However, the wave fronts can still be distinguished by the slope changes of the curves. In Fig. 7-5, the wave fronts can be easily seen on curves 1 and 2. For curve 1, the fronts of the waves from the left and right boundaries reach the positions $\bar{x}/\bar{x}_o = 0.25$ and $\bar{x}/\bar{x}_o = 0.75$, respectively. For curve 2, the two wave fronts meet each other at $\bar{x}/\bar{x}_o = 0.5$. However, after the waves from the left and right boundaries cross each other, it is difficult to discern the wave fronts, as is shown by curve 3. Curve 3 appears to be more like a distribution from the parabolic heat conduction model, but actually it is not the same as that from parabolic heat conduction (as will be shown in section 7.4).

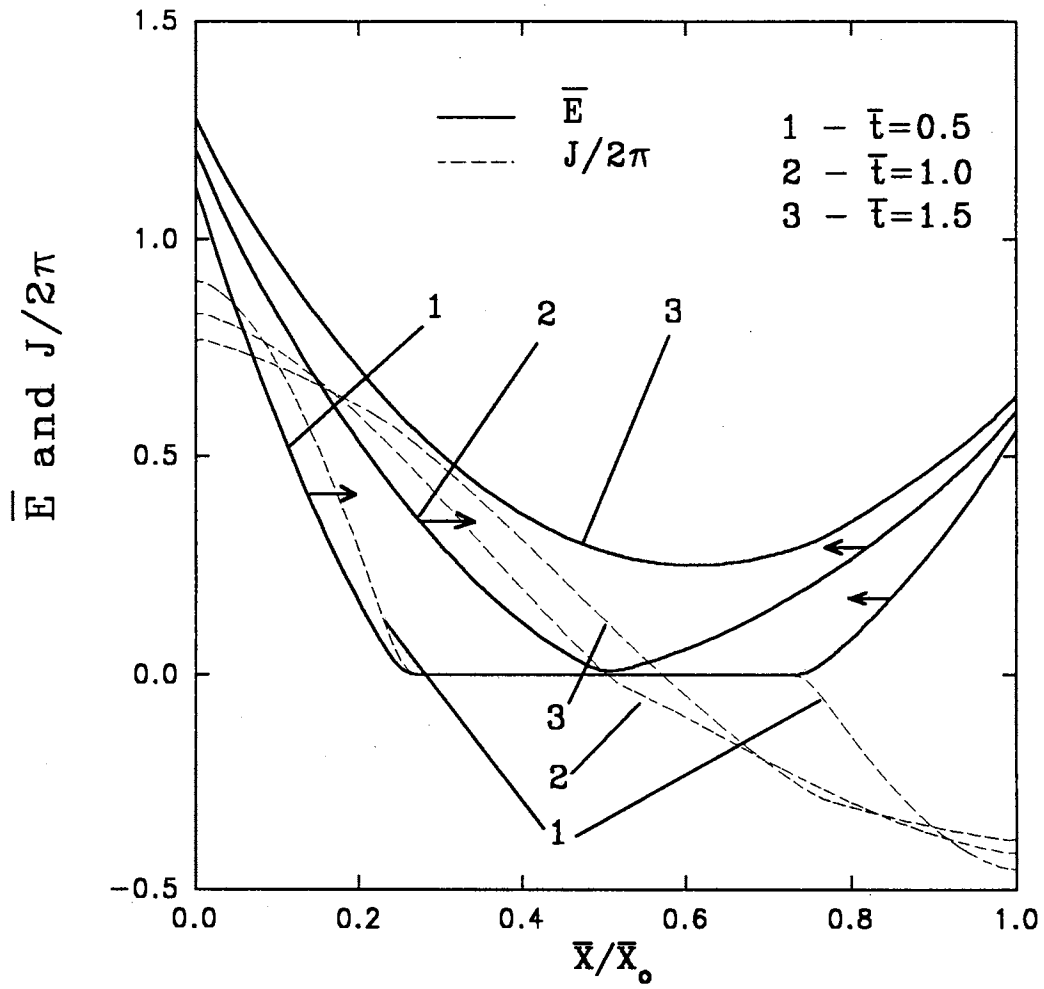

Fig. 7-5 Internal Energy and Heat Transfer ($\bar{x}_o = 2.0$)

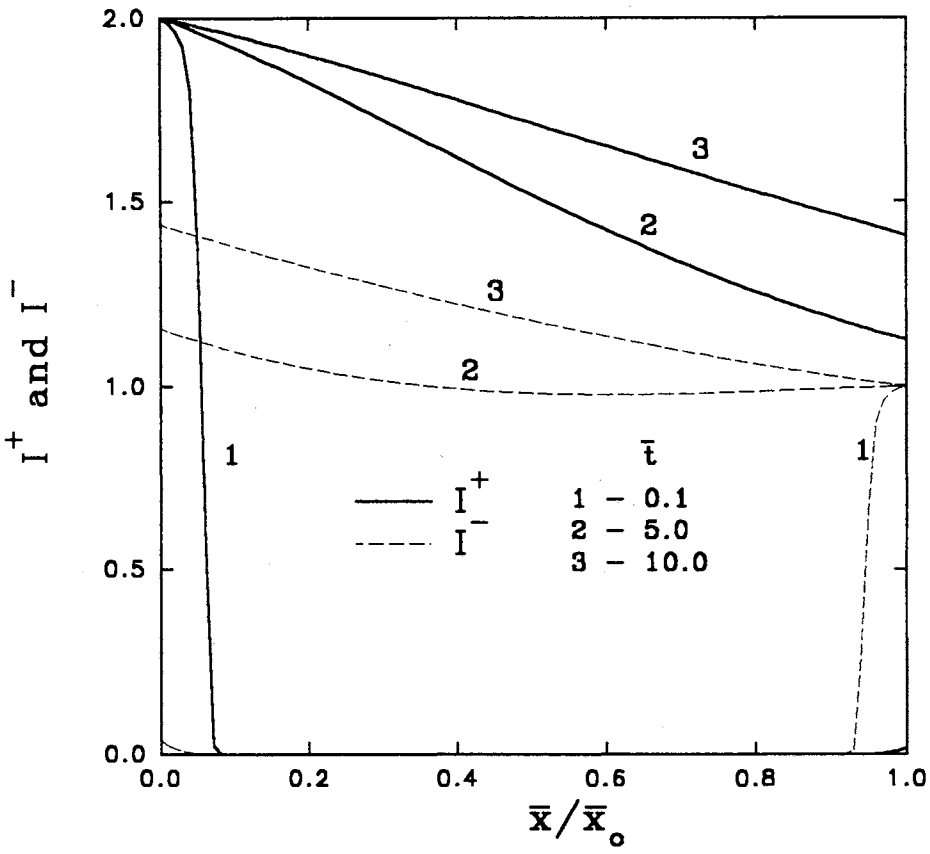

Fig. 7-6 Intensity ($\mu = 1.0$) at an Early Stage and Near the Final Stages of the Transient Process ($\bar{x}_o = 1.0$)

The intensity distributions at the early and near the final stages of the transient process are shown in Fig. 7-6. From the figure, we can see that at the early stage ($\bar{t}$ = 0.1), the wave fronts of the intensities in the positive and the negative directions along the $\bar{x}$-axis are near the boundaries. The waves have only moved small distances from the boundaries. When the process is near steady-state, for example, at $\bar{t}$ = 5.0, the wave fronts cannot be seen because they have passed completely through the material, and the boundaries were assumed to be completely absorbing boundaries. At this moment, the process is still not steady-state, and we can see from the figure that the intensities are two different distributions. At $\bar{t}$ = 10.0, the intensities are very similar distributions and they are almost parallel to each other. When the process is steady-state, the two curves for the two intensities will be similar to each other and exactly parallel to each other.

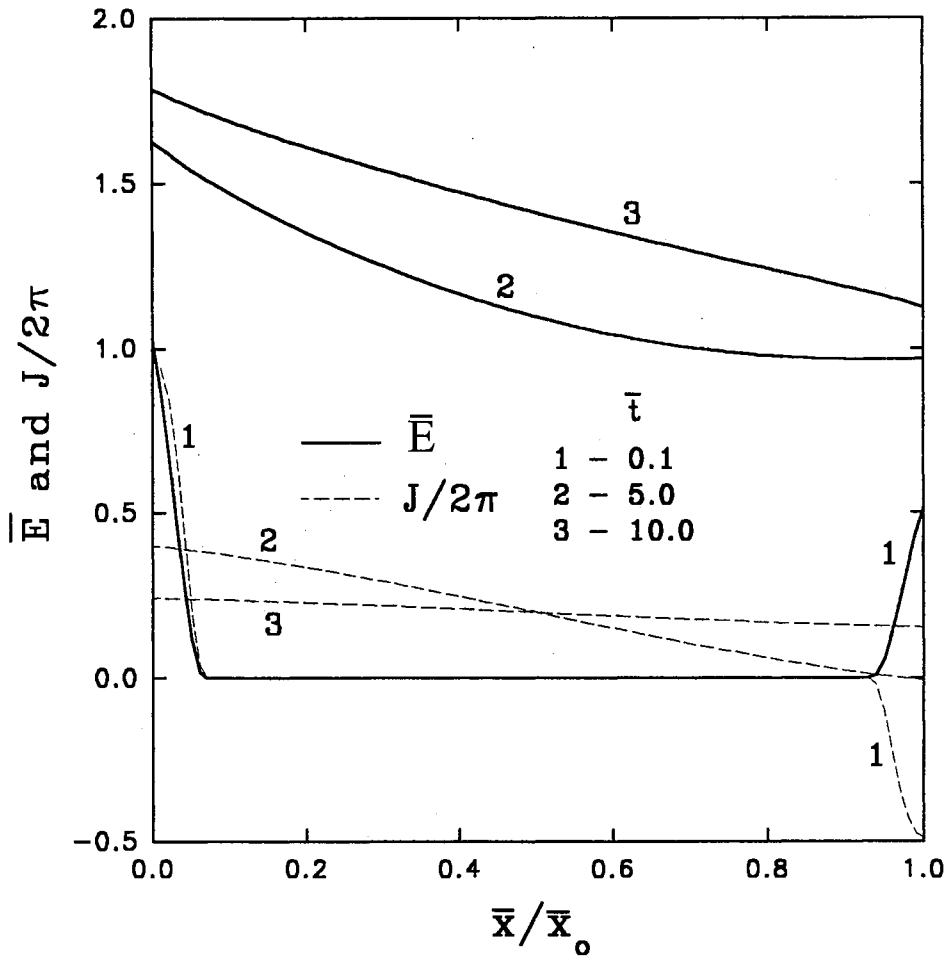

Fig. 7-7 Internal Energy and Heat Flux at an Early Stage and Near the Final Stages of the Transient Process ($\bar{x}_o$ = 1.0)

The internal energy and heat flux corresponding to the intensities shown in Fig. 7-6 are shown in Fig. 7-7. The early stage of the process is similar to the situation shown in Fig. 7-5. When the process is near steady-state, the heat flux teads to be uniform in the material. In the figure, we can see that at $\bar{t}$ = 5.0, the heat flux is close to a uniform distribution, and at $\bar{t}$ = 10.0, the distribution of heat flux is fairly uniform. The distribution of internal energy which is equivalent to temperature distribution is quite interesting. At the begining of the process, the internal energy wave is very clearly shown in the figure. As the process continues, the internal energy increases at the boundaries, the values of internal energy at the bounadries tend to the boundary conditions which are equal to 2.0 at

the left boundary and 1.0 at the right boundary. But the internal energy is not the same as the given boundary conditions even at $\bar{t} = 10.0$. As shown by curve 3 in Fig. 7-7, at the left boundary, the internal energy is less than the boundary value (2.0), and at the right boundary, it is higher than the boundary value (1.0). This phenomenon is called the boundary slip effect in radiative transfer. We will discuss this later as it applies to conduction.

From Fig. 7-7 and Fig. 7-5, we notice that the internal energy and heat flux waves are very different in their forms from the intensity waves shown in Fig. 7-3 and Fig. 7-6, especially in the early stages of the process. Now the question is why the waves of internal energy and heat flux do not have discontinuous wave fronts like the waves of the intensities. The reason is that the internal energy and heat flux are related to a combination of all of the intensities in all of the directions by integration. Since these intensities have different propagation speeds along the $\bar{x}$-axis, their distributions vary for different positions, but their integration smooths the discontinuities in the intensities. Figure 7-8 shows the intensity distributions at $\bar{t} = 1.5$. In this figure, the right boundary is set to $I_2^- = 0$, and the left boundary $I_1^+ = 1.0$. From this figure, we can see that the area under the intensity curve decreases as the position changes from 0.25 to 0.75 when the internal energy and heat current wave fronts are located at $\bar{t} = 1.5$. Since the area under the intensity curve changes (decreases) continuously, the wave fronts of internal energy and heat flux are not sharply discontinuous, but the slopes of these waves are discontinuous at the wave fronts.

The solution of internal energy (dimensionless temperature) at steady-state is shown in Fig. 7-9 for the boundary conditions given by Eq. (7-59). For this figure, we used Eq. (7-58b) to express the internal energy. If the temperature is much lower than Debye's temperature, the internal energy should be replaced by Eq. (7-58a). Since the phonon transport equation for the steady state process is the same as the radiation (photon) transport equation (Siegel and Howell, 1981), the result for the flux is the same

as that of the radiation transport equation. Majumdar (1993) also solved the same problem.

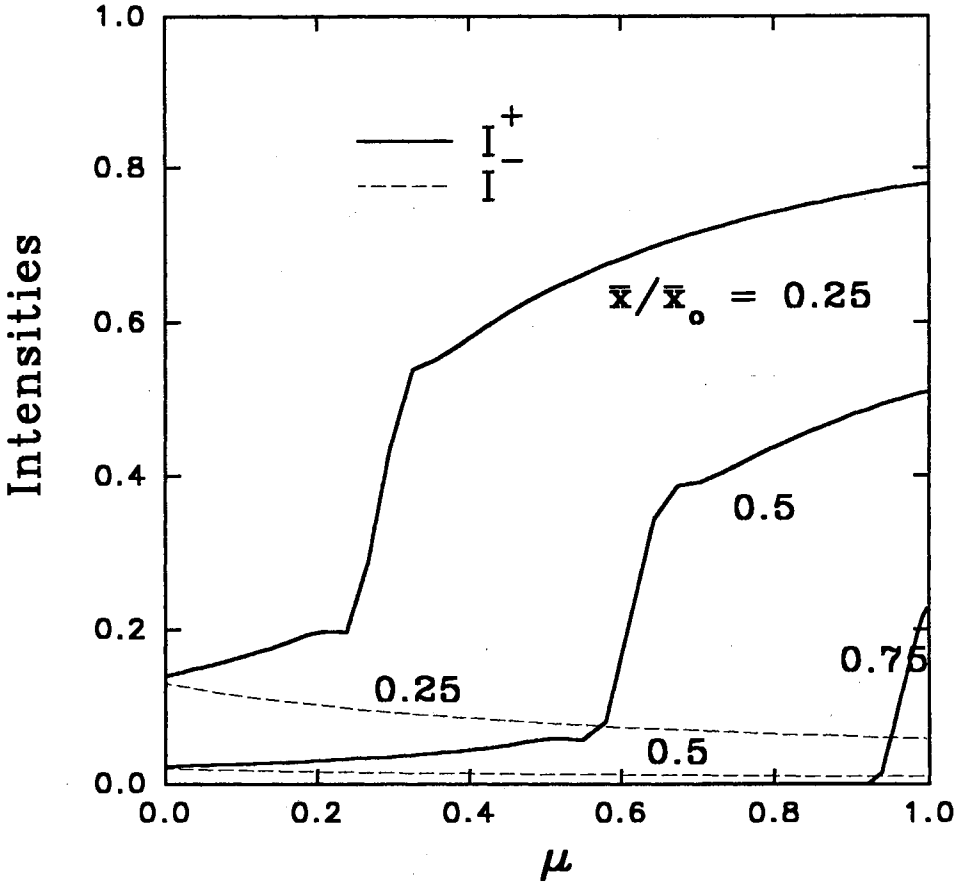

Fig. 7-8 Intensity Distribution at Different Positions and at Time $\bar{t}$ = 1.5

A comparison of our solution with the exact solution at the boundaries is given in Table 3. We can see that our numerical solution agrees very well with the exact solution for most situations except for $\bar{x}_o$ = 5.0. In the table, the exact solutions for $\bar{x}_o$ = 5.0 were not really exact because they were calculated using the suggested approximate relationships (Siegel and Howell, 1981). The approximate relationship is not very accurate for $\bar{x}_o$ = 5.0 because the acoustic thickness is not large enough for using the approximate relationship. This is the reason that the numerical solution in this case does not seem very accurate as compared to the exact solution.

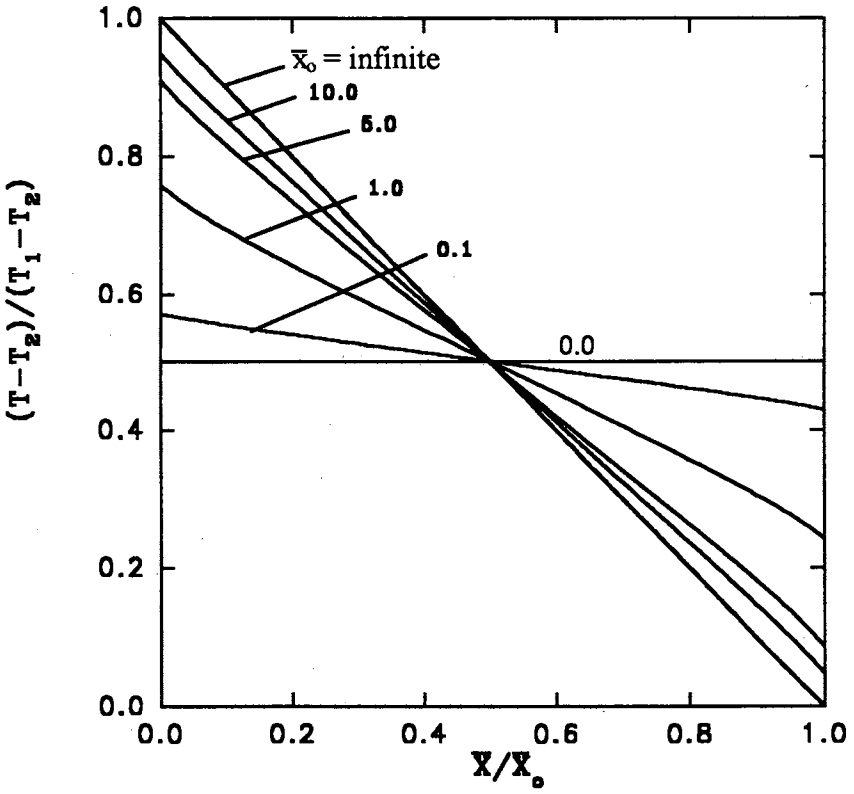

Fig. 7-9 Temperature Distribution Under Steady State Conditions

TABLE. 3 Comparison of Exact $\bar{E}$ with Numerical $\bar{E}$

$\bar{x}_o$	$\bar{E}(0)$ exact	$\bar{E}(0)$ num.	$\bar{E}(\bar{x}_o)$ exact	$\bar{E}(\bar{x}_o)$ num.
0.2	0.6114	0.6105	0.3886	0.3893
0.6	0.7051	0.7042	0.2948	0.2957
1.0	0.7581	0.7567	0.2418	0.2420
2.0	0.8307	0.8298	0.1692	0.1688
5.0	0.8935	0.9082	0.1065	0.0866

From Fig. 7-9, it is found that the temperature distributions for the acoustic thickness between 0.1 and infinity are not linear. This is caused by the internal scattering effect. When the acoustic thickness is infinite, the temperature distribution is linear and it is the same as the solution of the steady state parabolic heat conduction equation (Fourier's law).

The scattering effect is important for small acoustic thickness. From the figure, we also find that the temperatures are not continuous at the boundaries. At the left boundary, the given temperature is 1.0, but the temperatures inside the medium are less than the boundary temperature and the change is not continuous. Similarly, the temperatures are not continuous at the right boundary. This is called boundary slip in radiation. The cause of this effect is boundary scattering. The physical mechanism of boundary slip has been discussed in many radiation text books (Siegel and Howell, 1981, Sparrow and Cess, 1978). Majumdar (1993) has also discussed boundary slip for the phonon transport process. The steady state phonon process is basically the same as the photon process that is studied in radiation.

However, we are not very satisfied with the explanations given by the radiation theory. For heat conduction problems, boundary slip occurs only when the acoustic thickness of the material is fairly small. In this case, heat conduction is strongly non-equilibrium thermodynamically. We cannot even assume local thermodynamic equilibrium. Therefore, the temperature in the material is not well defined, or cannot be defined at all. Then what is meant by the temperature shown in Fig. 7-9 for small acoustic thickness? Our explanation is that the temperature does not represent the real temperature of the material. The temperature shown in Fig. 7-9 represents the local thermodynamic equilibrium states which represent the local non-equilibrium states in the material. At any local position in the material, if the local non-equilibrium state goes to an equilibrium state through an isentropic process, then the equilibrium state can represent the non-equilibrium state. Therefore, we can use the temperature for the equilibrium state to represent the non-equilibrium state. However, the temperature does not represent the real physical state. Based on this explanation, the boundary slip and even the temperature distribution for very small acoustic thickness really do not signify real physical states.

TABLE. 4 Comparison of $\overline{E}(\overline{x})$ by PTE with the Exact Solution

Parameters	$\overline{x}_o = 0.5$		$\overline{x}_o = 5.0$	
$\overline{x}/\overline{x}_o$	PTE	Exact	PTE	Exact
0.00	0.6844	0.6868	0.9068	0.9098
0.10	0.6409	0.6411	0.8093	0.8153
0.20	0.6043	0.6034	0.7243	0.7350
0.30	0.5648	0.5626	0.6460	0.6590
0.40	0.5301	0.5314	0.5611	0.5724
0.50	0.4987	0.4998	0.4853	0.4994
0.60	0.4636	0.4625	0.4024	0.4132
0.70	0.4272	0.4270	0.3283	0.3392
0.80	0.3951	0.3966	0.2462	0.2567
0.90	0.3571	0.3574	0.1706	0.1807
1.00	0.3118	0.3127	0.0851	0.0900

The numerical solution of PTE for long time period (near steady-state) is compared to the exact solution of the radiative transport equation. The boundary conditions for the problem are

$$I^{+}(\overline{x}=0,\mu)=1.0, \quad \text{and} \quad I^{-}(\overline{x}=\overline{x}_o,\mu)=0$$

The comparison given in Table. 4 shows that the difference between the numerical solution of the PTE and the exact solution is less than 5.5%. The accuracy of the numerical solution can be improved by solving the PTE for even longer time period so the solution is more close to steady-state solution.

7.4 Comparison of PHC, HHC, and Phonon Transport Theory

We have seen from section 7.3, that the internal energy and heat flux are waves that have non-dimensional propagation speeds equal to 1 (dimensionless). These waves are completely different from the waves given by the hyperbolic heat conduction model (HHC) in Chapter VI. In section 7.2, we have shown that both parabolic heat conduction (PHC) and hyperbolic heat conduction (HHC) can be derived from the transport equation. According to Majumdar (1993), the HHC is an approximation of the transport equation for large acoustic thickness. Also, according to radiative heat transfer (Siegel and Howell, 1981), and the discussion in section 7.2, parabolic heat conduction is a good approximation of the transport equation for large acoustic thickness. For steady state processes, the PHC is the same as the transport equation for very large acoustic thickness. This has been indicated in Fig. 7-7. However, for a transient process, the heat transfer is related to both acoustic thickness and time. Therefore, PHC and HHC may not be the same as the PTE even for large acoustic thickness.

In order to show the difference between these models, PHC and HHC will be compared with PTE. The PHC and HHC equations corresponding to transport equations (7-51) and (7-52) are

$$\frac{\partial U_0}{\partial \bar{t}} = -\frac{\partial U_1}{\partial \bar{x}}$$
$$\frac{\partial U_1}{\partial \bar{t}} + U_1 = -\frac{1}{3}\frac{\partial U_0}{\partial \bar{x}} \qquad (7\text{-}44)$$

for HHC, and

$$\frac{\partial U_0}{\partial \bar{t}} = -\frac{\partial U_1}{\partial \bar{x}}$$
$$U_1 = -\frac{1}{3}\frac{\partial U_0}{\partial \bar{x}}$$

for PHC. U_0 and U_1 are the first and second order moments of intensity. From Eqs. (7-56) and (7-57), these moments represent dimensionless temperature and heat flux

$$U_o = \frac{T - T_2}{T_1 - T_2} \quad \text{and} \quad U_1 = \frac{J}{2\pi}$$

and the initial temperature T_o is equal to T_2. The dimensionless time $\bar{t}$ and the dimensionless coordinate $\bar{x}$ are defined by Eq. (7-37).

Figure 7-10 shows the results from the three models for small acoustic thickness ($\bar{x}_o = 0.1$). At short times ($\bar{t} = 0.05$ and 0.5), we can see that the three models are very different from each other. Since acoustic thickness is small, the PHC solutions are almost steady state even at short time $\bar{t} = 0.05$. This is because the speed of heat transfer is infinite for the PHC, so it is very quick to get to steady state for small acoustic thickness. The HHC solutions are waves with discontinuous wave fronts, and the propagation speed is $(1/3)^{1/2}$. The magnitudes of the HHC solutions are higher than those of the PHC solutions. The solutions of the transport equation (PTE) are also waves. However, these waves are continuous at the wave fronts and have unit nondimensional propagation speed. The PTE solutions have very strong boundary scattering which is shown by the boundary slip in the temperature distribution. At time $\bar{t} = 5$, we see that HHC and PHC results are very close, except that HHC still shows a wave front. At time $\bar{t} = 8$, PHC and HHC are almost the same. However, they are very different from PTE. Obviously, both PHC and HHC are not accurate for small acoustic thickness.

Figures 7-11 and 7-12 show the comparison of the three models for acoustic thicknesses of $\bar{x}_o = 1.0$ and 5.0. Similar to Fig. 7-10, when the time is small, the three models are quite different from each other. When the time is large, the PHC and HHC results are very close, but they are different from PTE results because of boundary scattering (or boundary slip). When the acoustic thickness is very large, and the time is very long, the three models will be very close to each other, as shown in Fig. 7-12. In Fig. 7-12, the PHC results show that at the early time ($\bar{t} = 5$), the temperature is not linear, the physical process is still transient. Because the acoustic thickness is large, the process is still not steady even at $\bar{t} = 15$. Therefore, we can see that the PHC curve is not linear.

The results show that both PHC and HHC are good approximations for heat transfer for large acoustic thickness and long time periods. It was previously believed that the HHC is more accurate than the PHC for heat transfer for very small acoustic thickness and in extremely short time periods (Ozisik, 1984, Vick and Ozisik, 1983, Luikov, 1976, Taitel, 1972, Wiggert, 1977). From the results shown in Figs. 7-10, 7-11, and 7-12, we can conclude that the HHC is not accurate for small acoustic thickness or short time periods. Therefore, it appears that HHC should not be used to predict heat transfer for any engineering case. However, this does not mean that the hyperbolic heat conduction model is totally useless to engineering. In Fig. 7-13, we show the comparison of the temperature wave and heat flux wave from HHC with the Φ-wave and $\Psi/2$-wave for $\mu = 1.0$ from PTE. We can see that these waves are very similar in shape, although the speeds of the HHC waves are less than the speeds of the PTE waves. These waves all have discontinuous wave fronts, and dissipate during propagation. The waves of T and $\hat{q}$ from HHC are coupled together. Similarly, the waves of Φ and Ψ from PTE are also coupled with each other. These similarities between HHC waves and PTE waves are important, and they will be used to study the reflection properties of PTE waves in the next section.

Figure 7-14 shows the propagation of intensity waves ($\mu = 1.0$) and dimensionless temperature which are caused by a pulsed incident intensity from the left boundary. In this problem, the initial intensity was zero, and the magnitude of the pulsed incident intensity is 1.0, which corresponds to a pulsed temperature of T_s. The width of the pulsed incident intensity is $\Delta\bar{t}$ (= 0.025). From the figure, we find that the intensity along the $\bar{x}$-axis ($\mu =$ 1.0) is still a pulsed signal propagating in the medium with speed equal to 1. However, the temperature is not a pulsed wave, and the maximum value of the temperature is not at the position of the wave front when the time is large ($\bar{t} > 1.0$), but it is behind the wave front.

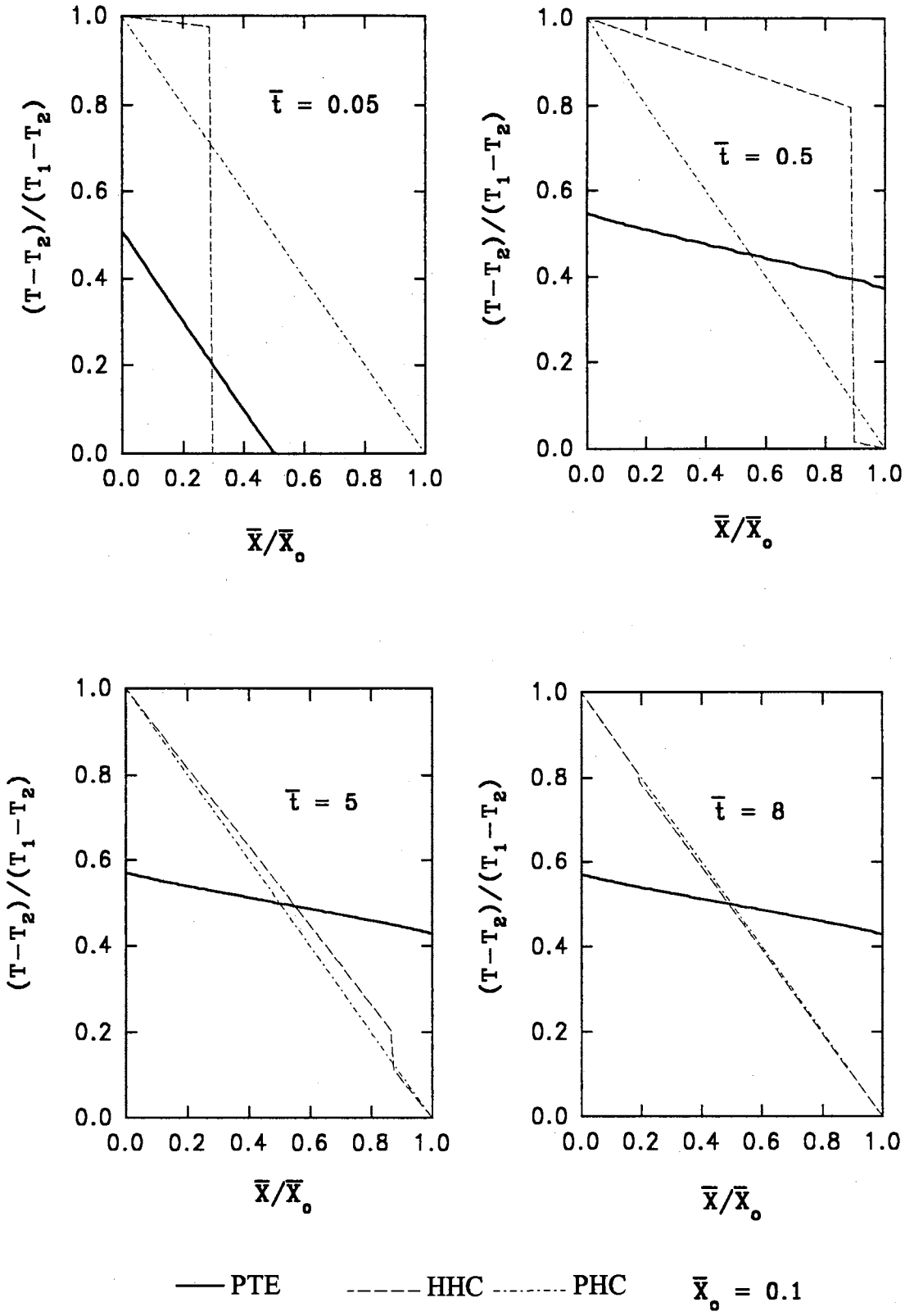

Fig. 7-10 Comparison of HHC, PHC and PTE for Small Acoustic Thickness

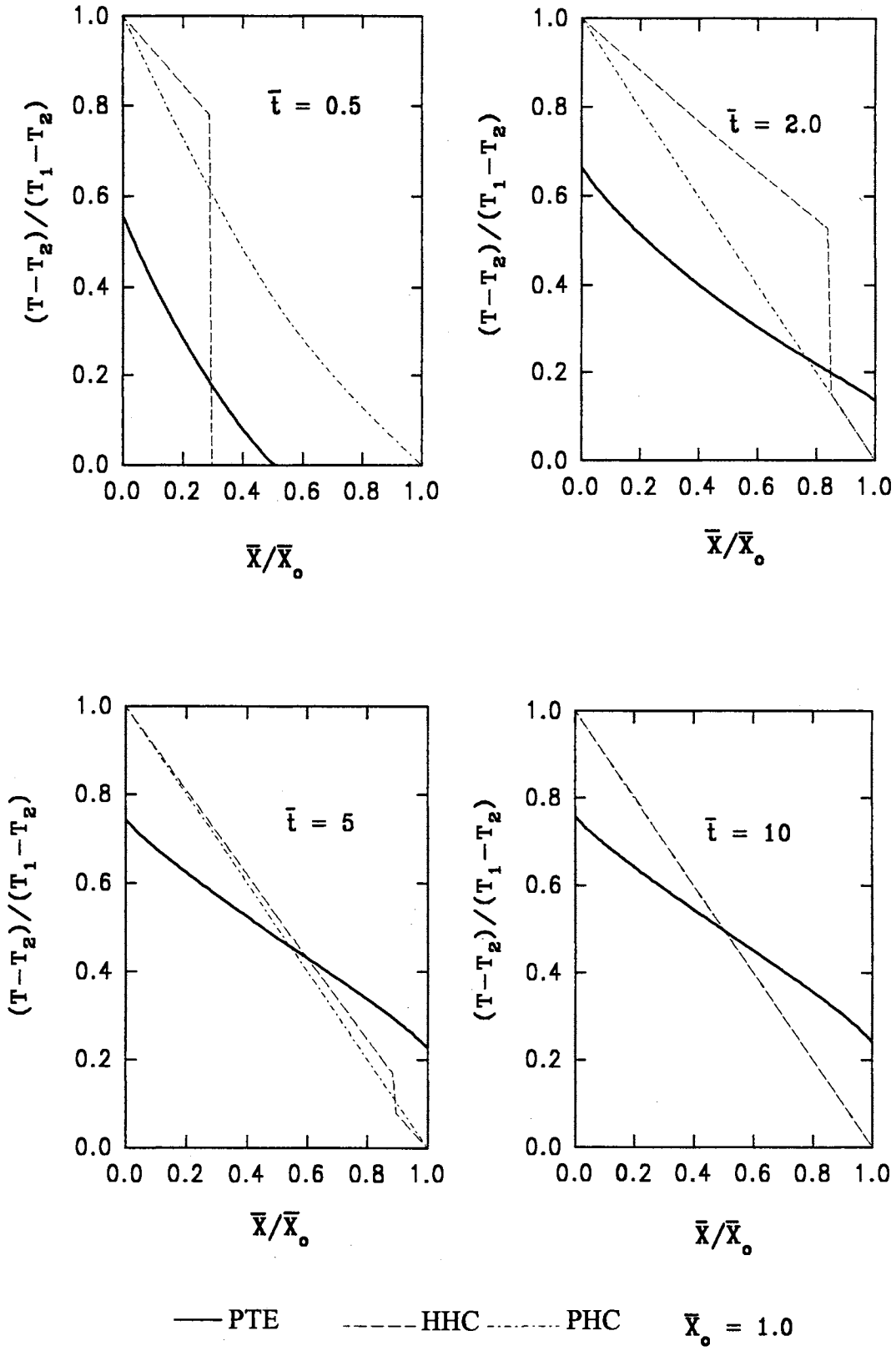

Fig. 7-11 Comparison of HHC, PHC and PTE for $\bar{x}_o = 1.0$

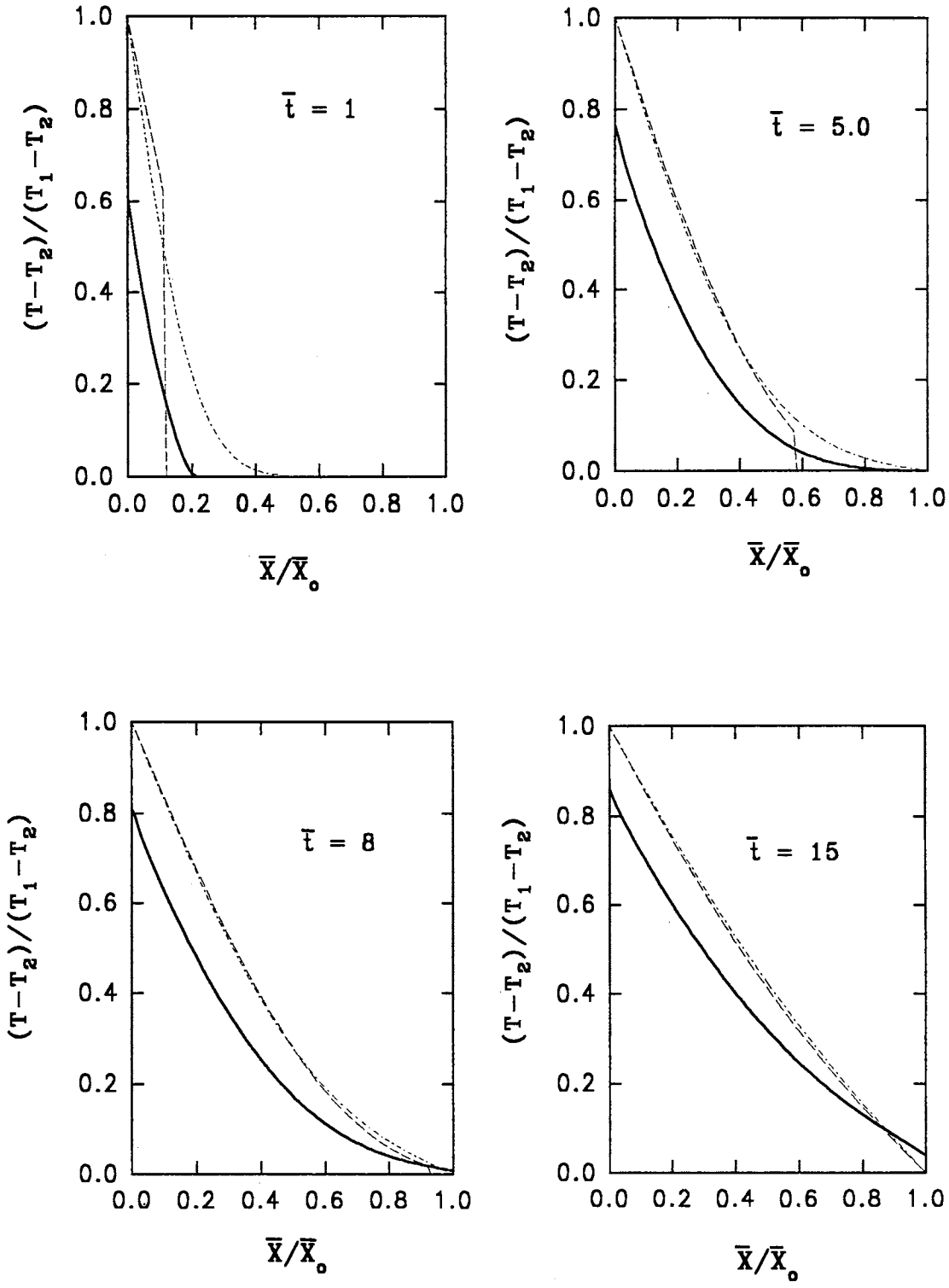

Fig. 7-12 Comparison of HHC, PHC and PTE for $\bar{x}_o = 5.0$

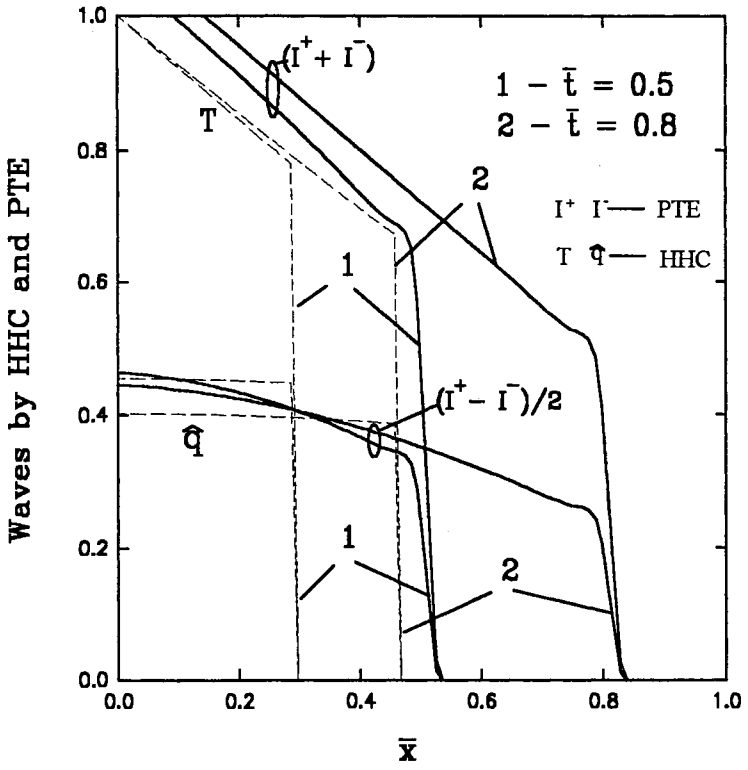

Fig. 7-13 Comparison of HHC Waves and PTE Waves

Since the intensities in different μ directions have different speeds which are in the range from 0 to 1, at any location behind the wave front, there always exists intensity that will contribute to the temperature change at that location.

The temperature change as a function of time is shown in Fig. 7-15. The results from HHC, PHC and PTE are compared with each other in the figure. As we can see from Fig. 7-15, the results from the three models are very different at the three different locations. The PHC results show that the pulsed change of the left boundary temperature can be felt immediately at any location in the medium, even very deep inside. This is because the propagation speed for the PHC model is infinite. The results from the transport equation (PTE) show that the pulsed change of the left boundary temperature cannot be felt at a certain location until the wave front reaches the location. It takes some time ($\bar{t} = \bar{x}/1.0$) for the wave front to get to location $\bar{x}$. From the figure, we find that the temperatures from the transport equation (PTE) are very similar to those from the PHC in

their trends. We believe that this is because of the scattering in the transport process. The scattering is strongly related to the diffusion process in the PHC model, and physically, the diffusion process is a strong scattering process. Therefore, it is not surprising that PHC and the transport equation (PTE) have some similar properties; and as we have discussed before, they are the same for large acoustic thickness and long time period processes.

The results from HHC are totally different from those of PHC and PTE. The temperature is a pulsed wave and its magnitude is much larger than those of PHC and PTE. This is because the HHC does not consider scattering effects, and thus the pulsed incident energy concentrates in a small region during its propagation in the medium. The temperature wave from HHC is similar to the intensity wave from PTE shown in Figs. 7-14 and 7-15. So the waves given by the HHC model are similar to the intensity waves given by the phonon transport equation (PTE).

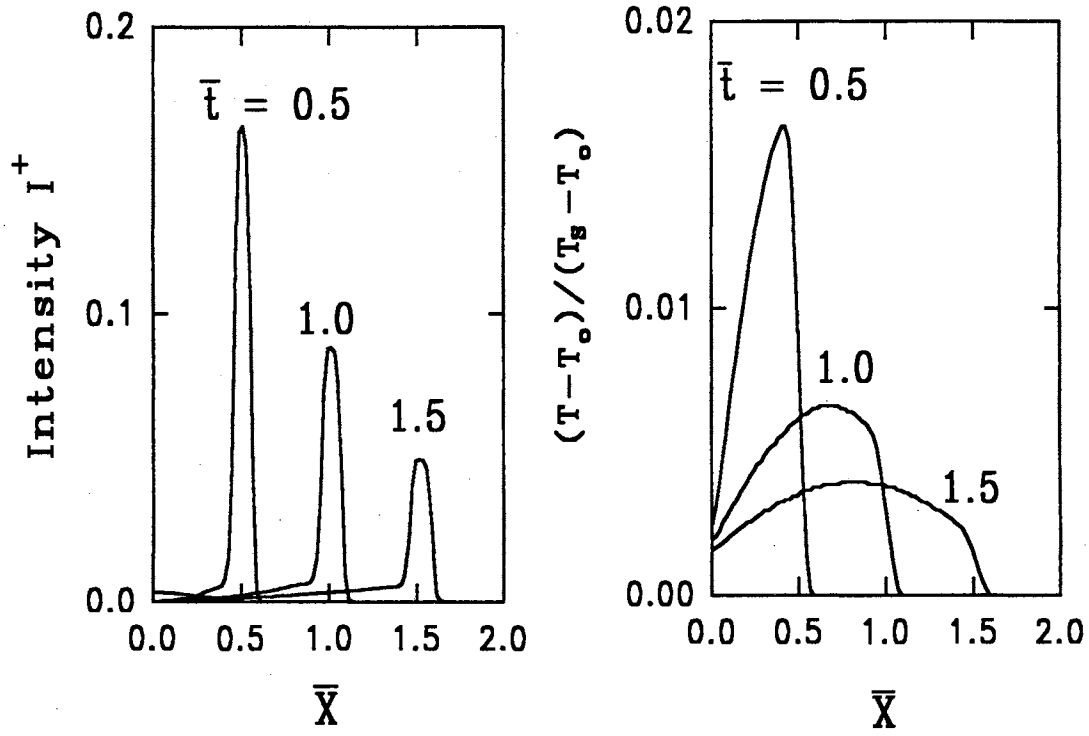

Fig. 7-14 Propagation of Pulsed Incident Intensity in One-Dimensional Medium

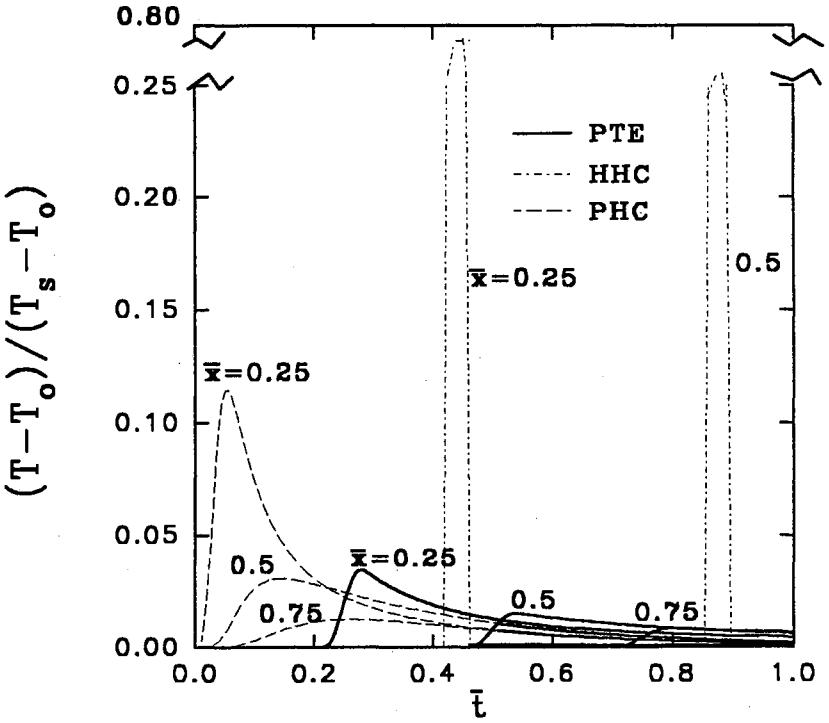

Fig. 7-15 Temperature Change as a Function of Different Positions

From the comparison between HHC, PHC and PTE, we see that these three models are very different for heat conduction problems with small acoustic thickness, or in very short time periods. We believe that phonon transport heat conduction is the most accurate model of these three heat conduction models. As we know, parabolic heat conduction was first developed as an empirical law (Fourier's law) based on experimental facts. Later, it was explained by using gas dynamics theory (Vincenti and Kruger, 1977, Roberts and Miller, 1960) for heat conduction in gases. In solid materials, heat conduction is explained successfully using phonon theory for most materials (Roberts and Miller, 1964). Both phonon theory and gas dynamics theory use the Boltzmann transport equation to derive Fourier's law.

It is believed that the Boltzmann transport equation is a very basic kinetic equation (based on Newton's law) to describe the behavior of all kinds of particles, including phonons and photons (Ziman, 1960, Kittel, 1986, Roberts and Miller, 1960, Bak, 1964).

Although the hyperbolic heat conduction model has been explained by many investigators using different theories, these explanations are not satisfactory for two reasons. The first is a theoretical reason. According to some explanations, thermal waves were assumed to be one-dimensional plane waves rather than diffusive waves. In other words, the particles were assumed to be moving one-dimensionally rather than randomly in all the directions in space. For example, in Weymann's (1967) random walk model, particles are assumed to be moving randomly in one-dimension by a step $\pm\ell$. Chester (1963) suggested that in the classic heat conduction equation

$$\frac{\partial T}{\partial t} = \alpha \nabla^2 T$$

the derivative with respect to time should be replaced by

$$\frac{\partial T}{\partial t} \rightarrow \tau \frac{\partial^2 T}{\partial t} + \frac{\partial T}{\partial t}$$

when heat conduction occurs in a very thin material during an extremely short time period, because the first order derivative is not accurate enough in this case. Other explanations made assumptions to simplify the original complicated Boltzmann transport equation. For example, in Cheng's (1989) study, the hyperbolic equation is the second approximation of the Boltzmann transport equation using the moment method. This is the same as the assumption we made in deriving Eqs. (7-51) and (7-52).

The second reason for the explanations of hyperbolic heat conduction being unsatisfactory is that so far we still do not have direct experimental proof to support the hyperbolic heat conduction theory. Although the thermal waves observed in liquid helium are very close to hyperbolic waves, they have been explained by using a two-fluid model (Bak, 1964) that are considered unique to liquid helium.

Therefore, due to the fundamental foundation of the Boltzmann equation as compared to the approximate treatment by HHC and PHC, we take the Boltzmann solutions or the phonon transport model as the benchmark. Both the parabolic model (PHC) and the hyperbolic model (HHC) are approximations of the transport theory. The

parabolic heat conduction model (PHC) is a good approximation for large acoustic thickness and large time scale. Although the hyperbolic model is also good for large acoustic thickness and large time scale, it is more complex than the parabolic model; and when the time period is not long enough, it is not as accurate as the parabolic model even for large acoustic thickness. For transient heat conduction problems, when acoustic thickness is very large, and the time period is very long, we can use the parabolic model to get good approximate results. This conclusion does not mean that the hyperbolic model is totally useless. Actually, the hyperbolic model is a very basic model that describes the thermal waves and their physical properties, although it cannot be directly used to predict heat transfer. We will discuss its applications in the prediction of reflection properties in the following section.

7.5 Reflection of Thermal Waves at an Interface

As we have presented in the previous sections, the temperature (or internal energy) and heat flux are two waves which are very different from the thermal waves according to the HHC model. Therefore, the reflection theory derived in Chapter III and Chapter IV cannot be applied directly to the waves from the transport theory. However, from section 7.4, we also notice that the waves from HHC are similar to the intensity waves from PTE in their propagation properties. Actually, the intensity waves in different μ directions are also hyperbolic waves with different speeds. Since intensity still possesses the features that hyperbolic waves have, the reflection theory derived for hyperbolic waves is still basic to the understanding of the reflection of internal energy and heat flux at an interface of two different media.

We have introduced wave functions Ψ and Φ in Eqs. (7-53) and (7-54). Since these functions are the basic functions of which internal energy and heat flux are composed, we call these two functions directional thermal waves. From Eqs. (7-51) - (7-54), the governing equations for Ψ and Φ can be derived

$$\frac{\partial \Psi(\bar{t},\bar{x},\mu)}{\partial \bar{t}}+\mu\frac{\partial \Phi(\bar{t},\bar{x},\mu)}{\partial \bar{x}}=-\Psi(\bar{t},\bar{x},\mu)+\int_0^1 \Psi(\bar{t},\bar{x},\mu')d\mu' \tag{7-61}$$

$$\frac{\partial \Phi(\bar{t},\bar{x},\mu)}{\partial \bar{t}}+\mu\frac{\partial \Psi(\bar{t},\bar{x},\mu)}{\partial \bar{x}}+\Phi(\bar{t},\bar{x},\mu)=0 \tag{7-62}$$

The terms on the right hand side of Eq. (7-61) do not make any contribution to the total heat transfer because the integration of Eq. (7-61) yields the energy conservation equation

$$\frac{\partial}{\partial \bar{t}}\int_{-1}^{1}\Psi(\bar{t},\bar{x},\mu)d\mu+\frac{\partial}{\partial \bar{x}}\int_{-1}^{1}\mu\Phi(\bar{t},\bar{x},\mu)d\mu=0 \tag{7-63a}$$

and thus

$$\int_0^1[-\Psi(\bar{t},\bar{x},\mu)+\int_0^1\Psi(\bar{t},\bar{x},\mu')d\mu']d\mu=0 \tag{7-63b}$$

So these terms only change the directional distribution of Ψ and Φ, and the changes are conservative over all directions. For this reason, we may approximate the above equations by

$$\frac{\partial \overline{\Psi}(\bar{t},\bar{x},\mu)}{\partial \bar{t}}+\mu\frac{\partial \overline{\Phi}(\bar{t},\bar{x},\mu)}{\partial \bar{x}}=0 \tag{7-64}$$

$$\frac{\partial \overline{\Phi}(\bar{t},\bar{x},\mu)}{\partial \bar{t}}+\mu\frac{\partial \overline{\Psi}(\bar{t},\bar{x},\mu)}{\partial \bar{x}}+\overline{\Phi}(\bar{t},\bar{x},\mu)=0 \tag{7-65}$$

Now the hat on the functions means that they are approximations. Equations (7-64) and (7-65) are the same hyperbolic wave equations as HHC Eq. (7-44) except that the dimensionless thermal conductivity in Eq. (7-65) is μ rather than 1/3. From these two equations and Eqs. (7-53) and (7-54), we can obtain the approximate intensity transport equations as

$$\frac{\partial \bar{I}^{+}(\bar{t},\bar{x},\mu)}{\partial \bar{t}}+\mu\frac{\partial \bar{I}^{+}(\bar{t},\bar{x},\mu)}{\partial \bar{x}}+\frac{1}{2}\bar{I}^{+}(\bar{t},\bar{x},\mu)=\frac{1}{2}\bar{I}^{-}(\bar{t},\bar{x},\mu) \tag{7-66}$$

$$\frac{\partial \bar{I}^{-}(\bar{t},\bar{x},\mu)}{\partial \bar{t}}-\mu\frac{\partial \bar{I}^{-}(\bar{t},\bar{x},\mu)}{\partial \bar{x}}+\frac{1}{2}\bar{I}^{-}(\bar{t},\bar{x},\mu)=\frac{1}{2}\bar{I}^{+}(\bar{t},\bar{x},\mu) \tag{7-67}$$

These equations can be solved and the results compared with those from Eqs. (7-51) and (7-52). Figure 7-16 shows the comparison of the results for small acoustic thickness ($\bar{x}_o$ = 0.1).

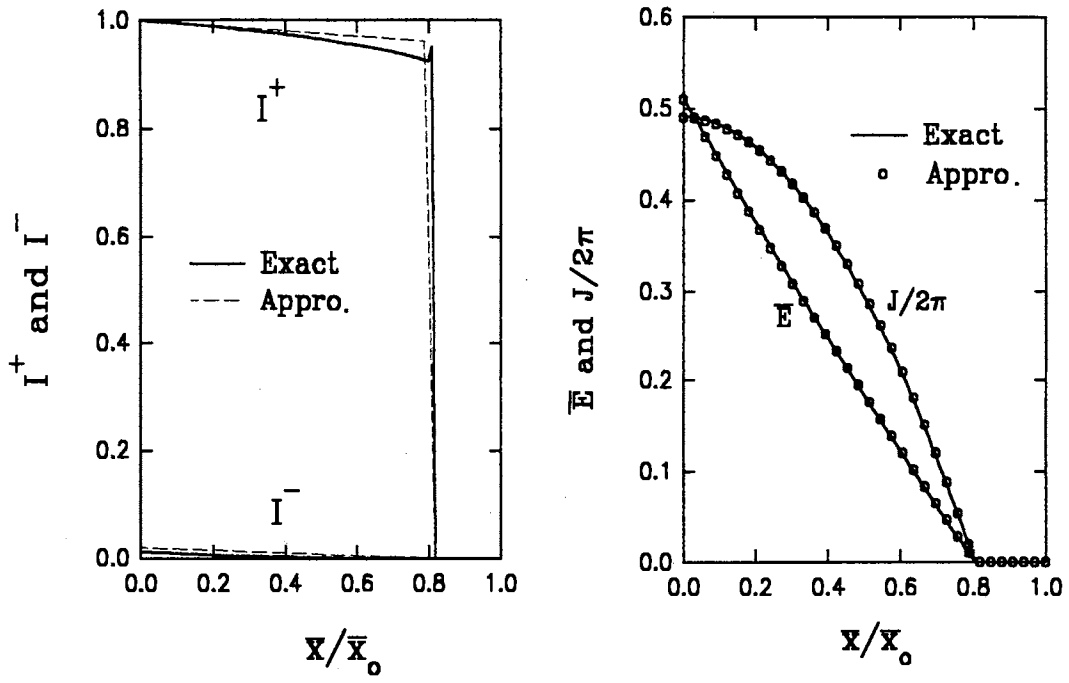

Fig. 7-16 Comparison of Intensity, Internal Energy and Heat Flux ($\bar{x}_o = 0.1$, $\bar{t} = 0.8$)

From the figure, we can see that the solutions from the approximate Eqs. (7-66) and (7-67) for intensity, internal energy and heat flux agree very well with the solutions from the exact Eqs. (7-51) and (7-52). Therefore, Eqs. (7-64) and (7-65) may be good approximations of Eqs. (7-61) and (7-62) for small acoustic thickness. For this reason, we propose to use Eqs. (7-64) and (7-65) to describe the wave behavior in the very small region around the interface between two different media. The reason that we use the approximation is that the approximate equations (Eqs. (7-64), (7-65)) are the same as the hyperbolic heat conduction equations that have been studied in detail in the previous chapters, then we may use the results from the previous chapters to study the reflection of phonon intensity.

As shown in Fig. 7-17, the wave propagating along the x'-axis can be written as

$$\frac{\partial \Psi(\bar{t}, x', \mu)}{\partial \bar{t}} + \frac{\partial \Phi(\bar{t}, x', \mu)}{\partial x'} = 0 \tag{7-66}$$

$$\frac{\partial \Phi(\bar{t}, x', \mu)}{\partial t} + \frac{\partial \Psi(\bar{t}, x', \mu)}{\partial x'} + \Phi(\bar{t}, x', \mu) = 0 \tag{7-67}$$

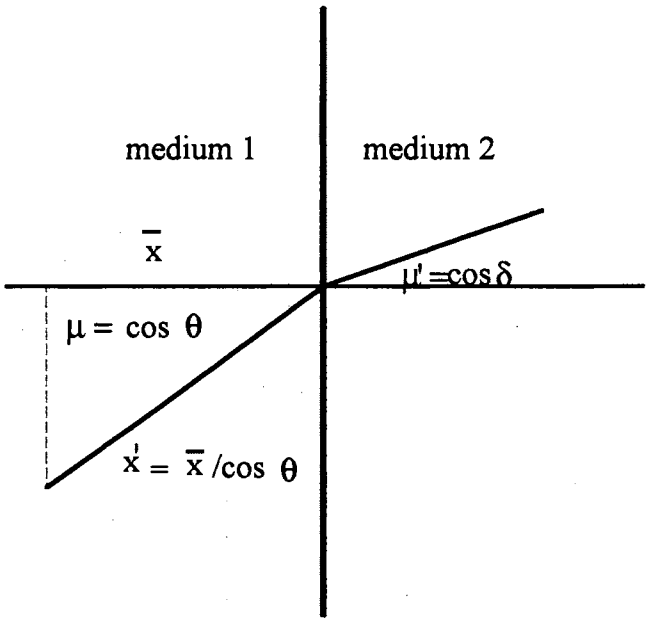

Fig. 7-17 The Interface and Incident Wave Directions

Equations (7-66) and (7-67) has the same form as the hyperbolic equations (Eqs. (1-1) and (1-4)) that have been studied in Chapter III and IV, except that the thermal capacity ρc_p is 1.0 and K is 1.0 for Eqs. (7-66) and (7-67). Therefore, we can directly use the conclusions obtained from those chapters.

The directional reflectivity for a harmonic wave is given by Eq. (3-24b)

$$\rho_{\lambda r} = \frac{TD\cdot\mu - \frac{\bar{n}_1}{\bar{n}_2}\mu'}{TD\cdot\mu + \frac{\bar{n}_1}{\bar{n}_2}\mu'} \tag{7-68}$$

where, TD is derived from Eq. (3-22), and is now the ratio of the acoustic speed in medium 1 to that in medium 2 since in Eqs. (7-66) and (7-67) the thermal capacity is unity, and the wave speed is the acoustic speed

$$TD = \frac{\bar{v}_1}{\bar{v}_2} \tag{7-69}$$

The incident angle and transmission angle are related to each other by the Snell's law given by Eq. (3-18). Then the reflection of the internal energy and heat flux can be found as (Eqs. (3-43))

$$\rho_{\lambda E} = \frac{\int_0^1 \rho_{\lambda r}(\mu)\Psi(\bar{t},\bar{x},\mu)d\mu}{\int_0^1 \Psi(\bar{t},\bar{x},\mu)d\mu} \tag{7-70}$$

and

$$\rho_{\lambda J} = \frac{\int_0^1 \rho_{\lambda r}(\mu)\mu\Phi(\bar{t},\bar{x},\mu)d\mu}{\int_0^1 \mu\Phi(\bar{t},\bar{x},\mu)d\mu} \tag{7-71}$$

where, $\bar{x}$ is the coordinate at the interface. Actually, when we solve the phonon transport equation, we need information about the reflection of intensities. The reflectivities given in the above equations are the reflectivities for functions Ψ and Φ. They are not the reflectivities for intensities which are needed in solving the transport equations. So Eqs. (7-70) and (7-71) are not very useful because we can not solve for internal energy and heat flux directly. Therefore, we must find the relationships for the intensities at the interface.

When the waves of Ψ and Φ strike the interface between two media, the incident waves, the reflected waves and transmitted waves are related to each other by the reflectivity $\rho_{\lambda r}$ (see Eqs. (3-14b) and (3-15))

$$\Psi_1(\bar{t},\bar{x},\mu)[1+\rho_{\lambda r}(\mu)] = \Psi_2(\bar{t},\bar{x},\mu') \tag{7-72}$$

and

$$\mu\Phi_1(\bar{t},\bar{x},\mu)[1-\rho_{\lambda r}(\mu)] = \mu'\Phi_2(\bar{t},\bar{x},\mu') \tag{7-73}$$

These two equations, especially Eq. (7-72) may not true for the actual physical process. These two equations seems to conflict each other. Actually, the temperature or Ψ will not be continuous at an interface of two materials. The discontinuity of interface temperature is discussed in Appendix II. Here, we assume that the temperature is continuous at an interface. Combining the above equations with Eqs. (7-53) and (7-54), we can obtain

$$I_2^+(\bar{t},\bar{x},\mu') = I_1^+(\bar{t},\bar{x},\mu)\frac{(\mu+\mu')+\rho_{\lambda r}(\mu)(\mu'-\mu)}{2\mu'}$$

$$+I_1^-(\bar{t},\bar{x},\mu)\frac{(\mu'-\mu)+\rho_{\lambda r}(\mu)(\mu'+\mu)}{2\mu'} \tag{7-74}$$

$$I_2^-(\bar{t},\bar{x},\mu') = I_1^-(\bar{t},\bar{x},\mu)\frac{(\mu+\mu')+\rho_{\lambda r}(\mu)(\mu'-\mu)}{2\mu'}$$
$$+I_1^+(\bar{t},\bar{x},\mu)\frac{(\mu'-\mu)+\rho_{\lambda r}(\mu)(\mu'+\mu)}{2\mu'} \tag{7-75}$$

where the subscript 1 represents the variables on the left side of the interface in medium 1, and the subscript 2 represents the variables on the right side of the interface in medium 2. These equations give the boundary conditions for intensities at an interface. These boundary conditions are very important when we solve the transport equations in non-homogeneous medium. The reflectivity can be obtained from Chapter III and Chapter IV. We can see from Eqs. (7-74) and (7-75) that the intensities at the interface are not continuous because of reflection. To solve for the four intensities, transport Eqs. (7-51) and (7-52) should be combined with the above two equations. Since we have discussed the reflection of hyperbolic waves in Chapter III and Chapter IV, we will not repeat our discussion here. However, from the study of this section, we realize that hyperbolic waves are the basic waves for intensity. Therefore, they are still very useful for the study of phonon transport processes. The hyperbolic model can be used to study the basic wave properties which are necessary and important for phonon transport processes. The study of reflection presented in this thesis is an example of the application of the hyperbolic heat conduction model.

CHAPTER VIII

CONCLUSIONS AND RECOMMENDATIONS

Through the previous study, we have seen that a thermal wave is a special wave which is different from other waves such as electromagnetic waves. First, as we have mentioned before, a thermal wave consists of two energy waves. One is the internal energy of the material, the other is the heat flow in the material. These two waves exchange energy during their propagation. Second, the heat flow is a vector, and the internal energy is a scalar wave. Therefore, they behave differently during propagation. In this chapter, we will draw conclusions on our research.

8.1 Conclusions

From the theoretical and numerical study of thermal waves presented in the previous chapters, we can arrive at the following conclusions:

1. According to the review of the previous studies of thermal waves, we realize that the reflection process of hyperbolic thermal waves by an interface between two different materials, or by the boundary of a material has not been studied very much. The knowledge of this important process is still very limited. There is not a formula for reflectivity that is readily available for engineering applications. There is not an investigation of two-dimensional reflection published in the open literature. Although the phonon transport theory has been studied by several investigators, transient processes have not been studied. The wave behavior of heat transfer in transient processes is very important, especially for small acoustic thickness and short time periods. No previous work exists to compare transport theory, hyperbolic heat conduction theory and parabolic heat conduction theory and to examine the accuracy of these theories.

2. The theoretical study of the reflection process of one-dimensional hyperbolic thermal waves in this research provides a theory that can be used the explain and calculate the reflectivity of a hyperbolic thermal wave which is reflected by either an interface in a composite material or at a boundary of a material. We have found that the parameter TD (defined in Chapter III) is a very important parameter for reflection. Depending on the value, the reflectivity can be positive, negative, or zero. Closed form equations are presented for the calculation of reflectivity for engineering applications.
3. The theoretical study of two-dimensional thermal waves provides us with the basic theory of the reflection process of a two-dimensional thermal wave at an interface in a composite material. The discussion of the mechanism of the reflection process and the wave propagation after being reflected at the interface shows that the reflection can be completely different for different situations. Relationships for directional reflectivity are presented for engineering applications.
4. So far, we have not found studies of numerical solutions of thermal waves in composite materials, neither for one-dimensional situations nor for two-dimensional situations. This research is the first one that has used several numerical methods to solve these types of problems. Also, in this research, the control volume finite difference method has been developed to solve for one and two-dimensional thermal waves in composite materials and homogeneous materials. Although we did not use the control volume finite difference method to solve for one-dimensional thermal waves in this study, the method can be easily used for 1-D, 2-D, and 3-D problems; and it can also be easily used for parabolic heat conduction problems.
5. The theoretical and numerical results have shown that the theory presented in this research can be directly applied to predict the reflection of one-dimensional hyperbolic thermal waves. By using the numerical solutions, we have explained the mechanism of negative reflectivity. We have seen that the exchange of energy between the internal energy (temperature wave) and the heat flow (heat flux wave) is very important

because it is this exchange that makes it possible for the reflectivity to be negative. The numerical solutions of two-dimensional hyperbolic thermal wave problems have shown the agreement of the trend in the reflection process between the closed form theory and the numerical results. The reflectivity does not agree with the closed form theory very well, and this appears to be due to several factors. One is that the numerical examples do not exactly satisfy the conditions of the closed form theory. There always exist the boundary reflection effects which interfere with the reflection at an interface. The closed form theory does not account for these but the numerical solution does. Secondly, the incident thermal wave for the two-dimensional situation is not a collimated plane wave as for a one-dimensional problem, but it is a directionally diffuse wave which arrives at the interface from all directions. Therefore, the reflectivity provided by the theory can not handle this wave since the theory treats the incident waves as plane waves only along one direction.

6. Debye's phonon theory is reviewed in this research. The general phonon transport equation (Eq. 7-22) has been derived based on Debye's phonon theory. The simplified one-dimensional phonon transport equation in an isotropic medium is solved numerically by using the TVD method. From the solutions for intensity, the temperature (or internal energy) and heat flux, we found that the intensity is a wave with similar wave properties to the hyperbolic waves studied in Chapters III, IV and VI. However, the temperature and heat flux are quite different from the hyperbolic thermal wave studies in those chapters. They do not have sharply discontinuous wave fronts, and their speed is larger than the speed of hyperbolic thermal waves.
7. The relationship between the transport equation, hyperbolic model, and Fourier's law is discussed. It is found that HHC and PHC are two different approximations of the transport equation (PTE). From numerical solutions for the PHC, HHC and PTE, the three models are compared. The comparison shows that the three models are very close when the time period and dimensional scales (acoustic thickness) are very large

compared to the relaxation time and the phonon mean free path. For small time period and small dimensional scales, the PHC does not have a wave behavior at all; while the HHC produces waves, but the wave speed is only $(1/3)^{1/2}$ of the actual acoustic speed, and the wave front is very sharp. Also HHC can not predict the boundary scattering effects. The phonon transport equation is much more realistic, and I believe that it accurately predicts temperature and heat flux waves and boundary scattering.

8. Although the hyperbolic thermal waves are not accurate in most cases, we found that the intensity waves from the transport equation are very similar to the hyperbolic thermal waves in their behavior. An approximate transport equation (Eqs. (7-66) and (7-67)) is derived for small acoustical thickness; and from this equation, we found that the intensity waves are actually the same kind of waves as hyperbolic thermal waves. Therefore, we can apply the conclusions for reflectivity obtained for hyperbolic thermal waves to phonon intensity reflection.

8.2 Topics for Future Research

As we can see from the present study, there are many important unsolved problems for thermal waves. We cannot solve all of these problems in this research. We realized from our study that the phonon transport theory is the key to solve heat conduction problems in microscale materials. However, this theory is still a framework and many details need to be filled in. Our understanding of the phonon transport process needs to be expanded. Based on our study, we would suggest several important topics for further research.

8.2.1. Thermal Wave Reflection Process

The phonon transport theory is especially useful for microscale heat conduction problems. One-dimensional heat transfer is very important because most of microscale heat conduction problems are one-dimensional. In our study, we have given a quite clear description of one-dimensional hyperbolic thermal waves and their reflection processes.

We also proved that phonon intensity waves are hyperbolic waves and the reflection of phonon intensity waves can be predicted by using the theory for hyperbolic thermal waves. However, our study still has not completely solved the phonon reflection problem, it only showed a way to approach this problem. Research is needed to determine the more general relationship between the reflection of hyperbolic waves and the reflection of phonon intensity waves.

With the study of the reflection of phonon intensity, we can further study the heat transfer in multi-layer materials, and predict the apparent physical properties of the materials such as apparent thermal conductivity. This is a very important step to put the phonon transport theory into engineering applications.

8.2.2. Phonon Scattering Process

In our study, we did not discuss in depth the phonon scattering process, for example, the collision between phonons and between phonons and other particles. We simply used the relaxation time approximation to simplify the scattering term in the Boltzmann transport equation and the phonon transport equation. Actually, the phonon scattering process is very complicated. There are two basic scattering processes, one is called the N-process, or normal process, and another is called the U-process, or Umklap process. For the N-process, the wave vectors of the phonons involved in a collision are conserved. For the U-process, the wave vectors of the phonons involved in a collision are not conserved. These processes are responsible for the heat conduction properties. So far, there is not easy way to link the achievements of physics to practical applications. These results are so complicated that they are not yet suitable for engineering computation. Therefore, there are diverse problems that need to be studied in this field.

The study of the phonon scattering process probably is the most difficult part in the phonon transport theory because it not only requires a strong knowledge of thermal science, but also requires strong background in physics, especially in solid state physics and in quantum theory.

8.2.3. Phonon-Electron Process in Conductors

Pure phonon heat transfer only occurs in dielectric materials. In conductors or semi-conductors, both phonons and electrons are important for heat transfer. Therefore, the contribution of electrons to heat conduction should be considered. Now the technique to include the electrons in a heat conduction process is to use Mathiessen's law (Ziman, 1960) to find the equivalent relaxation time for the scattering term in the phonon transport equation

$$\frac{1}{\tau} = \frac{1}{\tau_{ph}} + \frac{1}{\tau_{el}} + \frac{1}{\tau_{ph-el}}$$

where subscripts ph stands for the relaxation time for phonons, el stands for the relaxation time for electrons, and ph-el stands for the relaxation time for phonon-electron collision. With this approximation, we can only consider one kind of particle, either phonons or electrons, as the dominant particle in heat transfer. This is a very rough treatment. We actually should develop the transport equation for electrons (this is fairly easy after we have developed the phonon transport equation). The transport equations for phonons and electrons are coupled by the scattering (this is the difficulty). Then the total heat transfer is related to both phonons and electrons.

8.2.4. Effect of Polarization

Elastic waves in solids are polarized in three modes, two transverse modes and one longitudinal mode. Therefore, the physical states of phonons are related to the polarization modes. In our study, we did not consider the effect of polarization on heat transfer, but summed over all polarization modes.

The phonon speeds for different polarization modes are different. The wave frequency is also polarization-dependent. Therefore, in the phonon transport equation, the intensity will have three components corresponding to the three polarization modes. The three components may not be indepentent of each other. The first question that needs to be answered is how are the three components related to each other, and how can one

consider their relationships in the transport equations for the three components? The second step is how to solve the resulting transport equations.

The above listed topics are only few important ones that could be solved in near future. We consider them as the basic topics. With the solutions of these problems, the phonon transport theory will be fairly complete and portable for engineering applications, and it will be more like an *engineering* theory which is simple, clear, and practical. Two- and three-dimensional problems may be studied in the future, but these are not very significant for engineering because the phonon transport theory is basically applied to extremely thin (one-dimensional) materials. The thermal wave theory is a bright and important field in heat transfer. We believe many achievements will be made by many research studies in the near future.

REFERENCES

Bak, T. A. (Editor) (1964), **Phonons and Phonon Interactions,** W. A. Benjamin, Inc., New York.

Baumeister, K. J. and Hamill, T. D. (1969), "Hyperbolic Heat Conduction Equation- a Solution for the Semi-Infinite Body Problem," ***J. Heat Transfer,*** **91**, pp. 543-548.

Berkovsky, B. M. and Bashtovoi, V. G. (1977), "The Finite Velocity of Heat Propagation from the Viewpoint of Kinetic Theory," ***Int. J. Heat Mass Transfer,*** **20**, pp. 621-626.

Bertman, R. and Sandiford, D. J. (1970), "Second Sound in Solid Helium," ***Scient. Am.,*** **222(5)**, pp. 92-101.

Bland, D. R. (1988), **Wave Theory and Applications**, *Oxford Univ. Press*, New York.

Bohren, C. F. and Huffman, D. R. (1983), **Absorption and Scattering of Light by Small Particles,** *John Wiley & Sons, Inc.*, New York.

Chan, S. H. , Low, M. J. D. and Mueller, W. K. (1971), "Hyperbolic Heat Conduction in Catalytic Supported Crystallites," ***AICHE J.,*** **17**, pp. 1499-1501.

Cheng, K. J. (1989), "Wave Characteristics of Heat Conduction Using a Discrete Microscopic Model," ***J. Heat Transfer,*** **111**, pp. 225-231.

Chester, M. (1963), "Second Sound in Solids," ***Phys. Rev.,*** **131(5)**, pp. 2013-2015.

Curtin, M. E. and Pipkin, A. C. (1969), "A General Theory of Heat Conduction with Finite Wave Speeds," ***Arch. Rational. Mech. Anal.,*** **31**, pp. 113-126.

Cusumano, J. A. and Low, M. J. D. (1970), "Infrared Radiometry of Thermal Transients on Surfaces," ***J. Catalysis,*** **17**, pp. 98-105.

Del Grande, N. K., Dolan, K. W., Durbin, P. F. and Shapiro, A. B. (1993), "Dynamic Thermal Tomography for Nondestructive Inspection of Aging Aircraft," ***Proc. of Nondestructive Inspection of Aging Aircraft Conference,*** **2001**, Society of Photo-Optical Instrumentation Engineers, San Diego, CA, July 14-15.

Dougherty, R. L. and Price, C. E. (1994), "Corrosion Detection in Airframes," submitted to Oklahoma Center for the Advancement of Science and Technology (OCAST).

Frankel, J. I., Vick, B. and Ozisik, M. N. (1987), "General Formulation and Analysis of Hyperbolic Heat Conduction in Composite Media," ***Int. J. Heat Mass Transfer,* 30**, pp. 1295-1305.

Goodson, K. E. and Flik, M. I. (1993), "Electron and Phonon Thermal Conduction in Epitaxial High-T_c Superconducting Films," ***J. Heat Transfer,* 115**, pp. 17-24.

Harrington, R. E. (1966), "Anomalous Surface Heating Rates," ***J. Appl. Phys.,* 37**, pp. 2028-2034.

Hess, L. D., Kokorowski, S. A., Olson, G. L., and Yaron, G. (1981), "Laser Processing of Silicon for Advanced Microelectronic Devices and Circuits," in **Laser and Electron-Beam Solid Interactions and Material Processing,** edited by Gibbons, J. F., Hess, L. D., and Sigmon, T. W., New York, pp. 307-319.

Hus, Y. Y. (1962), "On the Size Range of Nucleation Cavities on a Heating Surface," ***J. of Heat Transfer,* 84**, pp. 207-216.

Kaminski, W. (1990), "Hyperbolic Heat Conduction Equation for Materials with a Nonhomogeneous Inner Structure," ***J. of Heat Transfer*, 112**, pp. 555-560.

Kazimi, M. S. and Erdman, C. A. (1975), "On The Interface Temperature of Two Suddenly Contacting Materials," ***J. Heat Transfer*, 97**, pp. 615-617.

Kittel, C. (1986), **Introduction to Solid Physics**, 6th ed., Wiley, New York.

Klitsner, T., VanCleve, J. E., Fischer, H. E., and Pohl, R. O. (1990), "Phonon Radiative Heat Transfer and Surface Scattering," ***Physics Review B,* 38,** pp. 7576-7594.

Kreyszig, E. (1983), **Advanced Engineering Mathematics**, *John Wiley & Sons*, New York.

Luikov, A. V. (1966), "Application of Irreversible Thermodynamics Methods to Investigation of Heat and Mass Transfer," ***Int. J. Heat Mass Transfer,* 9**, pp. 139-152.

Luikov, A. V., Bubnov, V. A. and Soloviev, I. A. (1976), "On Wave Solution of the Heat Conduction Equation," ***Int. J. Heat Mass Transfer,*** **19**, pp. 245-248.

Luss, D. and Amundson, N. R. (1969), "Maximum Temperature Rise in Gas-Solid Reactions," ***AICHE J.,*** **15**, pp. 194-198.

Maher, W. E. and Hall, R. B. (1980), "Pulsed Laser Heating Profile Width and Changes in Total Coupling with Pulse Length and Pressure," ***J. Appl. Phys.,*** **51(3)**, pp. 1338-1344.

Majumdar, A. (1993), "Microscale Heat Conduction in Dielectric Thin Films," ***J. Heat Transfer, 115,*** pp. 7-16.

Maldague, X., Krapex, J. C. and Cielo, P. (1991), "Subsurface Flaw Detection in Reflective Materials by Thermal Transfer Imaging," ***Optical Engineering,*** **30**, pp. 117-125.

Maxwell, J. C. (1867), "On the Dynamic Theory of Gases," ***Phil. PTE. R. Soc.,*** **157**, pp. 49-88.

Ozisik, M. N. (1984), "Propagation and Reflection of Thermal Waves in a Finite Medium," ***Int. J. Heat Mass Transfer,*** **27**, pp. 1845-1854.

Ozisik, M. N. (1980), **Heat Conduction**, John Wiley & Sons, Inc., New York.

Patankar, S. V. (1981), "A Calculation Procedure for Two-Dimensional Elliptic Situations," ***Numer. Heat Transfer,*** **4**, pp. 409-425.

Peshkov, V. (1944)," 'Second Sound' in Helium II," ***J. Phys., USSR VIII,*** p. 381.

Prater, C. D. (1958), "The Temperature Produced by Heat of Reaction in the Interior of Porous Particles," ***Chem. Eng. Sci.*** **8**, pp. 284-286.

Roberts, J. K. and Miller, A. R. (1960), **Heat and Thermodynamics,** 5th ed., Interscience Publishers, Inc., New York.

Siegel, R. and Howell, J. R. (1981), **Thermal Radiation Heat Transfer**, 2nd Edition, *Hemisphere Publishing Co.*, New York.

Sparrow, E. M. and Cess, R. D. (1978), **Radiative Heat Transfer**, Belmont, California.

Stritzker, B., Pospieszczyk, A., and Tagle, J. A. (1981), "Measurement of Lattice Temperature of Silicon During Pulsed Laser Annealing," ***Phys. Rev. Lett.*, 47(5)**, pp. 356-358.

Swartz, E. T. and Pohl, R. O. (1989), "Thermal Boundary Resistance," ***Reviewing of Modern Physics*, 61(3),** pp. 605-666.

Taitel, Y. (1972), "On the Parabolic, Hyperbolic and Discrete Formulation of the Heat Conduction Equation," ***Int. J. Heat Mass Transfer*, 15**, pp. 369-371.

Tzou, D. Y. (1989), "On the Thermal Shock Wave Induced by a Moving Heat Source," ***J. Heat Transfer*, 111**, pp. 232-238.

Tzou, D. Y. (1993), "Reflection and Refraction of Thermal Waves from a Surface or an Interface Between Dissimilar Materials," ***Int. J. Heat Mass Transfer*, 36**, pp. 401-410.

Tzou, D. Y. (1993), "An Engineering Assessment to the Relaxation Time in Thermal Wave Propagation," ***Int. J. Heat Mass Transfer*, 36**, pp. 1845-1851.

Vernotte, P. (1958), "Les Paradoxes de la Theorie Continue de Equation de la Chaleur", ***C. R.*, 246**, pp. 3154-3155.

Vick, B. and Ozisik, M. N. (1983), "Growth and Decay of a Thermal Pulse Predicted by the Hyperbolic Heat Conduction Equation," ***J. Heat Transfer*, 105**, pp. 902-907.

Vincenti, W. G. and Kruger, C. H. (1977), **Introduction to Physical Gas Dynamics**, Robert Krieger Publisher, New York.

Weymann, H. D. (1967), "Finite Speed of Propagation in Heat Conduction, Diffusion, and Viscous Shear Motion," ***Am. J. of Phys.*, 35**, pp. 488-496.

Wiggert, D. C. (1977), "Analysis of Early-Time Transient Heat Conduction by Method of Characteristics," ***J. Heat Transfer*, 99**, pp. 35-40.

Yang, H. Q. (1990), "Characteristic-Based, High-Order Non-Oscillatory Numerical Method for Hyperbolic Heat Conduction," ***Numer. Heat Transfer Part B*, 18,** pp. 221-241.

Yang, H. Q. (1992), "Solution of Two-Dimensional Hyperbolic Heat Conduction by High-Resolution Numerical Methods," AIAA-92-2937, ***AIAA 27th Thermophysics Conference,*** July 6-8, 1992, Nashville, TN.

Ziman, J. M. (1960), **Electrons and Phonons**, Oxford University Press, London.

APPENDIX I

1. PHC Code: This code was developed to solve one-dimensional diffusive heat conduction (PHC) problem using the control volume method. The thermal diffusivity is set to be equal to 1/3 (GAM = 1/3.0). The physical dimension is normalized by XL, the total thickness of the material.

```
C
C     THERMAL WAVE SOLUTION PHC MODEL
C                April 25, 1993
C     ---------------------------------------
      DIMENSION AP(100),AE(100),AW(100),B(100),X(100)
      DIMENSION T(100),F(100),T0(100),P(100),Q(100)
      OPEN(UNIT=1,FILE='phc.D')
      WRITE(*,10)
10    FORMAT(2X,'INPUT THE XL,TMAX:')
      READ(*,*)XL,TMAX
      GAM=1/3.0
      N=100
      DT=0.001
      DX=XL/FLOAT(N-1)
      TIME=DT
      DO 15 I=1,N
      X(I)=XL*FLOAT(I-1)/FLOAT(N-1)
      AE(I)=GAM*DT/DX
      AW(I)=GAM*DT/DX
      AP(I)=AE(I)+AW(I)+DX
      T(I)=0.
      T0(I)=0.
15    CONTINUE
      T(1)=1.0
      T0(1)=1.0
      AW(1)=0.
      AE(N)=0.
      iter=0
50    DO 25 I=2,N-1
      B(I)=T0(I)*DX
25    CONTINUE
      B(N)=T(N)
      B(1)=T(1)
      AP(N)=1.0
      AW(N)=0.0
      AP(1)=1.0
      AE(1)=0.0
      P(1)=0.0
      Q(1)=B(1)
      DO 30 I=2,N
      P(I)=AE(I)/(AP(I)-AW(I)*P(I-1))
      Q(I)=(Q(I-1)*AW(I)+B(I))/(AP(I)-AW(I)*P(I-1))
30    CONTINUE
      T(N)=Q(N)
      DO 35 I=2,N-1
```

```
      J=N+1-I
      T(J)=P(J)*T(J+1)+Q(J)
35    CONTINUE
      DO I=1,N
      T0(I)=T(I)
      END DO
      DO I=1,N-1
      F(I)=(T(I)-T(I+1))/DX*GAM
      END DO
      F(N)=F(N-1)
      TIME=TIME+DT
      IF(TIME.LT.TMAX) GOTO 50
      DO I=1,N
      XX=X(I)/XL
      WRITE(*,2)X(I),T(I),F(I)
      WRITE(1,2)XX,T(I),F(I)
      END DO
2     FORMAT(2X,F6.4,2X,F7.5,2X,F8.5)
      STOP
      END
```

2. HHC Code - layer 1: This code was developed to solve one-dimensional hyperbolic heat conduction (HHC) problems using the characteristics method. Only one layer of material is considered in this problem. Propagation speed is set to be equal to $(1/3)^{1/2}$. Both time and x coordinate are normalized. Total acoustic thickness is xl.

```
C     ------------------------------------------------------------------
C     WAVE BY THE METHOD OF CHARACTERISTICS
C                 July 15, 1993
C     ------------------------------------------------------------------
      implicit real*8 (A-H, O-Z)
      DIMENSION T(500),T0(500),Q(500),Q0(500),X(500)
      OPEN(UNIT=1,FILE='HHC.D')
      WRITE(*,*)'INPUT xl,TMAX'
      READ(*,*)xl,TMAX
      GAM=1/3.0
      N=200
      BI=0.0
      DX=xl/FLOAT(N-1)
      DO 10 I=1,N
      X(I)=xl*FLOAT(I-1)/FLOAT(N-1)
      T0(I)=0.
      Q0(I)=0.
10    CONTINUE
      T0(1)=1
      T(1)=1
      DT=DX/GAM**0.5
      DELTA=GAM**0.5
      TI=0.
      ITER=0.
50    ITER=ITER+1
```

```
      TI=TI+DT
      Q(1)=(Q0(2)*(DELTA-DX/2)+(T(1)-T0(2))*DELTA**2)/(DELTA+DX/2)
c     T(1)=T0(2)+(Q(1)*(DELTA+DX/2)-Q0(2)*(DELTA-DX/2))/DELTA**2
      Q(N)=(Q0(N-1)*(DELTA-DX/2)-(T(N)-T0(N-1))*DELTA**2)/(DELTA+DX/2)
c     T(N)=(T0(N-1)+Q0(N-1)*(DELTA-DX/2)/DELTA**2)/(1+BI*(DELTA+DX/2))
      DO 15 I=2,N-1
      T(I)=(T0(I-1)+T0(I+1)+(Q0(I-1)-Q0(I+1))*(DELTA-DX/2)/DELTA**2)
      T(I)=0.5*T(I)
      Q(I)=(Q0(I-1)+Q0(I+1))*(DELTA-DX/2)
      Q(I)=(Q(I)+(T0(I-1)-T0(I+1))*DELTA**2)/(2*(DELTA+DX/2))
15    CONTINUE
      T(1)=1.
      T(N)=0.
c     Q(N)=BI*GAM*T(N)
C     IF(TI.GT.TC-5*DT) THEN
C     IF(ITER.GE.M) THEN
      IF(TI.GT.TMAX) THEN
      ITER=0.
      DO 20 I=1,N
      XX=X(I)/xl
      WRITE(1,1)TI,XX,T(I),Q(I)
20    WRITE(*,1)TI,X(I),T(I),Q(I)
1     FORMAT(2X,4(F10.5,2X))
      stop
      ENDIF
      DO 25 I=1,N
      Q0(I)=Q(I)
      T0(I)=T(I)
25    CONTINUE
      TC=1/DELTA
c     IF(TI.GT.5*DT+TC) STOP
      GOTO 50
      STOP
      END
```

3. HHC Code - layer 2: This code was developed to solve for reflection of one-dimensional hyperbolic thermal waves at an interface of two materials. The characteristics method was used to develop the program.

```
C     ------------------------------------------------------------------
C     WAVE BY THE METHOD OF CHARACTERISTICS
C          FOR REFLECTION AT AN INTERFACE
C                  Aug. 20, 1993
C     ------------------------------------------------------------------
      IMPLICIT REAL*8(A-H,O-Z)
      DIMENSION T(1000),T0(1000),Q(1000),Q0(1000),X(1000)
      OPEN(UNIT=1,FILE='D.D')
      WRITE(*,*)'INPUT N,M'
      READ(*,*)N,M
      WRITE(*,*)'INPUT GAM1,GAM2,BI,OMEGA'
      READ(*,*)GAM1,GAM2,BI,OMEGA
```

```
      WRITE(*,*)'INPUT R1,TD,TMAX'
      READ(*,*)R1,TD,TMAX
      DX=0.5/FLOAT(M-1)
      DO I=1,M
      X(I)=0.5*FLOAT(I-1)/FLOAT(M-1)
      T0(I)=1.
      Q0(I)=0.
      END DO
      R2=1-R1
      T0(1)=1
      T(1)=2
      DT=DX*(R1/GAM1)**0.5
      DELTA1=(GAM1*R1)**0.5
      DX2=DT*(GAM2/R2)**0.5
      DELTA2=(GAM2*R2)**0.5
      BETA=(GAM1*R2/GAM2/R1)**0.5/TD
      DO I=M+1,N
      X(I)=0.5+DX2*(I-M)
      T0(I)=1.
      Q0(I)=0.
      END DO
      TI=0.
      ITER=0.
50    ITER=ITER+1
      TI=TI+DT
c     T(1)=1+SIN(OMEGA*TI)
      Q(1)=(Q0(2)*(R1-DT/2)+DELTA1*(T(1)-T0(2)))/(R1+DT/2)
      T(N)=BETA*DELTA2*(T0(N-1)+Q0(N-1)*(DELTA2-DT/2))
      T(N)=T(N)/(BETA*(DELTA2+BI*GAM2*(R2+DT/2)))
      Q(M)=DELTA1*(T0(M-1)-T0(M+1))+(R1-0.5*DT)*Q0(M-1)
      Q(M)=Q(M)+TD*(R1-0.5*DT*R1/R2)*Q0(M+1)
      Q(M)=Q(M)/((R1+0.5*DT)+TD*(R1+0.5*R1*DT/R2))
      T(M)=R1*TD*(R2+0.5*DT)*T0(M-1)+R2*(R1+0.5*DT)*T0(M+1)
      T(M)=T(M)+R1*TD*(Q0(M-1)*(R1-DT/2)*(R2+DT/2)-Q0(M+1)
     1 *(R1+DT/2)*(R2-DT/2))/DELTA1
      T(M)=T(M)/(R2*(R1+DT/2)+R1*TD*(R2+DT/2))
      DO  I=2,M-1
      T(I)=(T0(I-1)+T0(I+1)+(Q0(I-1)-Q0(I+1))*(R1-DT/2)/DELTA1)
      T(I)=0.5*T(I)
      Q(I)=(Q0(I-1)+Q0(I+1))*(R1-DT/2)
      Q(I)=(Q(I)+DELTA1*(T0(I-1)-T0(I+1)))/(2*(R1+DT/2))
      END DO
      DO I=M+1,N-1
      T(I)=(T0(I-1)+T0(I+1)+(Q0(I-1)-Q0(I+1))*(R2-DT/2)/DELTA2/BETA)
      T(I)=0.5*T(I)
      Q(I)=(Q0(I-1)+Q0(I+1))*(R2-DT/2)
      Q(I)=(Q(I)+BETA*DELTA2*(T0(I-1)-T0(I+1)))/(2*(R2+DT/2))
      END DO
      T(1)=2.
      Q(N)=BETA*BI*GAM2*T(N)
C     IF(TI.GT.TC-DT) THEN
      IF(TI.GE.TMAX) THEN
      ITER=0.
      DO 20 I=1,N
```

```
      WRITE(1,1)X(I),T(I),Q(I)
20    WRITE(*,1)X(I),T(I),Q(I)
1     FORMAT(2X,3(F10.5,2X))
      STOP
      ENDIF
      DO I=1,N
      Q0(I)=Q(I)
      T0(I)=T(I)
      END DO
      TC=1/DELTA1
C     IF(TI.GT.DT+TC) STOP
      GOTO 50
      STOP
      END
```

4. PTE Code: This code was developed to solve one-dimensional phonon transport (PTE) problems using the TVD method. Intensities U (forward) and V (backward) are solved, and temperature and heat flux are determined from U and V.

```
C     ------------------------------------------------------------
C     THE PROGRAM FOR THERMAL WAVE
C           TRANSPORT EQUATION
C                 Oct. 6, 1994
C     ------------------------------------------------------------
      IMPLICIT REAL*8 (A-H,O-Z)
      DIMENSION U(110,50),V(110,50),UO(110,50),VO(110,50),C(50)
      DIMENSION X(110),P(110),A(50),T(110),Q(110)
C     ------------------------------------------------------------
C     GRID DISCRETIZATION
C     -------------------
      OPEN (UNIT=1,FILE='PTE.D')
      WRITE(*,*)'INPUT THE TIME STEP:'
      READ(*,*) DT
      WRITE(*,*)'INPUT THE MAXIMUM TIME:'
      READ(*,*) TMAX
      WRITE(*,*)'INPUT THE AUSTICAL THICKNESS:'
      READ(*,*) X0
      TIME=0
      ITER=0
      AA=0.0
      BB=1.0
      NM=48
      NX=100
      CALL DXA(NM,AA,BB,C,A)
      SUM=0
      DX=X0/NX
      DO I=1,NX
      X(I)=X0*FLOAT(I-1)/FLOAT(NX-1)
      END DO
C     ------------------------------------------------------------
C     INPUT INITIAL AND BOUNDARY CONDITIONS
```

```
C     ------------------------------------
      WRITE(*,*)'INPUT THE TOP POSITIVE INTENSITY:'
      READ(*,*) U(1,1)
      WRITE(*,*)'INPUT THE BOTTOM NEGTIVE INTENSITY:'
      READ(*,*) V(1,1)
      WRITE(*,*)'INPUT THE INITIAL INTENSITY:'
      READ(*,*) UO(1,1)
      VO(1,1)=UO(1,1)
      DO I=1,NX
      DO J=1,NM
      UO(I,J)=UO(1,1)
      VO(I,J)=VO(1,1)
      END DO
      END DO
      DO J=1,NM
      UO(1,J)=U(1,1)
      VO(1,J)=V(1,1)
      END DO
C     ------------------------------------------------------------
C     SOLVE FOR THE INTENSITIES
C     -------------------------
10    DO I=1,NX
      SUM=0
      SUMQ=0
      DO J=1,NM
      SUM=SUM+(UO(I,J)+VO(NX+1-I,J))*A(J)
      SUMQ=SUMQ+(UO(I,J)-VO(NX+1-I,J))*C(J)*A(J)
      END DO
      T(I)=0.5*SUM
      Q(I)=SUMQ
      END DO
C     ---------- SOLVE FOR U ----------
      DO J=1,NM
      DO I=2,NX-1
      PUP=C(J)*UO(I,J)
      PLW=0.5*C(J)*(UO(I+1,J)+UO(I,J))
      PLW=PLW-0.5*C(J)*C(J)*DT/DX*(UO(I+1,J)-UO(I,J))
      R=(UO(I,J)-UO(I-1,J))/(UO(I+1,J)-UO(I,J)+1.0E-10)
      R1=2*R
      IF(R1.GT.1.0) R1=1.0
      IF(R.GT.2.0) R=2.0
      COEF=AMAX1(0, R1, R)
      P(I)=PUP+COEF*(PLW-PUP)
      END DO
      P(1)=C(J)*UO(1,J)
      DO I=2,NX-1
      U(I,J)=UO(I,J)-DT*(P(I)-P(I-1))/DX+DT*(T(I)-UO(I,J))
      END DO
      U(1,J)=UO(1,J)
      U(NX,J)=UO(NX,J)-DT*C(J)*(UO(NX,J)-UO(NX-1,J))/DX
      U(NX,J)=U(NX,J)+DT*(T(NX)-UO(NX,J))
      END DO
C     ---------- SOLVE FOR V ----------
      DO J=1,NM
```

```
      DO I=2,NX-1
      PUP=C(J)*VO(I,J)
      PLW=0.5*C(J)*(VO(I+1,J)+VO(I,J))
      PLW=PLW-0.5*C(J)*C(J)*DT/DX*(VO(I+1,J)-VO(I,J))
      R=(VO(I,J)-VO(I-1,J))/(VO(I+1,J)-VO(I,J)+1.0E-10)
      R1=2*R
      IF(R1.GT.1.0) R1=1.0
      IF(R.GT.2.0) R=2.0
      COEF=AMAX1(0, R1, R)
      P(I)=PUP+COEF*(PLW-PUP)
      END DO
      P(1)=C(J)*VO(1,J)
      DO I=2,NX-1
      V(I,J)=VO(I,J)-DT*(P(I)-P(I-1))/DX+DT*(T(NX+1-I)-VO(I,J))
      END DO
      V(1,J)=VO(1,J)
      V(NX,J)=VO(NX,J)-DT*C(J)*(VO(NX,J)-VO(NX-1,J))/DX
      V(NX,J)=V(NX,J)+DT*(T(1)-VO(NX,J))
      END DO
C     ---------- UPDATE U AND V ----------
      DO I=1,NX
      DO J=1,NM
      UO(I,J)=U(I,J)
      VO(I,J)=V(I,J)
      END DO
      END DO
C     ------------------------------------------------------
C     OUTPUT THE RESULTS
C     ------------------
      TIME=TIME+DT
      ITER=ITER+1
      IF(TIME.LT.TMAX) goto 10
c     IF(ITER.LT.100) GOTO 10
      ITER=0
      DO I=1,NX
      J=NX+1-I
      XX=X(I)/X0
C     do I=1,NM
      WRITE(*,20) XX,UO(I,NM),VO(J,NM),T(I),Q(I)
      WRITE(1,20) XX,UO(I,NM),VO(J,NM),T(I),Q(I)
C     WRITE(1,20) C(I),UO(25,I),VO(75,I),UO(50,I),
C    +  VO(50,I),UO(75,I),VO(25,I)
      END DO
c     IF(TIME.GT.TMAX) STOP
c     GOTO 10
20    FORMAT(2X,7(F8.4,2X))
      STOP
      END
```

5. Two-Dimensional Thermal Wave Code: This code was developed to solve two-dimensional hyperbolic heat conduction (HHC) problems in homogeneous materials using the TVD method.

```
C     ------------------------------------------------------------------------
C     TWO-DIMENSIONAL THERMAL WAVE SIMULATION
C                          SEPT. 7, 1993
C     ------------------------------------------------------------------
      DIMENSION X(150),Y(150),C(150,150),T(150,150)
      DIMENSION GX(150,150),GY(150,150),QX(150,150)
      DIMENSION QY(150,150),P(2,150)
      OPEN(UNIT=1,FILE='D.D')
C     ------------------ DISCRETIZATION ------------------
      WRITE(*,*)'INPUT N, M,MM,m1,m2:'
      READ(*,*)N,M,MM,m1,m2
      DX=1/FLOAT(N)
      DY=1/FLOAT(M)
      DO 10 I=1,N+1
10    X(I)=DX*(I-1)
      DO 15 J=1,M+1
15    Y(J)=DY*(J-1)
C     ------------------ INPUT THE PROPERTIES ------------
      WRITE(*,*)'INPUT C0,TAU'
      READ(*,*)C0,TAU0
      DO 20 I=1,N+1
      DO 20 J=1,M+1
      C(I,J)=C0
20    CONTINUE
      DT=0.25*DX/C0
      DTS=0.25*DY/C0
      IF(DTS.LT.DT) DT=DTS
C     ------------------ INPUT I.C. AND BC.S -------------
      DO 25 I=1,N+1
      DO 25 J=1,M+1
      T(I,J)=1.
      QX(I,J)=0.
      QY(I,J)=0.
25    CONTINUE
      TIME=0.
      ITER=0
130   DO 30 I=1,N+1
      QY(I,1)=0.
      QY(I,M+1)=0.
      T(I,1)=T(I,2)+(QY(I,1)*(1+0.5*DT)-QY(I,2)*(1-0.5*DT))/C(I,1)
C     IF(I.GE.M1) T(I,1)=2.0
C     QY(I,1)=(QY(I,2)*(1-DT/2.)+C(I,1)*(T(I,1)-T(I,2)))/(1+DT/2)
      T(I,M+1)=(QY(I,M)*(1-0.5*DT)-QY(I,M+1)*(1+0.5*DT))/C(I,M+1)
      T(I,M+1)=T(I,M+1)+T(I,M)
30    CONTINUE
      DO 35 J=1,M+1
      T(1,J)=2.0
      QX(N+1,J)=0.0
      QX(1,J)=QX(2,J)*(1-DT/2.)+C(1,J)*(T(1,J)-T(2,J))
```

```
      QX(1,J)=QX(1,J)/(1+DT/2.)
      if(J.LT.M1.OR.j.GT.m2) THEN
      QX(1,j)=0.
      T(1,J)=T(2,J)+(QX(1,J)*(1+0.5*DT)-QX(2,J)*(1-0.5*DT))/C(1,J)
      ENDIF
      T(N+1,J)=(QX(N+1,J)*(1+DT/2.)-QX(N,J)*(1-DT/2.))/C(N+1,J)
      T(N+1,J)=T(N,J)-T(N+1,J)
35    CONTINUE
C     ---------- X-DIRECTION ----------
      DO 40 I=1,N+1
      DO 40 J=1,M+1
      GX(I,J)=C(I,J)*T(I,J)+QX(I,J)
      GY(I,J)=-C(I,J)*T(I,J)+QX(I,J)
40    CONTINUE
      DO 45 J=2,M
      DO 50 I=1,N
      P(1,I)=C(I,J)*GX(I,J)
      P(2,I)=-0.5*C(I,J)*C(I,J)*DT*(GX(I+1,J)-GX(I,J))/DX
      P(2,I)=P(2,I)+0.5*C(I,J)*(GX(I+1,J)+GX(I,J))
      R=(GX(I,J)-GX(I-1,J))/(GX(I+1,J)-GX(I,J)+1.0E-08)
      RT=2*R
      IF(RT.GT.1.0) RT=1.0
      IF(R.GT.2.0) R=2.0
      F=AMAX1(0,RT,R)
      IF(I.EQ.1) F=0.
      P(1,I)=P(1,I)+F*(P(2,I)-P(1,I))
50    CONTINUE
      DO 55 I=2,N
      GX(I,J)=GX(I,J)-DT*(P(1,I)-P(1,I-1))/DX-DT*QX(I,J)
55    CONTINUE
      DO 60 I=2,N+1
      P(1,I-1)=-C(I,J)*GY(I,J)
      P(2,I-1)=-0.5*C(I,J)*(GY(I,J)+GY(I-1,J))
      P(2,I-1)=P(2,I-1)-0.5*C(I,J)**2.*DT*(GY(I,J)-GY(I-1,J))/DX
      R=(GY(I+1,J)-GY(I,J))/(GY(I,J)-GY(I-1,J)+1.0E-08)
      RT=2*R
      IF(RT.GT.1.0) RT=1.0
      IF(R.GT.2.0) R=2.0
      F=AMAX1(0,RT,R)
      IF(I.EQ.N+1) F=0.
      P(1,I-1)=P(1,I-1)+F*(P(2,I-1)-P(1,I-1))
60    CONTINUE
      DO 65 I=2,N
      GY(I,J)=GY(I,J)-DT*(P(1,I)-P(1,I-1))/DX-DT*QX(I,J)
65    CONTINUE
45    CONTINUE
      DO 70 I=2,N
      DO 70 J=2,M
      T(I,J)=0.5*(GX(I,J)-GY(I,J))/C(I,J)
      QX(I,J)=0.5*(GX(I,J)+GY(I,J))
      QY(I,J)=QY(I,J)*(1-DT)
70    CONTINUE
      DO 75 I=1,N+1
      QY(I,1)=0.
```

```
      QY(I,M+1)=0.
      T(I,1)=T(I,2)+(QY(I,1)*(1+0.5*DT)-QY(I,2)*(1-0.5*DT))/C(I,1)
C     T(I,1)=2.0
C     QY(I,1)=(QY(I,2)*(1-DT/2.)+C(I,1)*(T(I,1)-T(I,2)))/(1+DT/2)
      T(I,M+1)=(QY(I,M)*(1-0.5*DT)-QY(I,M+1)*(1+0.5*DT))/C(I,M+1)
      T(I,M+1)=T(I,M+1)+T(I,M)
75    CONTINUE
      DO 80 J=1,M+1
      T(1,J)=2.0
      QX(N+1,J)=0.0
      QX(1,J)=QX(2,J)*(1-DT/2.)+C(1,J)*(T(1,J)-T(2,J))
      QX(1,J)=QX(1,J)/(1+DT/2.)
      if(J.LT.M1.OR.j.GT.m2) THEN
      QX(1,j)=0.0
      T(1,J)=T(2,J)+(QX(1,J)*(1+0.5*DT)-QX(2,J)*(1-0.5*DT))/C(1,J)
      ENDIF
      T(N+1,J)=(QX(N+1,J)*(1+DT/2.)-QX(N,J)*(1-DT/2.))/C(N+1,J)
      T(N+1,J)=T(N,J)-T(N+1,J)
80    CONTINUE

C     ---------- Y-DIRECTION ----------
      DO 85 I=1,N+1
      DO 85 J=1,M+1
      GX(I,J)=C(I,J)*T(I,J)+QY(I,J)
      GY(I,J)=-C(I,J)*T(I,J)+QY(I,J)
85    CONTINUE
      DO 90 I=2,N
      DO 95 J=1,M
      P(1,J)=C(I,J)*GX(I,J)
      P(2,J)=0.5*C(I,J)*(GX(I,J+1)+GX(I,J))
      P(2,J)=P(2,J)-0.5*C(I,J)**2*DT*(GX(I,J+1)-GX(I,J))/DY
      R=(GX(I,J)-GX(I,J-1))/(GX(I,J+1)-GX(I,J)+1.0E-08)
      RT=2*R
      IF(RT.GT.1.0) RT=1.0
      IF(R.GT.2.0) R=2.0
      F=AMAX1(0,RT,R)
      IF(J.EQ.1) F=0.
      P(1,J)=P(1,J)+F*(P(2,J)-P(1,J))
95    CONTINUE
      DO 100 J=2,M
      GX(I,J)=GX(I,J)-DT*(P(1,J)-P(1,J-1))/DY-DT*QY(I,J)
100   CONTINUE
      DO 105 J=2,M+1
      P(1,J-1)=-C(I,J)*GY(I,J)
      P(2,J-1)=-0.5*C(I,J)*(GY(I,J)+GY(I,J-1))
      P(2,J-1)=P(2,J-1)-0.5*C(I,J)**2*DT*(GY(I,J)-GY(I,J-1))/DY
      R=(GY(I,J+1)-GY(I,J))/(GY(I,J)-GY(I,J-1)+1.0E-08)
      RT=2*R
      IF(RT.GT.1.0) RT=1.0
      IF(R.GT.2.0) R=2.0
      F=AMAX1(0,RT,R)
      IF(J.EQ.M+1) F=0.
      P(1,J-1)=P(1,J-1)+F*(P(2,J-1)-P(1,J-1))
105   CONTINUE
```

```
      DO 110 J=2,M
      GY(I,J)=GY(I,J)-DT*(P(1,J)-P(1,J-1))/DY-DT*QY(I,J)
110   CONTINUE
90    CONTINUE
      DO 115 I=2,N
      DO 115 J=2,M
      T(I,J)=0.5*(GX(I,J)-GY(I,J))/C(I,J)
      QY(I,J)=0.5*(GX(I,J)+GY(I,J))
      QX(I,J)=QX(I,J)*(1-DT)
115   CONTINUE
      TIME=TIME+2*DT
      ITER=ITER+1
      IF(ITER.GT.MM) THEN
      DO 120 I=2,N
      DO 120 J=2,M
      GX(I,J)=-(T(I,J)-T(I-1,J))/DX
      GY(I,J)=-(T(I,J)-T(I,J-1))/DY
      WRITE(*,180)X(I),Y(J),GX(I,J),GY(I,J),QX(I,J),QY(I,J)
      WRITE(1,180)X(I),Y(J),T(I,J),GY(I,J),QX(I,J),QY(I,J)
120   CONTINUE
      ITER=1
      stop
      ENDIF
C     IF(TIME.GE.1.) STOP
180   FORMAT(2X,6(E11.5,2X))
      GOTO 130
      STOP
      END
```

6. Two-Dimensional HHC Code: This code was developed to solve two-dimensional hyperbolic thermal wave problems in homogeneous or composite materials using the control volume finite difference method.

```
C-----------------------------------------------------------------
C        TWO-DIMENSIONAL THERMAL WAVES IN NON-HOMOGENEOUS
C          MATERIALS USING CONTROL VOLUME METHOD
C                APRIL 10, 1993
C-----------------------------------------------------------------
      DIMENSION AE(105,60),AW(105,60),AN(105,60),AS(105,60)
      DIMENSION AP(105,60),T0(105,60),TY(105,60),T(105,60)
      DIMENSION QX0(105,60),QY0(105,60),P(105),Q(105),B(105,60)
      DIMENSION X(105),Y(60),GAM(105,60),TAU(105,60),CP(105,60)
      OPEN(FILE='D.D',UNIT=1)
      open(FILE='d1.d',UNIT=2)
C--------------------INPUT PARAMETERS ---------------------------
      WRITE(*,*)'INPUT GRID NUMBER N AND M'
      READ(*,*)N,M
      WRITE(*,*)'INPUT INTERFACE M1'
      READ(*,*)M1
      WRITE(*,*)'INPUT TIME STEP DT'
      READ(*,*)DT
```

```
      WRITE(*,*)'INPUT COEFFICIENT F'
      READ(*,*)F
      WRITE(*,*)'RELAXATION TIME T1 AND T2'
      READ(*,*)T1,T2
      WRITE(*,*)'INPUT K1 AND K2'
      READ(*,*)G1,G2
      WRITE(*,*)'CP1 AND CP2'
      READ(*,*)CP1,CP2
      WRITE(*,*)'INPUT TMAX'
      READ(*,*)TMAX
C------------ GRID ----------------------------
      XL=0.5
      YL=0.25
      TIME=0
      DX=XL/FLOAT(N-1)
      DY=YL/FLOAT(M-1)
      DO I=1,N
      X(I)=XL*FLOAT(I-1)/FLOAT(N-1)
      END DO
      DO J=1,M
      Y(J)=YL*FLOAT(J-1)/FLOAT(M-1)
      END DO
      DVY=DY*DT*DT/DX*F
      DVX=DX*DT*DT/DY*F
C------------ CALCULATE AE AW AN AS AP B --------
      DO I=1,N
      DO J=1,M
      GAM(I,J)=G1
      TAU(I,J)=T1
      CP(I,J)=CP1
      T0(I,J)=0
      QX0(I,J)=0
      QY0(I,J)=0
      IF(J.GT.M1) THEN
      T0(1,J)=2.0
      GAM(I,J)=G2
      TAU(I,J)=T2
      CP(I,J)=CP2
      END IF
      T(I,J)=T0(I,J)
      TY(I,J)=T(I,J)
      END DO
      END DO
      DO J=1,M-1
      DO I=1,N-1
      AE(I,J)=DVY*GAM(I,J)/(TAU(I,J)+F*DT)
      AW(I+1,J)=AE(I,J)
      AN(I,J)=DVX*GAM(I,J)/(TAU(I,J)+F*DT)
      AS(I,J+1)=AN(I,J)
      END DO
      END DO

15    DO I=2,N-1
      DO J=2,M-1
```

```
      AP(I,J)=AE(I,J)+AW(I,J)+AN(I,J)+AS(I,J)+CP(I,J)*DX*DY
      B(I,J)=CP(I,J)*T0(I,J)*DX*DY+TAU(I,J)*DT/(TAU(I,J)+F*DT)*
     + ((QX0(I-1,J)-QX0(I,J))*DY+(QY0(I,J-1)-QY0(I,J))*DX)
      END DO
      END DO
C------------------ BOUNDARY CONDITIONS ---------------------
      DO I=1,N
      AS(I,1)=0
      AN(I,1)=1
      AP(I,1)=1
      B(I,1)=0
      AS(I,M)=1
      AN(I,M)=0
      AP(I,M)=1
      B(I,M)=0
      END DO
      DO J=1,M
      AE(N,J)=0
      AW(N,J)=1
      AP(N,J)=1
      B(N,J)=0
      AE(1,J)=0
      AW(1,J)=0
      AP(1,J)=1
      B(1,J)=T(1,J)
      IF(J.LE.M1) THEN
      AE(1,J)=1
      B(1,J)=0
      end if
      END DO
      TIME=TIME+DT
C--------------- X-DIRECTION TDMA ----------------
10     DO J=2,M-1
      P(1)=AE(1,J)/AP(1,J)
      Q(1)=B(1,J)/AP(1,J)
      DO I=2,N
      S=B(I,J)+AN(I,J)*T(I,J+1)+AS(I,J)*T(I,J-1)
      IF(I.EQ.N) S=B(I,J)
      P(I)=AE(I,J)/(AP(I,J)-AW(I,J)*P(I-1))
      Q(I)=(S+Q(I-1)*AW(I,J))/(AP(I,J)-AW(I,J)*P(I-1))
      END DO
      T(N,J)=Q(N)
      DO K=2,N
      I=N+1-K
      T(I,J)=P(I)*T(I+1,J)+Q(I)

      END DO
      END DO
C------------- Y-DIRECTION TDMA -------------------
      DO I=2,N-1
      P(1)=AN(I,1)/AP(I,1)
      Q(1)=B(I,1)/AP(I,1)
      DO J=2,M
      S=B(I,J)+AE(I,J)*T(I+1,J)+AW(I,J)*T(I-1,J)
```

```
      IF(J.EQ.M) S=B(I,J)
      P(J)=AN(I,J)/(AP(I,J)-AS(I,J)*P(J-1))
      Q(J)=(S+Q(J-1)*AS(I,J))/(AP(I,J)-AS(I,J)*P(J-1))
      END DO
      T(I,M)=Q(M)
      DO K=2,M
      J=M+1-K
      T(I,J)=P(J)*T(I,J+1)+Q(J)
      END DO
      END DO
      ERR=0
      DO I=2,N
      DO J=2,M
      ERR0=ABS(T(I,J)-TY(I,J))
      IF(ERR0.GT.ERR) ERR=ERR0
      TY(I,J)=T(I,J)
      END DO
      END DO
      WRITE(*,*)'ERR=',ERR
      IF(ERR.GT.0.001) GOTO 10
      DO I=1,N-1
      QY0(I,1)=0
      QY0(I,M)=0
      DO J=2,M-1
      QX0(I,J)=(TAU(I,J)-(1-F)*DT)*QX0(I,J)
      QX0(I,J)=QX0(I,J)+DT*GAM(I,J)*(T(I,J)-T(I+1,J))/DX
      QX0(I,J)=QX0(I,J)/(TAU(I,J)+F*DT)
      QY0(I,J)=(TAU(I,J)-(1-F)*DT)*QY0(I,J)
      QY0(I,J)=QY0(I,J)+DT*GAM(I,J)*(T(I,J)-T(I,J+1))/DY
      QY0(I,J)=QY0(I,J)/(TAU(I,J)+F*DT)
      QX0(N,J)=0
      T0(I,J)=T(I,J)
      END DO
      END DO
      IF(TIME.LT.TMAX) GOTO 15
      T(1,1)=0.5*(T(2,1)+T(1,2))
      WRITE(1,4)N,M
      DO I=1,N
      DO J=1,M
      WRITE(1,2)X(I), Y(J), T(I,J)
      END DO
      END DO
      DO I=1,N,2
      DO J=1,M,2
      WRITE(*,2)X(I), Y(J), T(I,J)
      WRITE(2,2)X(I), Y(J), T(I,J)
      END DO
      END DO

4     FORMAT(2X,I4,1X,I4)
2     FORMAT(2X,3(F8.4,2X))
      STOP
      END
```

7. Contour Code: This code was developed to find the points for contour plots presented in this thesis. The input data is obtained from the output file of Code #4. The output data is processed using Sigma Plot.

```
C     ------------------------------------------------------------------------
C      THIS PROGRAM FINDS CONTOUR POINTS
C                    (Oct. 5. 1993)
C     ------------------------------------------------------------
      DIMENSION X(150),Y(150),Z(150,150),XW(40,400),YW(40,400)
      OPEN(UNIT=1,FILE='D.D',STATUS='OLD')
      OPEN(UNIT=2,FILE='DD.D',STATUS='old')
      READ(1,*)N,M
      DO 10 I=1,N
      DO 15 J=1,M
      READ(1,*)X(I),Y(J),Z(I,J)
15    CONTINUE
10    CONTINUE
      DX=X(3)-X(2)
      DY=Y(3)-Y(2)
      VMIN=10.
      VMAX=-10.
      DO 2 I=1,N
      DO 2 J=1,M
      IF(Z(I,J).LE.VMIN)VMIN=Z(I,J)
      IF(Z(I,J).GT.VMAX)VMAX=Z(I,J)
2     CONTINUE
      l=1
      VALUE=2.00
      do 101 L=1,39
      VALUE=VALUE-0.05
      K=1
      DO 20 J=1,M
      DO 25 I=1,N-1
      VMIN=Z(I,J)
      VMAX=Z(I+1,J)
      IF(VMIN.GT.VMAX) THEN
      VMAX=VMIN
      VMIN=Z(I+1,J)
      ENDIF
      IF(VALUE.GE.VMIN.AND.VALUE.LE.VMAX) THEN
      YW(L,K)=Y(J)
      XW(L,K)=(X(I+1)-X(I))*(VALUE-Z(I,J))
      XW(L,K)=XW(L,K)/(Z(I+1,J)-Z(I,J)+1.e-8)+X(I)
      K=K+1
      ENDIF
25    CONTINUE
20    CONTINUE
      DO 30 I=1,N
      DO 35 J=1,M-1
      VMIN=Z(I,J)
      VMAX=Z(I,J+1)
```

```
      IF(VMIN.GT.VMAX) THEN
      VMAX=VMIN
      VMIN=Z(I,J+1)
      ENDIF
      IF(VALUE.GE.VMIN.AND.VALUE.LE.VMAX) THEN
      XW(L,K)=X(I)
      YW(L,K)=(Y(J+1)-Y(J))*(VALUE-Z(I,J))
      YW(L,K)=YW(L,K)/(Z(I,J+1)-Z(I,J)+1.e-8)+Y(J)
      K=K+1
      ENDIF
35    CONTINUE
30    CONTINUE
        DO 32 I=1,K-1
      WRITE(*,33)XW(L,I),YW(L,I)
      WRITE(2,33)XW(L,I),YW(L,I)
32    CONTINUE
101   continue
33    FORMAT(2X,2(E12.5,1x))
      end
```

APPENDIX II

Appendix II Nomenclature

c_v	constant volume specific heat (J/kgK).
$\overline{c}_v$	constant volume specific heat (J/m^3K).
G(S)	entropy production (W/Km^3).
I	phonon intensity (J/m^3 ster).
k	thermal wave extinction coefficient.
n	thermal wave real refractive index.
$\overline{n}$	thermal wave complex refractive index.
p	pressure (N/m^2).
Q	heat flow (J/m^2).
q	heat flux (W/m^2).
R_B	boundary resistance (m^2K/W).
s	specific entropy (J/Kkg).
S	specific entropy per unit volume (J/Km^3).
T	temperature (K).
TD	parameter defined by Eq. (II-43).
t	time (s).
u	internal energy (J/kg).
$\overline{u}$	displacement (m).
U	internal energy per unit volume (J/m^3).
v	specific volume (m^3/kg).
$\overline{v}$	acoustic speed (m/s).
x	coordinate (m).

Greek

α damping coefficient.

ρ density (kg/m^3).

$\hat{\rho}$ reflectivity.

$\Phi(S)$ entropy flow (W/Km^3).

μ cosine of the angle between the phonon propagation direction and the interface normal direction.

τ relaxation time (s).

ω frequency.

Subscripts and Superscripts

1 material 1.

2 material 2.

u $\bar{u}$ related variable.

+ the positive direction of x-axis.

- the negative direction of x-axis.

The two following sections are preliminary analysis that need further investigation to validate the ideas presented.

1. Thermodynamic Analysis of Hyperbolic Heat Conduction

In Chapters II-IV, we have discussed the thermal wave reflection phenomenon, and derived the relationships to predict the reflectivity. Tzou (1993) derived the relationships for the special case wherein the relaxation times of the two materials are the same. His results are the same as ours for one-dimensional thermal wave reflection when the two materials have the same relaxation times. However, he did not show that the reflectivity can be time dependent when the two relaxation times of the related materials are different, and he did not discuss the physical process of negative reflection. Tzou (1994) also presented a discussion of entropy production during the hyperbolic heat

conduction process. He claimed that the entropy production is always positive when the entropy is considered as a function of temperature, pressure, and heat flux

$$Tds(T,p,\vec{q}) = du(T,p) + pdv \qquad \text{(II-1)}$$

where s is the specific entropy, p is the pressure, and v is specific volume. Therefore, he believes that the hyperbolic heat conduction equations satisfy the requirements of the second law of thermodynamics. However, from our study, we have found that hyperbolic heat conduction does not always satisfy the second law of thermodynamics, especially when reflection takes place during the process.

A typical example is shown in Fig. II-1. In this figure, a one-dimensional heat conduction problem is solved. The right boundary of the material is set to be adiabatic, and the left boundary temperature is given (= 2.0). The initial temperature is 1.0. The wave speed is $5.0^{1/2}$. The temperature profiles at dimensionless times of 0.2 and 0.9 are shown in the figure. From the figure, we can see that at t = 0.2, the thermal wave is moving to the right boundary, and its value is decreasing because of attenuation. At t = 0.9, the wave is reflected by the right boundary, and moving back to the left boundary, but it has not arrived at the left boundary. We notice a significant increase in the temperature of the material from t = 0.2 to t = 0.9. At t = 0.9, the temperature in the material is larger than the left boundary temperature which is set to be 2.0. Suppose that at the moment t = 0.9, we remove the heat source from the left boundary, and set the left boundary to be adiabatic. Then the temperature in the material will finally get to be steady, and it will be larger than the temperature (= 2.0) of the heat source. This means that we can heat a material to a temperature which is even higher than the temperature of the heat source. We can repeat this process (at least theoretically) to transfer heat from a low temperature source to a high temperature material. This result illustrates that hyperbolic heat conduction does not satisfy the second law of thermodynamics in some cases.

Because of the above discussion, we need to reconsider the irreversibility of hyperbolic heat conduction, especially when reflection takes place. We consider a one-

dimensional heat conduction problem as shown in Fig. II-2. Because the time period of heat transfer is very small, we can use a second order Taylor's series expansion to represent the change of physical properties during a small time period δt

$$\delta U dx = [\frac{\partial U}{\partial t} + \tau \frac{\partial^2 U}{\partial t^2}]\delta t dx \tag{II-2}$$

where U is the internal energy per unit volume. The heat transfer through an unit area in an unit time is q. Then

$$\delta Q = [q + \tau \frac{\partial q}{\partial t}]\delta t \tag{II-3}$$

and the net heat transfer is

$$\{\delta Q + \frac{\partial}{\partial x}[\delta Q]dx\} - \delta Q = \frac{\partial}{\partial x}[q + \tau \frac{\partial q}{\partial t}]\delta t dx \tag{II-4}$$

Therefore, the energy conservation equation is

$$\delta U \delta t dx + \frac{\partial}{\partial x}[\delta Q]dx = 0 \tag{II-5a}$$

or

$$\frac{\partial U}{\partial t} + \tau \frac{\partial^2 U}{\partial t^2} + \frac{\partial}{\partial x}[q + \tau \frac{\partial q}{\partial t}] = 0 \tag{II-5}$$

Now if we use the hyperbolic model

$$q + \tau \frac{\partial q}{\partial t} = -\alpha \frac{\partial U}{\partial x} \tag{II-6}$$

we can obtain the thermal wave equation

$$\frac{\partial U}{\partial t} + \tau \frac{\partial^2 U}{\partial t^2} = \alpha \frac{\partial^2 U}{\partial x^2} \tag{II-7}$$

The entropy (per unit volume) change of the material in dx is

$$\delta S dx = [\frac{\partial S}{\partial t} + \tau \frac{\partial^2 S}{\partial t^2}]\delta t dx \tag{II-8}$$

This change is caused by the entropy flow $\Phi(S)$ and the entropy production G(S)

$$\delta S dx = [\Phi(S) + G(S)]\delta t dx \tag{II-9}$$

The entropy flow is related to the heat flow by

$$\Phi(S) = -\frac{\partial}{\partial x}\left[\frac{1}{T}\frac{\delta Q}{\delta t}\right] = -\frac{\partial}{\partial x}\left[\frac{1}{T}(q + \tau \frac{\partial q}{\partial t})\right] \tag{II-10}$$

or

$$\Phi(S) = \alpha \frac{\partial}{\partial x}\left[\frac{1}{T}\frac{\partial U}{\partial x}\right] \tag{II-11}$$

Then, by substituting Eqs. (II-11) and (II-8) into Eq. (II-9), we can obtain

$$\frac{\partial S}{\partial t}+\tau\frac{\partial^2 S}{\partial t^2}=\alpha\frac{\partial}{\partial x}\left[\frac{1}{T}\frac{\partial U}{\partial x}\right]+G(S) \tag{II-12}$$

This is the entropy equation. In the equation, the entropy production G(S) should be positive if the process satisfies the second law of thermodynamics. Since the entropy S and the internal energy U are local thermodynamic equilibrium properties, therefore, they satisfy the following thermodynamic relationship for constant specific volume

$$TdS = dU \tag{II-13}$$

Therefore, we have

$$\frac{\partial S}{\partial x}=\frac{1}{T}\frac{\partial U}{\partial x},\quad \frac{\partial S}{\partial t}=\frac{1}{T}\frac{\partial U}{\partial t},\quad U=\rho c_v T \tag{II-14}$$

Substituting Eq. (II-14) into Eq. (II-7), we can obtain

$$\frac{\partial S}{\partial t}+\tau\frac{\partial^2 S}{\partial t^2}=\alpha\frac{\partial^2 S}{\partial x^2}+\frac{1}{\rho c_v}\left[\alpha\left(\frac{\partial S}{\partial x}\right)^2-\tau\left(\frac{\partial S}{\partial t}\right)^2\right] \tag{II-15}$$

Comparing to Eq. (II-12), we can obtain

$$G(S)=\frac{1}{\rho c_v}\left[\alpha\left(\frac{\partial S}{\partial x}\right)^2-\tau\left(\frac{\partial S}{\partial t}\right)^2\right] \tag{II-16}$$

This equation shows that the entropy production may be negative if

$$\alpha\left(\frac{\partial S}{\partial x}\right)^2<\tau\left(\frac{\partial S}{\partial t}\right)^2 \tag{II-17}$$

Therefore, hyperbolic heat conduction may not satisfy the second law of thermodynamics. This situation occurs when reflection takes place, such as the situation shown in Fig. II-1. To discuss the reflection process, we use a harmonic wave as an example. Assume the incident internal energy shown in Fig. II-3 is

$$U_i = U_m \exp[i\omega(t-\frac{\bar{n}}{C}x) \tag{II-18}$$

Then, the reflected wave is

$$U_r = \hat{\rho}U_m \exp[i\omega(t+\frac{\bar{n}}{C}x) \tag{II-19}$$

After reflection, the internal energy is

$$U = U_m \exp(i\omega t)[\exp(-i\omega \frac{\bar{n}}{C} x) + \hat{\rho} \exp(i\omega \frac{\bar{n}}{C} x)] \quad \text{(II-20)}$$

Therefore, we can derive

$$\frac{\partial U}{\partial t} = i\omega U_m \exp(i\omega t)[\exp(-i\omega \frac{\bar{n}}{C} x) + \hat{\rho} \exp(i\omega \frac{\bar{n}}{C} x)] \quad \text{(II-21)}$$

and

$$\frac{\partial U}{\partial x} = i\omega \frac{\bar{n}}{C} U_m \exp(i\omega t)[-\exp(-i\omega \frac{\bar{n}}{C} x) + \hat{\rho} \exp(i\omega \frac{\bar{n}}{C} x)] \quad \text{(II-22)}$$

At the interface, x = 0, and we also have the following relationships from Eq. (II-14)

$$\frac{\partial S}{\partial x} = \rho c_v \frac{1}{U} \frac{\partial U}{\partial x}, \quad \frac{\partial S}{\partial t} = \rho c_v \frac{1}{U} \frac{\partial U}{\partial t} \quad \text{(II-23)}$$

Therefore, at x = 0

$$\frac{\partial S}{\partial t} = \rho c_v i\omega(1+\hat{\rho}), \quad \frac{\partial S}{\partial x} = \rho c_v i\omega(-1+\hat{\rho}) \frac{\bar{n}}{C} \quad \text{(II-24)}$$

From Eq. (II-16), for the harmonic wave, we have

$$G(S) = \frac{1}{\rho c_v}[\alpha \left\| \frac{\partial S}{\partial x} \right\|^2 - \tau \left\| \frac{\partial S}{\partial t} \right\|^2] \quad \text{(II-25)}$$

Therefore, from Eqs. (II-24) and (II-25), we obtain

$$G(S) = \rho c_v \omega^2 [\alpha(1-\hat{\rho})^2 \frac{n^2 + k^2}{C^2} - \tau(1+\hat{\rho})^2] \quad \text{(II-26)}$$

In order to ensure that G(S)>=0, the following conditions must be satisfied

$$(1-\hat{\rho})^2 (n^2 + k^2) - (1+\hat{\rho})^2 \geq 0 \quad \text{(II-27)}$$

where, we have used $C^2 = \alpha/\tau$. From Chapter II (Eqs. (3-7) and (3-8)), we know that n and k have the following relationship

$$n^2 + k^2 = [1 + (1/\omega\tau)^2]^{1/2} \quad \text{(II-28)}$$

and

$$\hat{\rho} = \frac{TD - 1}{TD + 1} \quad \text{(II-29)}$$

Substituting Eqs. (II-28) and (II-29) into Eq. (II-27), we obtain

$$TD \leq (n^2 + k^2)^{1/2} = [1 + (1/\omega\tau)^2]^{1/4} \quad \text{(II-30)}$$

For thermal waves, usually the frequency is very large. Then the parameter TD is limited by Eq. (II-30) as

$$TD \leq 1 \quad \text{(II-31)}$$

This result shows that basically the positive reflection process can not happen because it does not satisfy the second law of thermodynamics. The negative reflection is possible. However, since the hyperbolic heat conduction model conditionally satisfies the second law of thermodynamics, it should not be used to predict the reflection process.

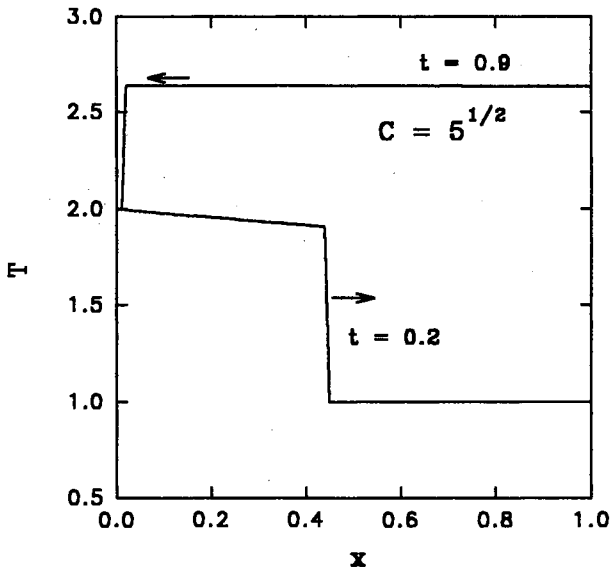

Fig. II-1 Temperature Distribution in a 1-D Medium

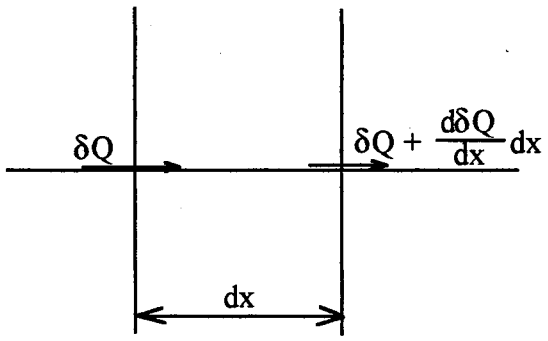

Fig. II-2 Control Volume of 1-D Heat Conduction

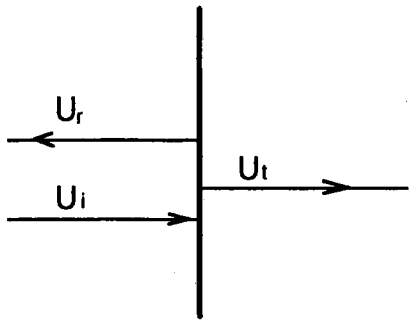

Fig. II-3 Interface Reflected and Transmitted Waves

2. Temperature Discontinuity at an Interface Based on Phonon Theory

In Chapter III, when we derived the relationship for reflectivity, we made an assumption that the temperature is continuous at an interface between two different materials. However, many experimental studies of phonon transport heat conduction have shown that the temperature is not continuous at the interface when reflection takes place. Swartz and Pohl (1989) have reviewed these experimental studies, and discussed the models to predict the boundary resistance that causes the discontinuity in temperature. At an interface, if the heat flux is q, and the boundary resistance is R_B, then

$$q = \frac{1}{R_B}\Delta T \tag{II-32}$$

where, ΔT is the difference between temperatures on the two sides of the interface. This fact cannot be predicted by using the hyperbolic heat conduction model and its reflection theory presented in Chapter III.

From the phonon transport theory, we can predict the boundary scattering (or temperature discontinuity) phenomenon. We have shown the boundary scattering process in the discussion in Chapter VII. Here, we will derive the temperature discontinuity at an interface based on the phonon transport theory.

Assume that at an interface, the phonon intensities are shown in Fig. II-4. The reflectivity of phonon intensity at the interface is $\hat{\rho}$. The reflectivity may be a function of phonon polarization mode, the frequency or wave vector, the incident angle, and the

phonon speed. Here, we will not discuss these factors. Then, the intensities satisfy the following conservation of energy equations at the interface of Fig. II-4

$$\mu_1\bar{v}_1 I_1^-(\mu_1) = \mu_1\bar{v}_1\hat{\rho}_{1-2} I_1^+(\mu_1) + \mu_2\bar{v}_2(1-\hat{\rho}_{2-1}) I_2^-(\mu_2) \tag{II-33}$$

$$\mu_2\bar{v}_2 I_2^+(\mu_2) = \mu_2\bar{v}_2\hat{\rho}_{2-1} I_2^-(\mu_2) + \mu_1\bar{v}_1(1-\hat{\rho}_{1-2}) I_1^+(\mu_1) \tag{II-34}$$

The phonon energy conservation through the interface in the μ_1 direction is

$$\mu_1\bar{v}_1[I_1^+(\mu_1) - I_1^-(\mu_1)] = \mu_2\bar{v}_2[I_2^+(\mu_2) - I_2^-(\mu_2)] \tag{II-35}$$

According to the Snell's law (Eq. (3-18)), we have

$$\frac{[1-\mu_1^2]}{[1-\mu_2^2]} = \left[\frac{\bar{v}_1}{\bar{v}_2}\right]^2 \tag{II-36}$$

We add and substract $\mu_1\bar{v}_1 I_1^+(\mu_1)$ to Eq. (II-33) and $\mu_2\bar{v}_2 I_2^-(\mu_2)$ to Eq. (II-34), then obtain

$$\mu_1\bar{v}_1[I_1^+(\mu_1) + I_1^-(\mu_1)] = \mu_1\bar{v}_1(1+\hat{\rho}_{1-2}) I_1^+(\mu_1) + \mu_2\bar{v}_2(1-\hat{\rho}_{2-1}) I_2^-(\mu_2) \tag{II-37}$$

$$\mu_2\bar{v}_2[I_2^+(\mu_2) + I_2^-(\mu_2)] = \mu_2\bar{v}_2(1+\hat{\rho}_{2-1}) I_2^-(\mu_2) + \mu_1\bar{v}_1(1-\hat{\rho}_{1-2}) I_1^+(\mu_1) \tag{II-38}$$

From Chapter VII, we know that temperature is related to the phonon intensity by

$$\bar{c}_v T = \frac{1}{2}\int_0^1 [I^+(\mu') + I^-(\mu')]d\mu' \tag{II-39}$$

Then, the temperature difference at the interface is

$$\bar{c}_v\Delta T = \bar{c}_v(T_1 - T_2) = \frac{1}{2}\int_0^1 \{[I_1^+(\mu_1) + I_1^-(\mu_1)] - [I_2^+(\mu_2) + I_2^-(\mu_2)]\}d\mu_1 \tag{II-40}$$

From Eqs. (II-37) and (II-38), we can obtain

$$\begin{aligned}[I_1^+(\mu_1) + I_1^-(\mu_1)] - [I_2^+(\mu_2) + I_2^-(\mu_2)] = {} & [(1+\hat{\rho}_{1-2}) - \frac{\mu_1\bar{v}_1}{\mu_2\bar{v}_2}(1-\hat{\rho}_{1-2})] I_1^+(\mu_1) \\ & -[(1+\hat{\rho}_{2-1}) - \frac{\mu_2\bar{v}_2}{\mu_1\bar{v}_1}(1-\hat{\rho}_{2-1})] I_2^-(\mu_2)\end{aligned} \tag{II-41}$$

Substituting Eq. (II-41) into Eq. (II-40), we obtain

$$\begin{aligned}\bar{c}_v\Delta T = \bar{c}_v(T_1 - T_2) = {} & \frac{1}{2}\int_0^1 [(1+\hat{\rho}_{1-2}) - \frac{\mu_1\bar{v}_1}{\mu_2\bar{v}_2}(1-\hat{\rho}_{1-2})] I_1^+(\mu_1)d\mu_1 \\ & -\frac{1}{2}\int_0^1 [(1+\hat{\rho}_{2-1}) - \frac{\mu_2\bar{v}_2}{\mu_1\bar{v}_1}(1-\hat{\rho}_{2-1})] I_2^-(\mu_2)d\mu_1\end{aligned} \tag{II-42}$$

Therefore, at the interface, the temperature is not continuous, and the difference of the temperatures on the two sides of the interface is related to the phonon reflectivity.

However, the heat transfer is continuous because it must satisfy the energy conservation at the interface.

As we have discussed in Chapter VII, the phonon intensities are also hyperbolic waves. However, the phonon reflection cannot exhibit the negative reflection process. This is because the phonons represent not only internal energy but also heat transfer, therefore, they are the only energy form during reflection. This is different from the hyperbolic thermal waves which can exchange energy between internal energy (temperature) and heat transfer, although this exchange is not always possible, as we discussed in the previous section. To understand phonon reflection, we have to consider the physical basis of phonons. Since phonons represent elastic waves in solid materials, the reflection of these elastic waves has to be considered. We may assume that the transverse elastic waves satisfy the following hyperbolic wave equation (Bland, 1988)

$$\frac{1}{\bar{v}^2}\frac{\partial^2 \bar{u}}{\partial t^2}+\frac{1}{\alpha}\frac{\partial \bar{u}}{\partial t}=\frac{\partial^2 \bar{u}}{\partial x^2} \tag{II-43}$$

where, α represents the damping of the wave because of the scattering, $\bar{u}$ is the displacement. The phonon energy is the kinetic energy of the wave. The reflection of the waves given by Eq. (3-24b) has been discussed in Chapter III, and the reflectivity is

$$\rho_u=\frac{TD\mu_1-\mu_2}{TD\mu_1+\mu_2},\quad TD=\frac{\bar{v}_1}{\bar{v}_2} \tag{II-43}$$

Because the phonon intensity or the total energy of a elastic wave is proportional to $\left(\frac{\partial \bar{u}}{\partial t}\right)^2$, the reflectivity of phonon intensity is

$$\hat{\rho}=\|\rho_u\|^2=\left\|\frac{TD\mu_1-\mu_2}{TD\mu_1+\mu_2}\right\|^2 \tag{II-44}$$

From Eq. (II-44), the reflectivities of Eq. (II-42) satisfy

$$\hat{\rho}_{1-2}=\hat{\rho}_{2-1}=\hat{\rho} \tag{II-45}$$

Since the heat flux is related to the intensities by (see Chapter VII)

$$q = 2\pi \int_0^1 \mu' [I^+(\mu') - I^-(\mu')] \bar{v} d\mu' \tag{II-46}$$

from Eqs. (II-46) and (II-33), we can obtain

$$q = 2\pi \int_0^1 (1-\hat{\rho})[\mu_1 \bar{v}_1 I_1^+(\mu_1) - \mu_2 \bar{v}_2 I_2^-(\mu_2)] d\mu_1 \tag{II-47}$$

where μ_1 and μ_2 are related by Eq. (II-36). Then, from Eq. (II-42), we can obtain

$$\begin{aligned} \bar{c}_v \Delta T = & \frac{1}{2} \int_0^1 (1+\hat{\rho})[I_1^+(\mu_1) - I_2^-(\mu_2)] d\mu_1 \\ & - \frac{1}{2} \int_0^1 (1-\hat{\rho})[\frac{\mu_1 \bar{v}_1}{\mu_2 \bar{v}_2} I_1^+(\mu_1) - \frac{\mu_2 \bar{v}_2}{\mu_1 \bar{v}_1} I_2^-(\mu_2)] d\mu_1 \end{aligned} \tag{II-48}$$

Then, the boundary resistance can be derived as

$$\frac{1}{R_B} = \frac{q}{\Delta T} \tag{II-49}$$

Substituting Eqs. (II-43) and (II-44) into Eq. (II-48), we obtain

$$\Delta T = \frac{1}{\bar{c}_v} \int_0^1 \frac{\mu_2 \bar{v}_2 - \mu_1 \bar{v}_1}{\mu_2 \bar{v}_2 + \mu_1 \bar{v}_1} \left[I_1^+(\mu_1) + I_2^-(\mu_2) \right] d\mu_1 \tag{II-50}$$

This result is very interesting. Suppose that the incident wave is collimated, and $I_1^+(\mu_1)$ is the only incident beam, $I_2^-(\mu_2) = 0$. Also assume that scattering near the interface is negligible. Then the temperature before reflection is

$$\bar{c}_v T = \int_0^1 I_1^+(\mu) \delta(\mu - \mu_1) d\mu = I_1^+(\mu_1) \tag{II-51}$$

After the reflection, the temperature change is

$$\Delta T = \frac{1}{\bar{c}_v} \frac{\mu_2 \bar{v}_2 - \mu_1 \bar{v}_1}{\mu_2 \bar{v}_2 + \mu_1 \bar{v}_1} I_1^+(\mu_1) = \rho_u T \tag{II-52}$$

This is the result obtained in Chapter III. The difference is that now the temperature is fixed at the interface, and it does not propagate in the material, which is typical of hyperbolic heat conduction. The question is how to explain physical meaning of this refult. This is an interesting topic for future study.

From Eq. (II-52), we can see that the temperature difference is zero when the ρ_u is zero. The temperature discontinuity always exists at an interface between two different

materials, and the temperature difference is directly proportional to the reflectivity. For phonon reflection, the reflectivity usually depends on the polarization mode. Since the heat transfer considered here is in microscale, the reflectivity will strongly depend on the crystal structure. Usually, the diffusive reflection assumption is not reasonable in this case. However, it is still a good approximate technique, and it is easy for engineering applications when there are not more realistic and more accurate methods to deal with this problem.

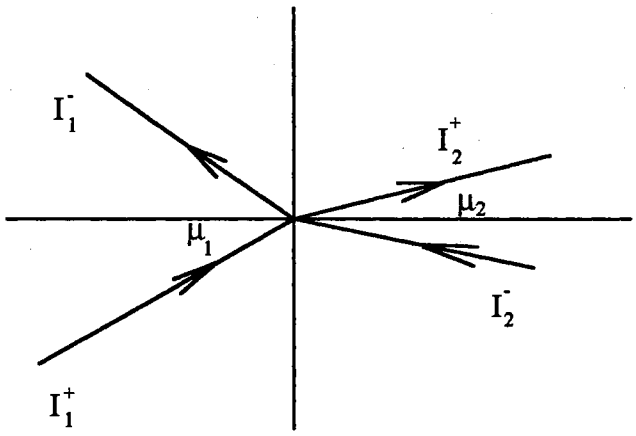

Fig. II-4 Interface Phonon Intensities

VITA

Ye Tian

Candidate for the Degree of
Doctor of Philosophy

Thesis: THEORETICAL INVESTIGATION OF TRANSPORT AND REFLECTION OF THERMAL WAVES

Major Field: Mechanical Engineering

Biographical:

Personal Data: Born in Xining City, QinHai, China, On September 12, 1962, the son of Tian, Jiu-Ting and Zhou, Yi-Xing.

Education: Graduated from Xining First High School, Xining, QinHai, China, in July, 1979; received Bachelor of Science degree in Mechanical Engineering from Xi'an Jiaotong University, Xi'an, Shaanxi, China, in August 1993; received Master of Science degree in Mechanical Engineering from Xi'an Jiaotong University in April 1986. Completed the requirements for the Doctor of Philosophy degree with a major in Mechanical Engineering at Oklahoma State University in July 1995.

Experience: Assistant Professor in Xi'an Jiaotong University, Department of Power and Mechanical Engineering, 1986 to 1990. Graduate research assistant at Oklahoma State University, School of Mechanical and Aerospace Engineering, 1990 to present.

Professional Memberships: American Society of Mechanical Engineers.